Aus der Klinik für Innere Medizin mit Schwerpunkt Nephrologie der
Medizinischer Fakultät der Charité - Universitätsmedizin Berlin

DISSERTATION

Effects of sex and enhanced nitric oxide/cGMP signalling on aortic remodelling in experimental mild renal insufficiency

zur Erlangung des akademischen Grades
Doctor medicinae (Dr. med.)

vorgelegt der Medizinischer Fakultät
Charité - Universitätsmedizin Berlin

von

Bianca Stancu

aus Timisoara, Rumänien

Datum der Promotion: 22.09.2017

TABLE OF CONTENTS

ABSTRACT

Cardiovascular disease is the leading comorbidity in patients with renal disease and has been related to impaired nitric oxide signalling. Estrogens exert protective effects on the vascular system. This study aims at investigating aortic morphological, cellular and molecular alterations in a rat model of mild renal insufficiency, with a focus on the effects of sex, the contribution of aortic NO/cGMP signal transduction and the therapeutic potential of the NO-independent sGC stimulator BAY 41-8543.

Age-matched male and female Wistar rats were assigned for 18 weeks into following groups: sham operated, subtotally nephrectomised (SNX), SNX+BAY 41-8543 and SNX+hydralazine. Analysis involved functional, histological and molecular kidney and thoracic aorta parameters. Statistical analyses were performed using Kruskal-Wallis and subsequent Mann-Whitney-U testing.

SNX significantly increased systolic blood pressure, which was comparably reduced to control levels by BAY 41-8543 and hydralazine. The degree of morphological kidney damage and renal function impairment was similar in males and females independent of treatment. In SNX males, uremic aortic remodelling was characterized by marked media thickening and increased media-to-lumen ratio, vascular smooth muscle cells (VSMC) proliferation, macrophage infiltration, extracellular matrix turnover, decreased aortic elastin/collagen ratio and endothelial NO-synthase (eNOS) mRNA expression. No significant alterations of aortic media-to-lumen ratio, VSMC proliferation, macrophage infiltration, metalloproteinase-2 and eNOS mRNA expressions were seen in female uremic animals. BAY 41-8543 significantly ameliorated uremic aortic remodelling and stiffening. BAY 41-8543 reduced aortic VSMC proliferation and also modulated aortic VSMC phenotype and consequently decreased collagen I deposition, extracellular matrix turnover with low TIMP-1 and MMP-2 expression and increased the elastic content of the aortic wall. Aortic eNOS mRNA expression was normalized in BAY 41-8543-treated uremic animals. Hydralazine treatment did not substantially influence aortic remodelling.

The present study shows that experimental mild renal insufficiency leads to pronounced aortic hypertrophic remodelling and stiffening in Wistar rats, and the underlying aortic morphological, cellular and molecular alterations undergo a sex-dependent regulatory process. Vascular disease was more severe in male rats and was related to reduced aortic eNOS expression. Specific sGC/cGMP stimulation by BAY 41-8543, but not hydralazine despite a similar reduction in blood pressure, significantly ameliorates the aortic wall remodelling and stiffening, indicating a blood pressure-independent mechanism. The findings in this experimental model of mild renal insufficiency suggest that pharmacological stimulation of the sGC enzyme

may be a novel therapy concept for pathological arterial wall remodelling seen in patients with chronic renal disease.

ABSTRACT

Kardiovaskuläre Erkrankungen sind die führende Komorbidität bei Patienten mit chronischer Nierenerkrankung und ihre Pathogenese wurde mit beeinträchtigter Stickstoffmonoxid-Signaltransduktion assoziiert. Östrogene üben schützende Effekte auf das Gefäßsystem aus. Ziel dieser Studie ist die Untersuchung morphologischer, zellulärer und molekularer Veränderungen der Aorta in einem Rattenmodell einer milden Niereninsuffizienz. Untersucht wurden der Einfluss des Geschlechts, die Rolle der Aorten-NO/cGMP-Signaltransduktion und das therapeutische Potential des NO-unabhängigen sGC-Stimulators BAY 41-8543.

Altersangepasste männliche und weibliche Wistar-Ratten wurden für 18 Wochen in schein-operierte, subtotal nephrektomierte (SNX), SNX + BAY 41-8543 und SNX + Hydralazin Gruppen eingeteilt. Untersucht wurden funktionale, histologische und molekulare Nieren- und thorakale Aorta-Parameter. Statistische Analysen wurden unter Verwendung von Kruskal-Wallis und anschließenden Mann-Whitney-U-Tests durchgeführt.

SNX führte zu einer signifikanten Erhöhung des systolischen Blutdrucks, der durch BAY 41-8543 und Hydralazin auf Werte vergleichbar mit schein-operierte Tieren gleichermaßen reduziert wurde. Der Grad der morphologischen Nierenschäden und Nierenfunktionseinschränkung war bei männlichen und weiblichen Tieren vergleichbar und unabhängig von der Therapie. Das urämischen Aortenremodelling in SNX Männchen war durch deutliche Zunahme der Mediadicke und des Media-Lumen-Verhältnisses, Proliferation der glatten Gefäßmuskelzelle (VSMC), Makrophageninfiltration, erhöhten Umsatz der extrazellulären Matrix, verringerte Aorten-Elastin/Kollagen-Verhältnis und endotheliale NO-Synthase (eNOS) mRNA-Expression gekennzeichnet. Bei weiblichen urämischen Tieren wurden keine signifikanten Veränderungen des Media-Lumen-Verhältnisses, der VSMC Proliferation, Makrophageninfiltration, Metallo-proteinase-2 und eNOS mRNA Expression in der Aortenwand wurden beobachtet. BAY 41-8543 verbesserte signifikant das urämische Aortenremodelling und -Versteifung. BAY 41-8543 verminderte Aorta-VSMC-Proliferation und modulierte auch den Phänotyp der Aorta-VSMC und demzufolge reduzierte die Kollagen I-Ablagerung, den Umsatz der extrazellulären Matrix mit verminderter TIMP-1 und MMP-2-Expression und erhöhte den Elastingehalt der Aortenwand. Die Aorta-eNOS-mRNA-Expression wurde in BAY 41-8543-

behandelten urämischen Tieren normalisiert. Der Prozess des Aortenremodelling wurde durch die Hydralazin-Therapie nicht wesentlich beeinflusst.

Die vorliegende Studie zeigt, dass die experimentelle milde Niereninsuffizienz zu einem ausgeprägten hypertrophischen Aortenremodelling und Versteifung bei Wistar-Ratten führt und die zugrundeliegenden morphologischen, zellulären und molekularen Veränderungen der Aorta einem geschlechtsabhängigen regulatorischen Prozess unterliegen. Die vaskuläre Erkrankung war bei männlichen Ratten deutlich ausgeprägter und mit einer verminderten Aorta-eNOS-Expression assoziiert. Eine spezifische sGC/cGMP-Stimulation durch BAY 41-8543, aber nicht die Gabe von Hydralazin, trotz einer ähnlichen Reduktion des Blutdrucks, vermindert signifikant das Remodelling und die Versteifung der Aortenwand, was auf einem blutdruckunabhängigen Mechanismus hinweist. Die Ergebnisse in diesem experimentellen Modell der milden Niereninsuffizienz deuten darauf hin, dass die pharmakologische Stimulation des sGC-Enzyms ein neues Konzept in der Therapie des pathologischen arteriellen Remodellings bei Patienten mit chronischen Nierenerkrankungen darstellen kann.

1. INTRODUCTION

Aortic remodelling and stiffening are identified as important independent risk and prognostic factors involved in increased cardiovascular morbidity, e.g. coronary heart disease and stroke, and mortality observed in patients with chronic kidney disease (CKD). Diffuse dilatation with hypertrophy and impaired elastic properties of the aortic wall are hallmarks of vascular alterations in hemodialysis patients, but their presence was demonstrated already in early stages of CKD, independent of age, mean blood pressure or other classic cardiovascular risk factors (1). This suggests that there are other hemodynamic and humoral factors characteristic of CKD, which trigger aortic structural and functional alterations. However, experimental and clinical studies failed to elucidate the cellular and molecular mechanisms underlying the process of aortic remodelling under uremic conditions. There is still a great need for further investigations in order to unravel the pathogenesis of aortic remodelling and enable the development of new therapeutic strategies that could reduce/prevent this process and thus improve aortic stiffness and, subsequently, the cardiovascular outcome in CKD patients.

Endothelial dysfunction resulting from low nitric oxide (NO) production and impaired NO signaling via cyclic guanosine monophosphate (cGMP) represents a central mechanism in the pathogenesis of aortic remodelling in CKD (2; 3). Multiple studies demonstrated the vasoprotective role of NO as signalling molecule responsible for vasodilatation, reduced platelet aggregation, platelet and monocyte adhesion to the endothelium, inhibition of vascular smooth muscle cell (VSMC) proliferation and migration and for extracellular matrix expansion. However, several *in vitro* and *in vivo* studies report proatherogenic and pro-proliferative effects of NO/cGMP signalling. These data raise several questions regarding the cardiovascular actions of the NO/cGMP pathway and the therapeutic effects of pharmacological interventions on different components of this pathway.

In addition to NO-cGMP, sex hormones (estrogens, progesterone and androgens) and their receptors are critical determinants in sex differences of renal and cardiovascular disease (4). Premenopausal women show a reduced incidence and slower progression of cardiovascular disease compared with age-matched men and women in postmenopause, but data regarding the role of sex hormones in pathogenesis of vascular disease are controversial. Multiple clinical and experimental studies pointed towards estrogens exerting vasoprotective effects, among others by increasing NO production and bioavailability. In contrast, interventional trials in postmenopausal women suggested neutral or even adverse vascular actions of hormone replacement therapy.

The present study was designed to characterize the morpho- and physiopathological features of aortic remodelling in a rat model of mild renal insufficiency, with focus on the role played by the NO-cGMP pathway and the modulator effect of gender. We also address the question whether pharmacological enhancement of the NO/cGMP signalling, by using the novel soluble guanylate cyclase stimulator BAY 41-8543, exerts beneficial effects on the development of vascular disease.

1.1. Aortic remodelling in chronic kidney disease

1.1.1. The physiology and pathophysiology of aortic remodelling

Vascular remodelling represents a physiological structural and functional adaptation of the vessel wall to chronic hemodynamic and humoral changes, and to direct injury, but it can also underlie the pathogenesis of many severe cardiovascular diseases. Arteries should be regarded as dynamic structures, whith a continuous active interplay at their level between different cell types (endothelial cells, VSMC, fibroblasts) and components of extracellular matrix (ECM). The structural alterations that occur in the process of aortic remodelling are characterized by changes in aortic lumen and/or wall thickness and composition caused by activation, proliferation and migration of VSMC, rearrangements of different cellular elements, as well as imbalanced production and degradation of ECM.

Endothelial cells are involved in detection and transformation of mechanical and humoral stimuli into biological signals that will modulate vascular structure and function. This makes the presence of an intact endothelium a pre-condition for normal vascular adaptation (5).

Depending on the association/predominance of factors that act on the vessel wall, there are different types of aortic remodelling. Elevated blood pressure and alterations in blood flow with increased shear stress are the major hemodynamic factors that induce mechanical stimulation of the aortic wall and are responsible for induction and progression of the remodelling process. Hypertension, a common finding in patients with CKD, results in increased aortic transmural pressure and wall stretch. According to Laplace´s law ($\sigma = P \; x \; r \; / \; h$), an increase in arterial transmural pressure (P) or radius (r) induces an elevation of the tensile stress (σ), which will then be compensated by a thickening of the arterial wall (h). Thus, pressure overload is characterized by a hypertrophic remodelling of the aortic wall with decreased lumen diameter and increased media-to-lumen ratio. The other important mechanical force acting on the vascular wall is represented by shear stress (τ), the dragging frictional force acting on the vessel surface,

which is directly influenced by changes in blood flow according to the formula $\tau = (Q \times \eta) / (\pi \times r^3)$ (6). The shear stress is directly proportional to blood flow (Q) and viscosity (η) and inversely proportional to the arterial radius (r), so that any increase in arterial blood flow results in an enlargement of arterial lumen. These two adaptive mechanisms are closely interrelated, since the increase of aortic lumen following flow overload is attended by aortic wall thickening in order to maintain the tensile stress in physiological range. This explains why pathological conditions characterized by flow/volume overload are accompanied by a proportional increase in aortic lumen diameter and wall thickness, so that media-to-lumen ratio is relatively preserved (7).

Changes in aortic structure in response to different trigger factors are reflecting in functional alterations. Large conduit arteries, like aorta, accomplish two important functions: conduit and cushioning (dampening) functions. The conduit function assures an optimal perfusion of the peripheral tissues according to their metabolic demands and depends mostly on the arterial diameter. The cushioning function refers to the capacity to dampen blood pressure oscillation due to intermittent ventricular ejection, thus transforming pulsatile flow into laminar flow in peripheral arteries. The efficiency of this process depends on the viscoelastic properties of the aortic wall but also on vessel diameter. Stiffness, defined as resistance of an elastic body to deformation, represents an important parameter of viscoelastic properties and depends, among others, on elastin and collagen content of the aortic wall. Aortic stiffening leads to systolic blood pressure elevation with high pulse wave velocity (PWV) and reduced diastolic pressure at aortic level (6). These hemodynamic changes, by increasing left ventricle preload, are detrimental and lead to left ventricle hypertrophy, high myocardial oxygen consumption and functional impairment. In addition, low diastolic blood pressure is reflecting in reduced myocardial perfusion and disturbed coronary blood flow distribution (8). Furthermore, elevated blood pressure accelerates the arterial degenerative processes and aggravates aortic stiffness (6). Reduced cushioning function is a hallmark of the aging process, but is also present in diseases associated with increased vascular collagen content and alterations in extracellular matrix, condition known as arteriosclerosis. Arteriosclerosis is a primary arterial media degenerative disease that affects large conduit arteries and manifests as lumen dilatation with diffuse hypertrophy and stiffening of the arterial wall. Morphologically, arteriosclerosis is characterized by fibroelastic intima thickening, increased collagen and ground substance content in the media with fragmentation of elastic lamellae, and consecutive fibrosis and calcification of arterial wall (7).

1.1.2. Pathophysiology of aortic remodelling in CKD

In patients with CKD, remodelling of large conduit arteries represents a major factor that contributes to increased cardiovascular morbidity and mortality. Besides accelerated atherosclerosis, which is one of the main pathophysiological processes underlying this increased cardiovascular burden, the spectrum of vascular alterations in CKD is broader, including non-occlusive remodelling with modification of the viscoelastic properties of large capacitive arteries. Aortic stiffening was identified already in patients with mild to moderate renal disease and was found to be associated with reduced creatinine clearance (7).

Multiple interrelated trigger factors like hemodynamic overload, humoral and metabolic alterations, some of them specific to uremic condition, act on the aortic wall and are responsible for the initiation and progression of vascular disease (Fig.1).
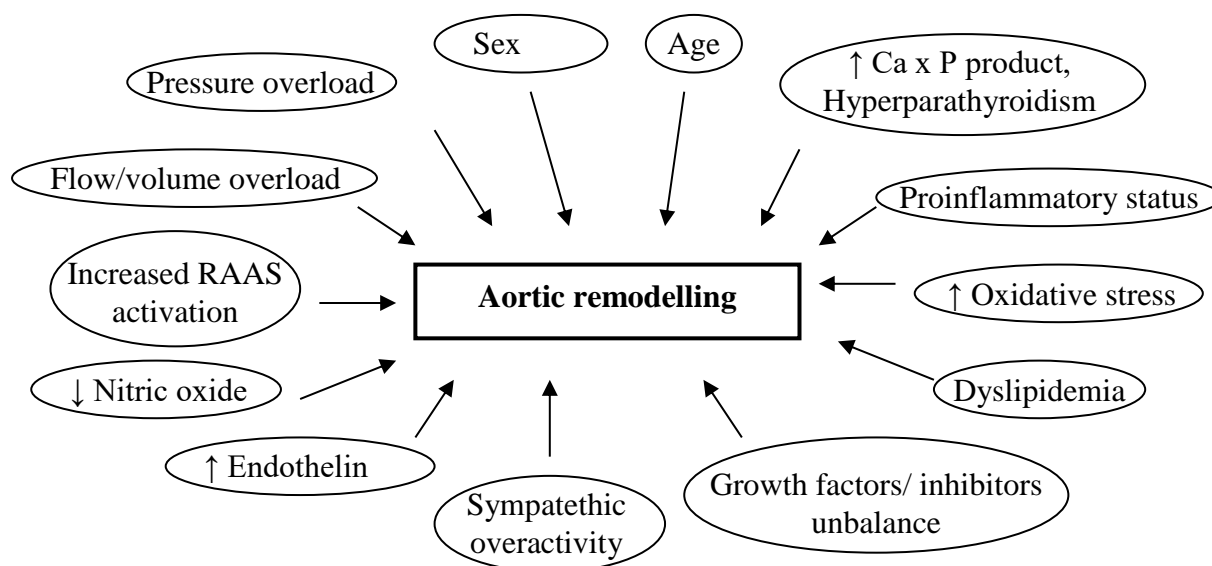
Figure 1. Trigger and modulating factors involved in the pathogenesis of aortic remodelling in chronic renal disease (adapted after London et al (7)).

Pressure and volume overload are almost constant findings in patients with CKD and represent main trigger factors involved in the pathogenesis of aortic remodelling. The underlying pathophysiological mechanisms involve activation of the renin-angiotensin-aldosterone system (RAAS), with increased concentrations of angiotensin II (Ang II) and aldosterone, and increased water-sodium retention. In addition, elevated endothelin levels (9) and reduced NO production/bioavailability, as well as sympathetic overactivity contribute to increased vascular

tonus and aortic remodelling. Other factors more specific to CKD, like arteriovenous shunts, anemia and over-hydration, largely contribute to high blood flow velocity (7).

Endothelial dysfunction represents a central mechanism in the pathogenesis of many different cardiovascular complications in CKD, including aortic remodelling. Experimental and clinical studies demonstrated the prominent role of reduced nitric oxide production and impaired signalling in CKD-associated endothelial dysfunction (10; 11). As suggested by the HOORN study, altered endothelial function may contribute to increased cardiovascular mortality even in mild renal insufficiency (2). In addition, the complex association of increased oxidative stress, proinflammatory status and dyslipidemia in CKD patients further contributes to the pathogenesis of aortic wall remodelling and stiffening, partially by down-regulating NO/cGMP signalling (7; 12).

Clinical studies showed that large capacitance arteries of ESRD (end-stage renal disease) patients, when compared with age-, sex- and blood pressure-matched non-uremic patients, are subject to a remodelling process characterized by lumen enlargement and media thickening, with qualitative changes of aortic wall components. Aortic remodelling in renal patients is associated with increased aortic stiffness, while in patients with essential hypertension the elastic properties of aorta are preserved (1; 13).

Experimental models of hypertension brought important information concerning structural alterations that occur in the aortic wall and can explain the increased wall thickness. Studies investigating the aorta of rats with renovascular hypertension, spontaneously hypertensive (SHR) (14; 15; 16) or subtotally nephrectomised rats (17) found VSMC hypertrophy and/or hyperplasia, and increased ECM deposition as cellular mechanisms involved in aortic media thickening. The endothelin system and parathyroid hormone were shown to be involved in vascular and cardiac structural alterations occurring in renal failure (18; 19).

ECM proteins, besides providing structural support, also play an important role in modulating cell function. Aortic remodelling involves ECM reorganization and therefore an active process of proteolysis and re-synthesis of ECM proteins. Both endothelial cells and VSMC were demonstrated to constitutively express MMP-2 (matrix metalloproteinase-2) and the inhibitory TIMP-1 (tissue inhibitor of metalloproteinase-1) and TIMP-2, the production of these proteins being enhanced in various models of arterial disease (20; 21).

1.1.3. Therapeutic interventions in aortic remodelling and stiffening

Aortic stiffness was recognized as an independent cardiovascular risk factor that negatively affects left ventricular hypertrophy and function. This explains why treatment of CKD patients should include strategies to prevent large artery remodelling.

Clinical studies demonstrated the beneficial effect of antihypertensive therapy on aortic remodelling in non-uremic patients with essential hypertension (22). Blocking RAAS with ACE inhibitors, angiotensin receptor blockers, direct renin inhibitor or aldosterone antagonists exerts beneficial effects on arterial remodelling and stiffening in hypertension (23; 24; 25). Natriuretic peptides, by increasing cyclic guanosine monophosphate (cGMP) levels, were found to reduce arterial stiffness and to exert antiproliferative and antifibrotic effects in experimental studies. This was confirmed in clinical trials using the association of an endopeptidase inhibitor (Omapatrilat), which reduces ANP degradation, with an ACE inhibitor (26; 27; 28). Sildenafil, a phosphodiesterase-5 inhibitor that increases cGMP concentration by reducing its degradation, could also reduce pulse pressure and improve arterial stiffness (29). Aldosterone synthase inhibitors, the combination angiotensin receptor blocker with neprilysin inhibitors, as well as baroreceptor stimulation are new therapeutic approaches that could beneficially influence the process of arterial remodelling (22).

In controlled clinical studies in CKD patients, long-term treatment with ACE inhibitors and calcium channel blockers managed to lower blood pressure and significantly reduce PWV, thus improving the function of large conduit arteries (30; 31), which reflects in regression of left ventricular hypertrophy and better survival in this population (32).

1.2. NO/cGMP signalling in vascular system

In 1980 Furchgott et al. (33) were the first to show that the vasodilative effects of acetylcholine depend on the presence of an intact endothelium that secretes a signalling molecule named endothelium-derived relaxing factor (EDRF), which acts on VSMC and promotes vascular relaxation. In 1987 EDRF was finally identified as the small gas molecule NO (34; 35), for this discovery and further research in the area R.F. Furchgott, L.J. Ignarro and F. Murad were awarded in 1998 the Nobel Prize for Medicine and Physiology.

1.2.1. Nitric oxide synthases and NO production

NO is a small, highly lipophilic and diffusible free radical gas molecule, whit physical and chemical properties that allow it to rapidly disperse and traverse different cell membranes, and confer it a high chemical reactivity. Thus, besides acting as a signalling molecule, NO can react with a multitude of molecules and radicals, especially superoxide and oxyhaemoglobin, this considerably reduces its half-life and operating distance. NO half-life ranges from milliseconds to a few seconds, depending on environmental conditions, and the maximal action range is about 100 μm (36). Despite being one of the simplest biological molecules, NO is implicated in a variety of physiological and pathological processes in nearly every organ and system, from vasodilatation, inflammation, platelet adhesion and aggregation, cell proliferation/apoptosis to phenotype regulation and neurotransmission.

NO is produced in the organism by a family of enzymes called nitric oxide synthases (NOS) from the amino acid L-arginine (37). There are tree enzyme isoforms known so far: endothelial, neuronal and inducible NOS (eNOS, nNOS and iNOS). All these isoforms use oxygen (O_2) and nicotinamide adenine dinucleotide phosphate (NADPH) as co-substrates for the oxidation of L-arginine, with formation of L-citruline as co-product, and require co-factors like tetrahydrobiopterin, flavin adenine mono- and dinucleotide and calmodulin. L-arginine is a semi-essential amino acid that is endogenously synthesized primarily in proximal tubule of the kidney, but in small quantities also in endothelial cells and macrophages (38).

eNOS and nNOS, also called constitutive NOSs, are constitutively expressed and their activity is modulated by intracellular Ca^{2+} concentration, calmodulin and by post-translational regulation. eNOS is expressed in endothelial cells, VSMC, cardiac myocytes but also in neurons. In endothelial cells, eNOS is responsible for the basal, well regulated NO generation that sensitively and continuously modulates the vascular tonus by cGMP-dependent VSMC relaxation and, in addition, it inhibits platelet aggregation and adhesion as well as leukocyte adhesion. Shear stress, by mechanically stimulating endothelial cells, is an important eNOS modulator in the vasculature. nNOS was first described in the central and peripheral nervous system as being involved especially in neurotransmission, but it was also found to be expressed in endothelial cells and kidney, where it regulates glomerular hemodynamics (39).

iNOS is an inducible enzyme expressed primarily in macrophages and neutrophils, but also in endothelial and smooth muscle cells, heart and diseased kidney in response to inflammatory cytokines like IL-1, IFN-γ and TNF-α (39; 40). Regulation of iNOS occurs at transcriptional level. The enzyme produces high levels of NO in a Ca^{2+}-independent manner and

for a longer period of time compared with constitutive NOSs. The resulting high NO concentration has cytotoxic effects and is involved in inflammatory and immune responses (41).

1.2.2. *The dual role of NO*

NO can act via two different main pathways in order to exert its various effects: indirect, as a signalling molecule, or direct, as an effector molecule.

At low physiological concentrations, NO diffuses freely and rapidly through cell membranes, its diffusion coefficient being 1.4 fold higher than that of oxygen, and acts as a signalling molecule. Due to its chemical properties, NO reacts especially with haem-containing enzymes, like soluble guanylate cyclase (sGC), NOSs and cytochrome P450, and proteins containing thiol groups (42). Binding of NO to sGC increases the catalytic activity of this enzyme and thus increases intracellular cGMP concentration, which is responsible for the further downstream biological effects of NO: vasodilatation, inhibition of leukocyte adhesion and of platelet activation (43).

At high concentrations, as found in inflammatory states, NO becomes a destructive effector molecule involved in host defence and autoimmunity. In these conditions, NO irreversibly reacts with superoxide radicals (O_2^-) forming peroxynitrite ($ONOO^-$). High concentrations of peroxynitrite exert cytostatic and cytotoxic actions, among others by nitrosylation of tyrosine residues in proteins, DNA fragmentation, and inhibition of DNA synthesis and key enzymes of respiratory chain (36). In addition, autooxidation of NO results in production of dinitrogen trioxide and induces DNA alterations.

1.2.3. *Physiology of NO/cGMP signalling in vascular system*

In the vasculature, eNOS-derived NO diffuses through the endothelial cell membrane into underlying VSMC or in vessel lumen and then into platelets and leukocytes. There, NO exerts its effects by activation of sGC, resulting in increased intracellular concentration of cGMP, the second messenger molecule of the pathway. Both transmembrane particulate GC, activated by natriuretic peptides, and sGC, whose ligands are represented by NO and carbon monoxide (CO), convert 5´-guanosinetriphosphate (GTP) into cGMP and pyrophosphate.

sGC is ubiquitously expressed in mammalian cells and has a heterodimeric structure consisting of an α- and β-subunit, each with two isoforms, the α_1/β_1 dimer having the most important role in the cardiovascular system. Characteristically, sGC contains a prosthetic haem moiety attached to the haem-binding domain. NO binds to the haem group and induces

conformational changes by shifting the iron atom out of the porphyrin ring plane, thus leading to an allosteric activation of the enzyme. Exposure of sGC to low 10-100nM concentrations of NO results in a 500-fold enhancement of its catalytic activity, while other ligands, like CO, induce only a slight 6-fold increase (44). Besides being its activator, NO can also physiologically modulate the expression of sGC, high NO levels reducing mRNA and protein expression of the enzyme (45).

cGMP directly and indirectly modulates various target proteins like cGMP-dependent protein kinases (PKG-I and PKG-II), phosphodiesterases (PDEs), ion channels but also tyrosine kinases and phosphatases, G-protein-coupled receptors and others (46).
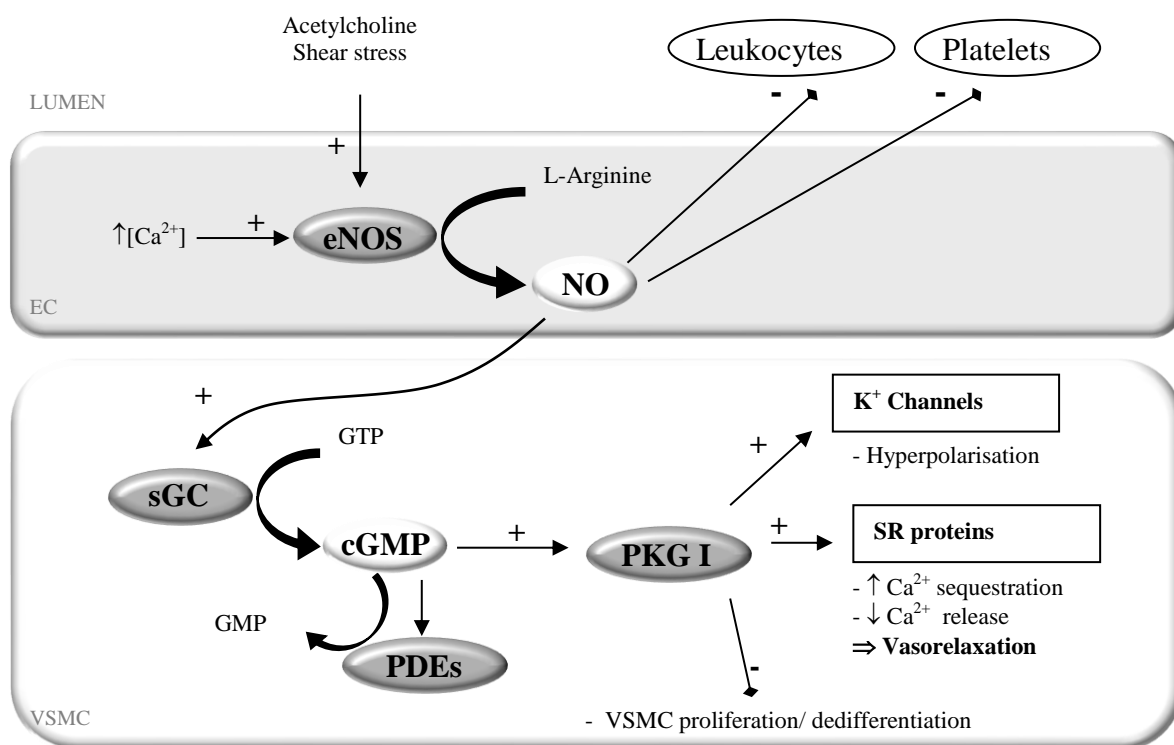
Figure 2. Schematic representation of NO/cGMP signal transduction in arterial wall (EC – endothelial cell; SR - sarcoplasmic reticulum).

PKG-I is highly expressed in smooth muscle cells and platelets, but lower concentrations were also found in endothelial cells, cardiomyocytes, fibroblasts, renal mesangial cells, and leukocytes. cGMP-activated PKG-I induces phosphorylation of different proteins in the sarcoplasmic reticulum, i.e. phospholamban and 1,4,5-inositoltriphosphat receptor-associated cGMP kinase substrate (IRAG), thus increasing Ca2+ sequestration in and inhibiting Ca2+ release from sarcoplasmic reticulum. In addition, PKG-I can activate Ca2+-dependent K+

channels, resulting in hyprerpolarisation of the cell membrane and lower Ca2+ influx. Through all these mechanisms, PKG-I effectively decreases intracellular Ca2+ concentration, thus being responsible for NO-induced relaxation of VSMC with vasodilatation. PKG-I also regulates VSMC proliferation and phenotype, and inhibits platelet aggregation and adhesion (46; 47).

PDEs inactivate cGMP by hydrolyzing its 3´-phosphoester bond with formation of biological inactive metabolite 5´-GMP. PDE-5 and PDE-1 were found to play a major role in the vasculature. cGMP can regulate the activity of some PDEs, like PDE-2 and PDE-3, thus interfering with degradation of cAMP (48). Pharmacological PDEs inhibition represents already a therapeutic approach in clinical practice, unspecific inhibitors (methylxanthines) or specific inhibitors of PDE-4 (i.e. roflumilast), PDE-3 (i.e. milrinone, cilostazol) or PDE-5 (i.e. sildenafil) being successfully used in treatment of chronic obstructive pulmonary disease, acute heart failure, peripheral artery disease, pulmonary hypertension and erectile dysfunction, respectively (49).

1.2.4. *Pathophysiology of NO/cGMP signalling*

1.2.4.1. NO/cGMP signalling in CKD

CKD is characterized, among others, by reduction of the overall NO production and bioavailability, which contributes to further progression of renal disease and to pathogenesis of cardiovascular complications. Reduced NO production, reflected in low urinary nitrite/nitrate levels, was demonstrated in both humans and animals with CKD and is a marker of endothelial dysfunction. Multiple conditions associate and explain the NO deficiency in renal disease.

Impaired NO production in CKD can be partially explained by substrate deficiency due to decreased L-arginine endogenous production and/or dietary intake, by consumption of available L-arginine in other metabolic pathways (arginase) and impairment of L-arginine transport into endothelial cells (50).

Alteration of renal and aortic NOSs expression further contributes to NO deficiency, as shown in rat remnant kidney model. Down-regulation of renal NOSs expression was associated with increased aortic NOSs expression and activity in infarction model (51), whereas reduced aortic eNOS and iNOS levels were found in ablation model (52; 53; 54).

Furthermore, CKD patients present high plasma levels of asymmetric dimethylarginine, a competitive NOS inhibitor, which accumulates due to enhanced synthesis and reduced degradation (50). Dyslipidemia is associated with elevated endothelial caveolin-1 expression, a regulatory protein that co-localizes and binds to eNOS in caveole, forming an inactive complex.

CKD is also characterized by increased oxidative stress. Thus, besides impaired NO production, available NO is scavenged by reactive oxygen species (ROS) with subsequent production of highly cytotoxic compounds like peroxynitrite, mechanism involved in the pathogenesis of uremic hypertension (55).

1.2.4.2.   Role of NO/cGMP pathway in aortic remodelling

NO represents the most important endogenous vasodilator, this being confirmed by development of hypertension in eNOS knock-out mice (56). However, the vasoprotective role of NO goes far beyond vascular tone regulation. Multiple studies in different animal models of vascular injury demonstrated that NO effectively prevents vascular remodelling in a PKGI-dependent or independent manner by maintaining the balance between VSMC proliferation and apoptosis and inhibiting VSMC transition to a fibroproliferative phenotype characterized by high production of ECM proteins (collagen I, MMPs, thrombospondin etc). Enhanced NO/cGMP signalling using a sGC stimulator prevented vascular remodelling through suppression of MMP2 and MMP9 expression and activity (57). In contrast, other *in vitro* and *in vivo* data point towards a proproliferative and proatherogenic effect of the NO/cGMP pathway (58; 59).

In addition, activation of the NO/cGMP pathway can efficiently inhibit platelet aggregation and adhesion as well as leukocyte adhesion, the latter as a result of suppressed VCAM-1 and NFkB expression (60). The antiinflammatory action of NO is doubled by antioxidative effects, both being major pathophysiological processes involved in vascular remodelling (36; 39).

At the functional level, the regulatory effect of NO on large artery stiffness was investigated in clinical and experimental studies. Aortic PWV was shown to be increased in eNOS knock-out mice and after L-nitro-arginine methyl ester (L-NAME) administration (61).

1.2.5.   Pharmacological stimulators of sGC

Pharmacological manipulation of sGC represents a valuable tool for both further elucidation of NO/cGMP signal transduction and investigation of potential therapeutic implications. By only increasing cGMP levels, sGC stimulation overcomes the possible negative actions of NO as effector molecule, which were described after L-arginine supplementation, and the tolerance phenomenon associated with chronic NO-donors therapy.

YC-1 (3-(5´-hydroxymethyl-2´-furyl)-1-benzylindazole) was the first NO-independent sGC stimulator discovered, which induces a moderate 10-fold increase in sGC activity. Its

actions depend on the presence of reduced prosthetic haem moiety of sGC, are synergistic with NO, and include also PDE inhibition (62).

Stasch et al. discovered and characterized the new NO-independent, haem-dependent sGC stimulators BAY 41-2272 and BAY 41-8543, both synthesized based on YC-1 as lead structure but with a two orders of magnitude higher potency (63; 64). BAY 41-8543 (chemically, 2-[1-[(2-fluorophenyl)methyl]-1H-pyrazolo[3,4-b]pyridin-3-yl]-5(4-morpholinyl)-4,6-pyrimidinediamine) is about 3-fold more potent *in vivo* after oral administration when compared with BAY 41-2272. BAY 41-8543 has no PDE inhibitory effect and synergizes with NO over a wide range of concentrations. The latter characteristic is probably related to the fact that BAY 41-8543 does not bind to the haem moiety, instead, it was proposed to interact with a new NO-independent regulatory site on the α_1-subunit of sGC, thus increasing the catalytic rate and the responsiveness to NO. In a high renin, low NO rat model of hypertension, chronic BAY 41-8543 treatment prevented elevation of blood pressure, had renal protective effects and anti-platelet actions, and consequently increased survival (65). sGC stimulators were shown to exert vascular and cardio-renal protective effects in animal models of chronic pulmonary hypertension and congestive heart failure (66; 67), as well as in patients with pulmonary hypertension (68; 69). In addition to the beneficial cardiovascular effects, previous work of our group indicated that sGC stimulators are able to reduce progression of renal disease in experimental glomerulosclerosis (70; 71).

For its effects on both renal and cardiovascular systems and its higher potency, BAY 41-8543 was chosen in this study to stimulate the NO/cGMP pathway, in order to investigate the role of NO/cGMP signal transduction in the pathogenesis of uremic vascular remodelling and as potential therapeutic target.

1.3. Sex-related aspects in vascular system

Sex hormones (estrogens, progesterone and androgens) and their receptors are critical determinants of renal and cardiovascular sex differences. The two main estrogen receptor subtypes, ERα and ERβ, were both found to be expressed in kidney (72) and vasculature, ERβ being the predominant receptor in human VSMC. The presence of androgen receptor (AR) was also demonstrated in renal and vascular tissues. Sex hormone receptors, after binding with their ligands in the cytosolic cellular compartment, translocate into the nucleus where they act as transcription factors. They bind as hetero- or homodimers to hormone-responsive DNA elements of hormone-sensitive genes and subsequently regulate their transcription. This mechanism is

responsible for the genomic, long-term effects of sex hormones. In addition, both estrogens and androgens are capable of rapid, nongenomic actions, especially in the vasculature, where they induce acute vasodilatation. This mechanism involves plasma-associated sex hormone receptors and subsequent activation of various signalling pathways (72; 73).

1.3.1. *Sex-related differences in arterial remodelling*

The incidence of cardiovascular disease, including hypertension, is much lower in premenopausal women compared with age-matched males, but it rises sharply after the menopause. This suggests sex differences in physiological and pathological cardiovascular processes, and cardiovascular protective effects of female sex hormones (74).

However, studies investigating sex differences in arterial remodelling and stiffness provided contradictory data. Several epidemiological studies, including one in elderly population with mild renal insufficiency, found PWV, as marker of arterial stiffness, to be higher in men than in premenopausal women (75; 76). In contrast, in type 2 diabetes, women have a greater incidence of aortic stiffening and left ventricular hypertrophy than men (73).

Experimental data on the vascular effects of estrogen are controversial, too. Several studies in SHR, Dahl salt-sensitive and deoxycorticosterone-salt hypertensive rats showed that blood pressure levels are higher in males than in females (72). Ovariectomy (OVX) induced different effects on aortic remodelling and function: it abolished the protective effects of female sex and accentuated media thickening, or had no influence on the aortic remodelling process. The effects of estrogen replacement therapy varied also from reduction of aortic wall remodelling to neutral or even detrimental effects, the outcome varying with animal model and vascular bed (77; 78; 79).

Estrogens exert multiple direct and indirect effects on the arterial wall that can account for their vascular protection. The rapid vasodilator effect of estrogens is mediated by nongenomic mechanisms involving enhanced NO production in endothelial cells and decreased Ca^{2+} entry with relaxation of VSMC. In addition, estrogens exhibit long-term effects on the vasculature by modulating the expression of genes encoding important mediators of vascular function (cyclooxygenase and prostacyclin synthetase, endothelin-1) and extracellular matrix components. Moreover, estrogens exhibit antiinflammatory and antioxidant effects by decreasing expression of endothelial adhesion molecules and NADPH oxidase. Sex differences in the expression and activity of RAAS components were also reported. Female sex hormones are associated with increased angiotensinogen but lower renin and angiotensin-converting enzyme

levels and down-regulation of Ang II receptor 1 (AT-1). In contrast, male sex is characterized by higher renin and reactive oxygen species concentrations (73). Besides the direct effects on the vascular wall, estrogens exert systemic effects: they reduce LDL-cholesterol, increase HDL-cholesterol but also triglyceride plasma levels, and enhance fibrinolysis (74; 80). In various experimental models of vascular injury, estrogens were described to promote endothelial cell growth and rapid reendothelialization, but inhibit proliferation and migration of VSMC (74; 81), and modulate VSMC phenotype (82; 83).

It is important to mention that studies in humans and animal models showed variable effects of sex hormones, depending on the investigated species, strain, disease model, vascular bed and cell type.

1.3.2. *Effects of sex on the NO/cGMP signalling pathway*

In healthy humans, total NO production is higher in premenopausal women than in men (84), this has been confirmed by animal studies (72).

Estrogens can increase NO production and bioactivity by different mechanisms: genomic and rapid nongenomic pathways. Estrogens induce up-regulation of eNOS mRNA expression, this transcription activation being ERβ-mediated (85). Also, estrogens can indirectly reduce NO scavenging by ROS by downregulating the expression of different NADPH oxidase subunits (86).

In addition to genomic actions, estrogens are capable of rapidly (5-10 min) activating eNOS, thus inducing acute modulation of NO release and regulation of vascular tone. This effect is mediated by a plasma membrane-associated subpopulation of ERs that colocalises with eNOS to caveolae in endothelial cells, forming, together with other regulatory proteins, a functional signalling complex. Binding of estrogens to ER in caveolae leads to activation of further downstream pathways such as tyrosine kinase/mitogen-activated protein kinase (MAPK) pathway and phosphatidylinositol 3 (PI-3) kinase/Akt signalling, and hence stimulation of eNOS activity. Moreover, high NO release and cGMP production upon estrogens stimulation occurs also through elevation of intracellular Ca^{2+} concentration and induction of heat shock protein 90/eNOS active complex (87; 88; 89).
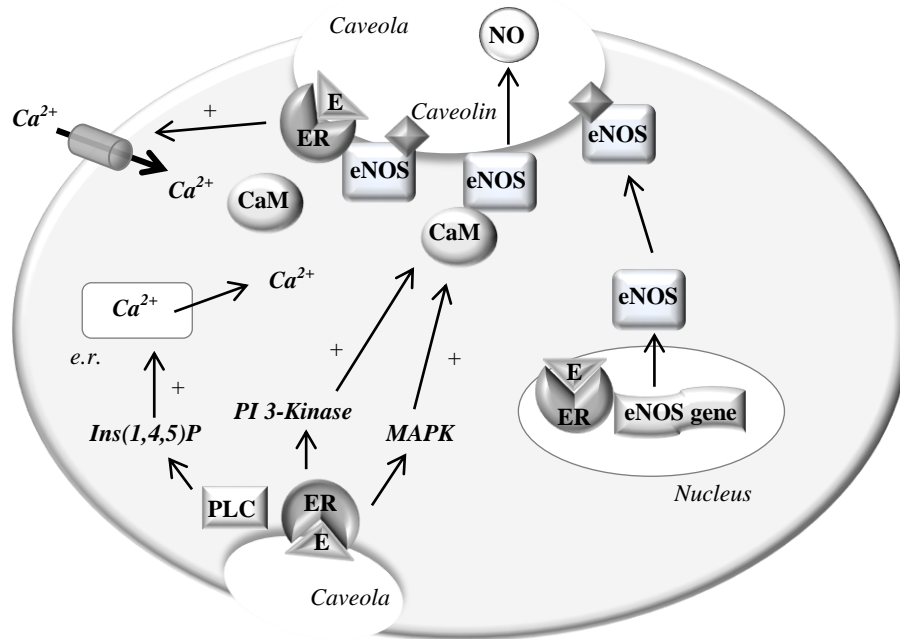
Figure 3. Proposed signalling mechanisms of genomic and nongenomic regulation of eNOS by estrogen (E) in endothelial cells (CaM – calmodulin; PLC – phospholipase C; Ins $(1,4,5)P_3$ – Inositol 1,4,5-triphosphate; e.r. – endoplasmic reticulum). Modified after Gray GA et al. (90).

Testosterone was also demonstrated to induce NO-mediated vasodilatation in some arterial preparations, while dehydroepiandrosterone enhanced NO production by increasing the expression of eNOS in human endothelial cells (89).

1.4. Aim of the study

Aortic remodelling with increased wall stiffness represents an independent cardiovascular risk factor in patients with CKD by promoting and accelerating left ventricular hypertrophy and functional impairment. Extracellular matrix expansion and VSMC proliferation were shown to be involved in aortic media thickening, but there is a great need for further elucidation of the underlying mechanisms. Based on its multiple vascular effects, we hypothesized that NO/cGMP signalling represents one of the important pathomechanisms and therefore a promising therapeutic target in uremic arterial remodelling. Sexual dimorphism in aortic remodelling and function could be partially explained by enhanced NO production and signalling induced by estrogens (91).

In a rat model of mild uremia induced by subtotal nephrectomy (SNX), the present study had the following goals:

1. Characterization of morphological, cellular and molecular changes occurring in the aortic wall in response to renal disease, by analysing
   - the involvement of different pathophysiological processes (VSMC proliferation, ECM expansion, chronic inflammatory infiltration of vascular wall),
   - aortic elastin-to-collagen ratio as an indirect parameter of arterial wall stiffness,
   - the impact of SNX on aortic expression of NO/cGMP signalling pathway components,
   - whether uremic aortic remodelling develops independently of blood pressure levels, hydralazine-treated SNX rats being used as non-hypertensive controls.

2. Identification of sex-related differences in the uremic aortic remodelling process, by looking for
   - blood pressure-independent effects of sex on aortic morphological and molecular alterations,
   - sex-dependent differences in NO/cGMP signal transduction at aortic level.

3. Further investigation of the role played by NO/cGMP signalling pathway in the process of uremic aortic remodelling by enhancing sGC/cGMP signalling:
   - evaluation of the therapeutic potential of BAY 41-8543, a NO-independent sGC stimulator, in preventing/attenuating uremic aortic remodelling.
   - Treatment with the sole vasodilator hydralazine served as control in order to assess the blood pressure-independent effects of BAY 41-8543.

2. MATERIALS AND METHODS

2.1. Materials

2.1.1. Chemicals, instruments and tools

All chemicals used were purchased from Sigma Chemical-Aldrich Co. (Taufkirchen, Germany), unless otherwise stated.

The following table lists instruments and tools that were used during the experiments.

Table 1. Instruments and tools used during the experiments

Centrifuge 5417R	Eppendorf-Netheler-Hinz GmbH, Hamburg, Germany
Combitips plus, 0.5/2.5/5.0 ml	Eppendorf AG, Hamburg, Germany
Computerized Blood Pressure Monitor IITC Model 31	Life Science Instruments, California, USA
Cryo Tube™ Vials	NUNC™ Brand Products, Roskilde, Denmark
ECHO MRI™ Whole Body Composition Analyser	Echo Medical Systems, Houston, Texas, USA
Electrophoresis Power Supply EPS 300	Pharmacia Biotech, Uppsala, Sweden
Electrophoresis Camber	Hoefer Scientific Instruments, California, USA
Eppendorf Pipette/Multipette	Eppendorf-Netheler-Hinz GmbH, Hamburg, Germany
Eppendorf Tips	Eppendorf AG, Hamburg, Germany
Eppendorf Tubes 0.5/1.5/2.0 ml	Eppendorf AG, Hamburg, Germany
Examination Gloves	Ulma International GmbH, Darmstadt, Germany
Homogenizer	ART-moderne Labortechnik, Müllheim, Germany
Isoflurane Anesthesia Systems	Völker GmbH, Kaltenkirchen, Germany
MasterCycler ep realplex^{2}S	Eppendorf AG, Hamburg, Germany

Megafuge 2.0R	Heraeus Instruments, Hanau, Germany
Metabolic Cages	3701M081, Tecniplast, Buguggiate, Italia
Microplate Reader (MRX)	DYNEX Technologies, Sullyfield Circle, USA
Microscope	Carl Zeiss Inc., Berlin, Germany
Microscope Slides, Super Frost Plus	R. Langenbrinck, Emmendingen, Germany
Microscope Cover Glasses	Gerhard Menzel GmbH, Braunschweig, Germany
Microtest^{TM} Tissue Culture Plates, 96well	Becton Dickinson GmbH, Heidelberg, Germany
Microtiter Plate Shaker TITRAMAX 101	Heidolph Instruments, Schwabach, Germany
Microtome Rotary 2003	pfm. Produkte für die Medizin AG, Köln, Germany
Microwave	Robert Bosch GmbH, Stuttgart, Germany
Minishaker MS1	IKA Works Inc., Wilmington, Germany
Multifly Needle Set	Sarstedt, Nümbrecht, Germany
Needles Gr. 20	B.Braun Melsungen AG, Melsungen, Germany
Parafilm	American National Can™, Greenwich, USA
pH Meter	Wissenschaftlich Technische Werkstätten, Weilheim, Germany
Polypropylene Conical Tube, 15/50ml	Becton Dickinson GmbH, Heidelberg, Germany
Prolene Monofil Suture 4-0	Ethicon Inc., Somerville, New Jersey, USA
Scale	Sartorius, Göttingen, Germany
S-Monovette 9ml with EDTA	Sarstedt, Nümbrecht, Germany
Shaker, "Big squid"	IKA-WERKE GmbH, Staufen, Germany
Shaver	Wella AG, Darmstadt, Germany

Sterile Syringe 1/20 ml	Becton Dickinson GmbH, Heidelberg, Germany
Surgical Instruments	Medicalis Medizintechnologie, Garbsen, Germany
Thermomixer Compact	Eppendorf AG, Hamburg, Germany
Tissue Embedding Station 4004	pfm. Produkte für die Medizin AG, Köln, Germany
Tissue Flotation Bath 45	Medite GmbH, Burgdorf, Germany
TP 472 T/Pump-System	Gaymar Industries Inc., Orchard Park, New York, USA
TRIO-Thermoblock	Biotron GmbH, Pliezhausen, Germany
Twin.tec PCR-Plates	Eppendorf AG, Hamburg, Germany

2.1.2. Software

1. EchoMRI™ Whole Body Composition Analyser Software (Echo Medical Systems, Houston, Texas, USA) was used to assess whole body composition parameters.

2. Measurements and calculations of echocardiography parameters were performed using Vevo 770^{TM} V2.3.0 (VisualSonics Inc., Toronto, Canada).

3. Histomorphometric analyses were performed by applying the Axiovision 4.2 computer-based quantification program (Carl Zeiss, Berlin, Germany).

4. ELISA measurements and data analysis were carried out using BioLinx™ (Dynatech Laboratories Inc., Sullyfield Circle, USA).

5. For *Real time*-PCR analysis, MasterCycler ep *realplex*^{2}S (MasterCycler-Software, Eppendorf AG, Hamburg, Germany) was used.

6. Statistical analysis was done using SPSS 11.0 (SPSS Inc., Chicago, USA) and Excel 2003 (Microsoft Corporation, USA).

7. Graphical representations were performed using Excel 2003 (under Windows XP, Microsoft Corporation, USA).

8. The thesis was written using Word 2003 (under Windows XP, Microsoft Corporation, USA).

2.2. Animal experiment

Animal handling and experiment were performed according to the European Union guidelines and approved by local authorities (animal experiments register No. G 0354/06, Landesamt für Arbeitsschutz, Gesundheitsschutz und technische Sicherheit Berlin).

2.2.1. Animals

Nine-week-old male and female Wistar rats (Charles River, Sulzfeld, Germany) with an initial body weight of 265-275 g and 210-220 g, respectively, were used in the study. Animals were housed in the animal facility of the Center for Cardiovascular Research (Hessische Str. 3-4, 10115 Berlin, Germany) under standard conditions with a 12-h dark/12-h light cycle, caged in pairs with free access to food and drinking water. Animals were monitored daily and body weight, food and drinking water consumption were monitored during the entire study.

2.2.2. Model of subtotal nephrectomy

The reduction of renal mass was achieved using the renal ablation method based on the protocol introduced by Amman et al. (92). The surgical procedure was performed by Dr. med. vet. Stephanie Krämer, who previously optimized the protocol, as described below, in order to standardize the method and to reduce postoperative complications. In the first surgical intervention, the right kidney was removed under inhalator anesthesia with isoflurane (Forene[®], Abbott AG, Wiesbaden, Germany). Anesthesia was induced by using an isoflurane concentration of 3.5% in the inhaled air, which was then reduced to 2% in the maintenance phase. Rats were positioned in left lateral decubitus, the coat was shaved in the region of renal bed and the tegument was disinfected with alcohol and Braunoderm (B.Braun Melsungen AG, Melsungen, Germany). An incision of the skin and underlying musculature was made 1 cm caudally from the costal arch. After opening the peritoneal cavity, the right kidney was exposed and carefully decapsulated without damaging the adrenal gland. The renal pedicle was clamped in the hilus and then ligated with a non-resolvable fibre right under the clamping site. The kidney was then cut off and weighed. The peritoneum with the muscular layer and skin were sutured separately. The wound was protected by disinfection with Braunoderm (B.Braun Melsungen AG, Melsungen, Germany) and application of a spray-plaster (Band-Aid[®], Ethicon GmbH, Norderstedt, Germany). After two weeks, under the same anesthesia protocol, rats underwent the second surgical intervention, in which two-thirds of the left kidney cortex were ablated. The left kidney was exposed as described above. After decapsulation, the two poles of the kidney were

successively cut off using a scalpel. The ablated renal mass corresponded approximately to two-thirds of the right kidney weight. Special care was taken not to injure the renal pelvis. To achieve haemostasis, a tissue adhesive (Spongostan Film® 200x70x0.5 mm, Johnson & Johnson, Norderstedt, Germany) was wrapped around the remaining renal tissue. The kidney was afterwards placed back into abdominal cavity. An antibiotic (Duphamox LA, Fort Dodge Veterinär GmbH, Würselen, Germany) was administered intraperitoneally to prevent infectious complications, and the wound was closed as described before. Analgesia was attained by administration of Fluonixin (Finadyne®, Essex Pharma GmbH, München, Germany). Two doses of 2.5 mg/kg body weight were applied i.m., first administration was intraoperative and the second after 12 hours. If necessary, additional analgesia was performed. To avoid hypothermia, during the intervention the rats were placed on a 39°C warmed pad (Gaymar Industries Inc., Orchard Park, USA). Animals assigned into the sham group underwent the same procedure, but with preservation of the renal mass (91).

2.2.3. Food and drinking water

All animals had free access to food and tap drinking water, food and water consumption being monitored daily during the entire experiment.

Table 2. Food content (Altromin No.1314 modified with 40% protein)

Diet ingredients	Content / 100g
Protein	40 g
Fat	5.5 g
Fibers	3.6 g
Ash	6.7 g
Arginine	2.4 g
Sodium	0.4 g
Calcium	0.8 g
Phosphorus	0.7 g
Vitamin A	1500 I.E.
Vitamin D_3	60 I.E.
Vitamin E	11 I.E.
Iron	0.01g

The animals were fed a normal breading diet (Altromin No.1311 with 22% protein, Altromin, Lage, Germany) during the first two weeks, until the second surgical procedure. Afterwards, all animals received a high protein diet (Altromin No.1314 modified with 40% protein, Altromin, Lage, Germany) in order to accelerate the progression of renal disease.

2.2.4. Drug administration

Depending on body weight and food and water intake, the appropriate amounts of drugs were added to food or drinking water of treated animals (91).

BAY 41-8543 (2-[1-[(2-fluorophenyl)methyl]-1H-pyrazolo[3,4-b]pyridin-3-yl]-5(4-morpholinyl)-4,6-pyrimidinediamine) is a novel haem-dependent NO-independent stimulator of soluble guanylate cyclase. Previous studies showed that sGC stimulators induce potent relaxation of systemic and pulmonary arteries and have antiproliferative effects on VSMC and antiaggregant effects on platelets (93). The dosage of BAY 41-8543 administered p.o. was 10 mg/kg body weight and was added in the food starting from the second week after subtotal nephrectomy. This dosage was previously described to induce a sufficient and constant blood pressure reduction in spontaneously hypertensive rats (65). The calculated amount of drug was added to 1 kg flour of the rat chow and mixed evenly. Then, 600 ml fresh tap water was added to the mixture and mixed until a homogeneous dough developed. The dough was then rolled out about 1 cm thick and shaped by means of a biscuit mold. The biscuits were put on a metal grid and air-dried. BAY 41-8543 was generously provided by Dr. Johannes-Peter Stasch, Pharma Research Center, Bayer AG, Wuppertal, Germany.

Hydralazine (Hydralazine hydrochloride, Sigma-Aldrich GmbH, Steinheim, Germany) was administered in fresh tap drinking water starting from the second week after renal ablation. The dosage used was 15 mg/kg body weight/day in females and 5 mg/kg body weight/day in males. This dosage was chosen because it reduced and maintained systolic blood pressure at levels comparable with those of sham-operated rats. Hydralazine is a potent arteriolar vasodilator, which induces relaxation of vascular smooth muscle cells. Although the mechanism of action is not completely understood, there is evidence that hydralazine inhibits calcium release from the vascular smooth muscle cell sarcoplasmic reticulum by blocking inositol triphosphate (IP3)-calcium release, thus reducing the calcium turnover in the cell (94).

2.2.5. Experimental design

Male (M) and female (F) Wistar rats were randomized and allocated to subtotal (5/6) nephrectomy (SNX) or sham operation. Initial body weight, systolic blood pressure and whole body composition were determined (basal values). After 5 days of adaptation, the animals underwent subtotal nephrectomy or sham operation (as described above). Subtotally nephrectomised rats were then randomized into untreated groups, BAY 41-8543-treated (SNX+BAY) and hydralazine-treated (SNX+Hydr) groups, respectively. Since previous studies showed that subtotally nephrectomised rats present a higher mortality during the experimental period, an increased number of rats were allocated to these groups so that in the end, all study groups would be equilibrated. Table 3 shows the distribution of the study groups, with the number of rats allocated to each group.

BAY 41-8543 and hydralazine treatments were started one week after complete surgery, allowing the animals a recovery period in which food and water consumption normalized. Systolic blood pressure, heart rate and whole body composition were assessed at weeks 0, 4, 12 and 18 during the study. At weeks 2, 6, 10, 14 and 18 after renal mass ablation, the animals were housed in metabolic cages and 24 hours total protein excretion was measured. At the end of the experiment, 18 weeks after subtotal nephrectomy, the animals were sacrificed and blood samples, kidney and aorta were harvested for further analyses (91).

Table 3. Study design according to sex, surgical procedure and treatment.

Groups	Number	Total
F-Sham	n=5	
F-SNX	n=12	
F-SNX+BAY	n=12	$N_{total}=39$
F-SNX+Hydr	n=10	
M-Sham	n=5	
M-SNX	n=12	
M-SNX+BAY	n=12	$N_{total}=39$
M-SNX+Hydr	n=10	

2.3. Harvesting of materials

2.3.1. Urine collection

For urine collection, the animals were individually housed in metabolic cages for 24 hours, with free access to food and drinking water. The metabolic cages are equipped with a special funnel and cone design that effectively separates urine from feces and food rests. In order to avoid excessive bacterial growth leading to changes in analysed parameters, 100 µl Penicillin/Streptomycin (10000 U/10000 µg/ml) were pipetted into the urine collector tube. 24-hour urine was collected, centrifuged for 10 min at 14000 rpm to remove particulate matter and frozen at -20°C for later measurements.

2.3.2. Blood and organ removal

At the end of the experiment, the animals were anesthetized with isoflurane, as described in the surgery protocol, and sacrificed by exsanguination. The animals were fixed in dorsal decubitus and a U-shaped incision was made from pelvis to both costal arch endings. Caudal abdominal aorta was cannulated and blood was drawn until heartbeat stopped. Blood samples were collected in EDTA-coated tubes and placed on ice until further handling. Immediately, ice-cold phosphate-buffered saline (PBS) was injected via the same cannula, until the heart began to beat again. The inferior vena cava was cut caudally to renal veins to ensure the drainage. The animals were then perfused under constant pressure with 120 ml ice-cold PBS. The perfused kidneys were removed, thoracotomy was then performed and the descending thoracic aorta was harvested. All organs were stored on ice in 50 ml ice-cold PBS until further processing. Blood samples were centrifuged for 10 min at 3000 rpm, 4°C, aliquoted according to analysed parameters, e.g. creatinine, urea, cholesterol, triglycerides and cGMP, and frozen at -20°C. For cGMP measurement 20 µl IBMX 5mM (Alexis GmbH, Grünberg, Germany), a non-specific phosphodiesterases inhibitor, was added to 980 µl plasma in order to block cGMP degradation. Kidney and transverse sectioned fragments of thoracic aorta were fixed in Carnoy solution (60% ethanol, 30% chloroform and 10% acetic acid) or frozen in liquid nitrogen and stored at -80°C for mRNA analyses.

2.4. Measurements

2.4.1. Systolic blood pressure and heart rate

Systolic blood pressure was measured in trained conscious animals by non-invasive tail cuff plethysmography. The animals were fixed in a dark acryl glass pipe that was maintained at a moderate temperature in an ambient chamber. After 5 min acclimatization, a seal with an integrated sensor was put around the rat's tails about 1 cm before the tail root, inflated and three measurements were made, whose values were averaged. In order to avoid misleading high values caused by stress, the animals were accustomed to the procedure before the actual start of the experiment.

2.4.2. Urinary protein excretion

In order to determine proteinuria, 24h urine was collected as described before. Total urinary protein was measured by pyrogallol red-molybdate colorimetric method (Fluitest® USP, Biocon Diagnostik, Marienhagen, Germany). The test principle is based on the binding of pyrogallol red-molybdate complexes to proteins, thus causing a shift of the absorbance peak to 600 nm. Due to the presence of detergents in the reagents, different types of proteins give similar recoveries. Therefore, the color intensity is directly proportional to the total protein concentration in the sample. Standard dilutions with protein concentrations between 0 and 5 g/l and urine sample dilutions (1:2 to 1:32 in 0.9% NaCl solution) were prepared. 10µl standards and samples were pipetted into a 96 well microplate and 350 µl reagent was added into each well. All measurements were done in duplicate. After 10 min incubation time, the absorbance (A) of the developed colour was assessed at 570 nm using the plate reader. The daily urinary protein excretion was calculated as follows:

Urinary Protein Excretion (mg/24h) = A_{Sample} / $A_{Standard}$ x Urine Volume (ml) x Dilution.

2.4.3. Renal function

Plasma and urine creatinine levels, as markers of renal excretory function, as well as hematocrit, reflecting the renal endocrine erythropoietin-producing capacity, were determined. Plasma and urine creatinine concentrations were measured with a Roche Modular (Roche/Hitachi, Roche Diagnostics, Mannheim, Deutschland) using the Jaffé method, which is based on the reaction between creatinine and picric acid in an alkaline medium with formation of yellow-orange colour complexes. The creatinine concentration is directly proportional to the

developed color intensity that is photometrically measured. Creatinine clearance was calculated as follows:

Clearance$_{Creatinine}$ = (Creatinine$_{Urine}$ x Urine volume) / (Creatinine$_{Plasma}$ x 1440 min),

where 1440 min represents the urine collection time. The hematocrit was measured as percent of blood cells (sediment) in the blood sample after 10 min centrifugation at 3000 rpm, 4°C.

2.4.4. Histology

Following 2.5 h fixation in Carnoy solution, thoracic aorta and renal cortex sections were kept overnight in 100% ethanol, 1 h in xylene (J.T.Baker, Deventer, Holland) and then embedded in paraffin. The paraffin-impregnated tissues were then poured in blocks and cut after hardening in 3-4 μm thick sections. Before staining, the slides were deparaffinized in xylene and descending alcohol row. For immunohistology, the slides were boiled in citrate buffer (pH 6.5) in a steamer at 96°C for 5 min and preserved, after cooling, in distilled water until further processing.

2.4.4.1. Periodic acid Schiff (PAS) staining

The following solutions were first prepared for this staining:

- Alcoholic periodic acid solution: 1 g periodic acid was dissolved in 30 ml distilled water and afterwards 70 ml 100% ethanol was added.
- Alcoholic disulphide solution: 0.5 g Potassium disulphide was dissolved in 30 ml distilled water. Then 70 ml 100% ethanol was mixed in the solution.
- Schiff´s reagent commercial mixture (Merck, Darmstadt, Germany).

The deparaffinized slides were immersed into 1% periodic acid solution for 10 minutes. After washing the slides in tap water twice for 5 minutes, they were incubated at 40°C for 20 minutes in previously heated Schiff`s reagent. Then the slides were dipped shortly in disulphide solution, washed for 10 minutes in tap water and counterstained 5 minutes in Mayer´s hematoxylin. Afterwards the slides were blued 10 minutes in tap water, transferred through ascending alcohol raw and finally covered up with Shandon-Mount™ (Anatomical Pathology International, Runcorn, United Kingdom).

Staining result: nuclei = blue-black

cytoplasm = pink

connective tissue = blue

acid mucopolysaccharides = bright magenta.

2.4.4.2. Hematoxylin-eosin (HE) staining

Following deparaffinisation, the slides were brought for 2 min into Meyer's hematoxylin solution and then blued for 5 min in tap water. The slides were transferred afterwards into 1% eosin solution for 3 min, washed in distilled water, subsequently dehydrated in ascending alcohol dilutions and mounted with Aquatex® (Merck, Darmstadt, Germany).

Staining result: nuclei = blue-violet

connective tissue = pink

muscle = red

erythrocytes = bright red.

2.4.4.3. Weigert´s resorcin-fuchsine staining of elastic fibers

Deparaffinised slides were immersed in Weigert´s resorcin-fuchsine commercially available solution for 15 min at 40°C. After washing in distilled water, the slides were dehydrated and mounted with Aquatex®.

Staining result: elastic fibres – violet.

2.4.4.4. Immunohistological staining

PCNA (proliferating cell nuclear antigen), Collagen I and ED1 (macrophage marker) were evaluated using the HRP (horseradish peroxidase) immunohistological staining method. This method is based on the binding of the primary antibody to an HRP-conjugated secondary antibody, this being responsible of the generated colour reaction in the presence of the AEC (3-Amino-9-Ethylcarbazol) substrate.

Before staining, Tris-buffered saline (TBS) had to be prepared. At first, two master solutions were set:

- Master solution A: 0.5 M Tris-solution, consisting of 60.55 g Tris (hydroxymethyl)-aminomethane /1 l distilled water.
- Master solution B: 1.5 M NaCl solution, consisting of 87.66 g NaCl/1 l distilled water.

The master solutions were kept at 4°C. TBS was set before use in a ratio of 1 part solution A + 1 part solution B + 8 parts distilled water and then adjusted to pH 7.6 with 0.5 M HCl.

Immunohistological staining was performed with the paraffin slides in a humidified chamber. The slides were first deparaffinised, rehydrated and cooked in citrate buffer as described above. Then the sections on the slides were circled with a tallow pencil (DAKO

Cytomation, Hamburg, Germany) and TBS buffer was added to each of them. The sections were then blocked with inactivated fetal calf serum for 30 minutes. Afterwards, the sections were incubated with the primary antibody:

- Mouse anti-rat PCNA (DAKO Cytomation GmbH, Hamburg, Germany) for 60 min, dilution 1:50;
- Goat anti-rat collagen I (Southern Biotech, Birmingham, USA) for 60 min, dilution 1:10;
- Mouse anti-rat ED1 (Serotec GmbH, Düsseldorf, Germany) for 60 min, dilution 1:100.

The antibodies were diluted with an antibody dilution medium (Dako Cytomation GmbH, Hamburg, Germany). There were three cuts on each slide. One cut served as negative control and was incubated only with antibody dilution medium instead of the primary antibody. The slides were then rinsed with TBS buffer. Then, incubation with the secondary antibody for 30 min followed:

- Anti-mouse-Ig/HRP (DAKO Cytomation GmbH, Hamburg, Germany) for PCNA and ED1 staining;
- Anti-goat-Ig/HRP (DAKO Cytomation GmbH, Hamburg, Germany) for collagen I staining.

The sections were rinsed again with TBS buffer and incubated for about 5 min with AEC substrate chromogen (DAKO Cytomation GmbH, Hamburg, Germany). The colour reaction was microscopically controlled. The sections were then rinsed with distilled water and counterstained with Mayer's hematoxylin for 1 min. Then they were washed with running tap water for 10 min and covered up with ImmuMount (Shandon, Pittsburgh PA, U.S.A.).

Staining result: positive area = reddish-brown

2.4.4.5. Morphological evaluation

For all morphological studies, the images were obtained by using a high-resolution camera connected to the microscope. The measurements were then performed in a blind fashion by applying a computer-based quantification program (Axiovision 4.2, Carl Zeiss Berlin, Germany).

2.4.4.5.1. Renal damage scores

The degree of renal injury was quantified by assessing the glomerulosclerosis and tubulointerstitial matrix scores. To this end, using light microscopy, the entire PAS stained slide was analysed at 400x magnification and each 5th glomerulus was evaluated. The glomerular

damage was quantified using the method described by El Nahas et al (1991), which classifies glomerular lesions into five stages (Table 4). The glomerulosclerosis index was calculated as follows:

$$GSI = [(0 \times no)+(1 \times n1)+(2 \times n2)+(3 \times n3)+(4 \times n4)] / (n0+n1+n2+n3+n4) \,,$$

where n0-n4 are the numbers of glomeruli with stage 0-4.

Table 4. Glomerular injury score

Stage	Histological aspect	Percent of injured glomerular tuft
0	Normal glomerulus	0%
1	Mesangial expansion with/without mesangial cell proliferation	<25%
2	Segmental sclerosis. Mesangial proliferation with partial involvement of capillary wall	>50%
3	Diffuse sclerosis. Extended capillary obliteration by proliferated mesangium or fibrotic scar.	<75%
4	Diffuse sclerosis with capillary collapse with/without capillary thromboses.	100%

Tubulointerstitial matrix score was determined in 15 randomly selected cortical areas per sample observed at 200x magnification. The relative degree of tubulointerstitial injury (i.e. interstitial fibrosis, tubular dilatation and atrophy, and inflammatory infiltration) was expressed as percentage of the affected area in relation to total area analysed.

2.4.4.5.2. Glomerular volume

In order to evaluate the degree of glomerular hypertrophy, as a marker of hyperfiltration, the volume of thirty glomeruli for each animal was assessed using the Weibel and Gomez method. First, the glomerular cross-sectional area (A_G) was obtained by tracing the glomerular tuft contour at 400x magnification. To ensure the maximum diameter, only glomeruli cross-sectioned at their vascular pole and without pronounced fibrotic lesions were measured. The glomerular tuft volume (V_G) was then calculated according to the formula:

$$V_G \ (\mu m^3) = \beta/k \times (A_G)^{1.5}$$

where β=1.38 is the shape coefficient for spheres (the ideal shape of glomeruli) and k=1.1 is the size distribution coefficient (91).

2.4.4.5.3. Aortic histomorphometric parameters

Lumen diameter and area as well as media cross sectional area of aorta were evaluated in HE-stained sections of descending thoracic aorta at 25x magnification. To avoid errors due to tissue deformation during embedding, the aortic lumen and external media perimeter were measured by tracing it with the cursor. Aortic lumen diameter and area as well as total area (without adventitia) were calculated using the following geometrical formulas:

$$D_{Lumen} = P_{Lumen} / \pi$$

$$A_{Lumen} = P_{Lumen}^{2} / 4\pi$$

$$A_{Total} = P_{Media}^{2} / 4\pi$$

where *D*=diameter, *P*=perimeter, *π*=Pi constant=3.14 and *A*=area. Media cross sectional area was calculated as the difference between total and lumen area of aorta. Intima and media thickness of aortic wall were measured on the same slides at 400x magnification on four opposite sites of the aortic wall, randomly selected, in order to minimize the effects of cutting plan. The thickness of intima and media (distance between elastica interna and externa) was measured at the same level and the average value for each animal was calculated (91). Aortic wall remodelling was further characterized by computing the intima-media and media-to-lumen ratio as follows:

Intima-Media ratio = Intima thickness / Media thickness and

Media-to-Lumen ratio = Media area / Lumen area.

2.4.4.5.4. Aortic collagen I and elastin content

To quantify the collagen I and elastin content of the aortic wall, immunohistologic collagen I and Weigert´s resorcin-fuchsin stainings of transverse sections of descending thoracic aorta were used. The entire section of aortic wall was analysed at 200x magnification on successive microphotographs. Collagen I and elastin content of aortic wall were expressed as percent of positive stained area of the examined aortic media area, the final content of aortic collagen I or elastic fibers being represented by the mean of the values obtained.

2.4.4.5.5. Aortic PCNA and ED-1 expression

Aortic PCNA and ED-1 staining served to investigate aortic VSMC proliferation and macrophage infiltration, respectively. Results were expressed as number of PCNA-positive cells

per total aortic media cross-section and number of ED-1-positive cells per total aortic cross-section.

2.4.5. *Enzyme-linked immunosorbent assay (ELISA)*

The plasmatic concentration of cGMP was determined using a cGMP competitive enzyme immunoassay system (Amersham, Freiburg, Germany). The kit includes novel lysis reagents in order to facilitate simple and rapid extraction of cGMP from cells. Lysis reagent 1 hydrolyses cell membranes to release intracellular cGMP. Lysis reagent 2 sequesters the key component in lysis reagent 1 and ensures that cGMP is free for subsequent analysis. The assay is based on competition between unlabelled cGMP (from samples) and a fixed quantity of peroxidase-labelled cGMP for a limited number of binding sites on a GMP-specific antibody.

The assay buffer working solutions and working standards (0, 2, 4, 8, 16, 32, 64, 128, 256, 512 fmol/well) were prepared according to the manufactur´s instructions. 10 µl acetylation reagent was added to 100 µl standards and samples. 100 µl rabbit anti-cGMP antibody was added to all wells precoated with donkey anti-rabbit IgG except the blank and NSB (non-specific binding) wells. Then, 50 µl standards or samples was pipetted into the appropriate wells. 150 µl assay buffer were pipetted into the NSB wells. The plate was incubated at 3-5 °C for 2 hours. Then, 100 µl diluted peroxidase-labelled cGMP conjugate was added to all wells except the blank and the plate was incubated at 3-5 °C for 1 hour. Then all wells were aspirated and washed with washing buffer. Immediately, 200 µl tetramethylbenzidine substrate was pipetted into all wells. The plate was fixed on a microplate shaker for exactly 30 min at room temperature. Finally, 100 µl of 1 M H_2SO_4 was added to all wells to block the reaction prior to end point determination. The optical density was read at 450 nm within 30 min. Finally, the concentrations were computed according to the standard curve.

2.4.6. *mRNA analyses*

2.4.6.1. RNA isolation by Trizol

Total RNA was extracted by using Trizol Reagent according to the manufacturer's instructions. 20-50 mg tissue was transferred into 1 ml Trizol reagent and homogenized with the homogenizer for 30 sec. The samples were then incubated at room temperature for 5 min. 200 µl chloroform (Merck, Darmstadt, Germany) was added. After 15 sec vigorously vortexing, the mixture was incubated at room temperature for 3 min and then centrifuged at 14000 rpm and 4°C for 15 min. RNA remains exclusively in the upper aqueous phase. The aqueous phase was

transferred carefully into a fresh tube (about 400-500 µl) and the remainder was discarded. 500 µl isopropyl alcohol (J. T. Baker, Deventer, Holland) was added. The sample was mixed by gently swivelling, incubated for 10 min at room temperature and then centrifuged again at 14000 rpm and 4°C for 10 min. The supernatant was removed and the remaining RNA pellet was washed with 1 ml 75% ethanol (Merck, Darmstadt, Germany) and then centrifuged at 14000 rpm and 4°C for 5 min. The supernatant was removed and the RNA pellet was air-dried in laminar flow for 5-10 min. Subsequently the RNA pellet was dissolved in 10 µl DEPC-treated water and incubated at 60°C in the thermal mixer for 10 min to ensure total resuspension.

Two investigation procedures for examination of the quality and concentration of isolated RNA content were performed. The quality of the RNA was analysed using 2% agarose gel electrophoresis. 1 µl RNA was dissolved in 9 µl DEPC-treated water. Then 8 µl bromine-phenol-blue (Carl Roth GmbH, Karlsruhe, Germany) was added and the sample was pipetted into the gel pockets. The gel was run at 100 volts for 1 hour. Two bands, 18S and 28S ribosomal RNA, can be seen under ultraviolet light. The RNA concentration in the sample was spectrophotometrically quantified. 1 µl RNA was mixed with 99 µl DEPC-treated water. The zero value of the spectrometer was set with DEPC-treated water. The sample was measured at a wavelength of 260 nm against zero. RNA concentration was adjusted to 0.5 µg/µl with DEPC-treated water. RNA samples were kept at -80°C until further analyses.

2.4.6.2 Reverse transcription-polymerase chain reaction (RT-PCR)

RT-PCR is a highly sensitive method for determining gene expression at the RNA level and for quantifying the strength of gene expression. "Two-step" RT-PCR was used. A cDNA copy is created with reverse transcriptase from the RNA PCR Core kit (Roche, Applied Biosystems, New Jersey, USA). Reverse transcription was carried out in a thermocycler using the following conditions: 25°C for 10 minutes, 42°C for 45 min, 95°C for 5 min, 4°C continuously. The cDNA obtained in this reaction was then used for the subsequent PCR.

2.4.6.3 Polymerase chain reaction

PCR is a method for oligonucleotide primer-directed enzymatic amplification of a specific DNA sequence of interest. The PCR product is amplified from a DNA template using a heat-stable DNA polymerase and an automated thermocycler by repeating 30 or more cycles of denaturing, annealing of primers and polymerization.

Table 5. Mixture of reverse transcription components

Components	Volume (µl)
$MgCl_2$	4
10xPCR buffer	2
DEPC-treated water	2
dGTP	2
dATP	2
dTTP	2
dCTP	2
RNase inhibitor	1
MuLV reverse transcriptase	1
Random hexamers	1
RNA (0,5µg/µl)	1

Quantitative analyses of the genes of interest were performed with a MasterCycler System using the Real-time PCR method. The amount of PCR product increases logarithmically in the first few PCR cycles before reaching a plateau. Real-time PCR refers to the continuous monitoring of the progress of the amplification during the whole PCR reaction and allows measurements to be made during the log-linear phase of a PCR. Utilization of a dsDNA-binding dye, SYBR Green I (Quiagen, Hilden, Germany), is more specific, since it only fluoresces when bound to dsDNA. The MasterCycler System typically measures fluorescence once every cycle, to monitor the increase in PCR product formation.

Table 6. Mixture of PCR components

Components	Volume (µl)
QMix	5
Primer (sense)	0.75
Primer (antisense)	0.75
DEPC-treated water	1,5
cDNA	2

Therefore, the cDNA obtained after reverse transcription was diluted 1:2 in DEPC-treated water and then a mixture of the reaction components was prepared as shown in table 6. For Real-time PCR, 10 µl of the mixture was used and all samples were measured in duplicate.

The MasterCycler System is capable of providing sequence confirmation of the amplified product by melting curve analysis, thus excluding unspecific products or primer-dimers. Each dsDNA product has its own specific melting temperature (Tm), determined by the guanine/cytosine base pair content.

Table 7. Real-time PCR program

Steps	Temperature	Time (seconds)	Fluorescence measurement	
Initial denaturizing	95°C	120		
Denaturizing	95°C	10		50 cycles
Annealing	Primer-dependent	10		
Elongation	72°C	10	Yes	
Melting curve	65°C-95°C	1200	yes	

Relative mRNA expression was calculated using a relative quantification method that is based on the relative expression of a target gene versus a reference gene, β-actin in this study. Amplification is described as $N=N_0 \; x \; E^{\Delta CP}$ (N = number of amplified molecules; N_0 = initial number of molecules; E = amplification efficiency; ΔCP = crossing point deviation expressed as $\Delta CP=CP_{Target} - CP_{\beta\text{-}Actin}$). In this quantification method, CP represents the "crossing point" defined as the point at which the fluorescence rises appreciably above the background fluorescence. The N_0 of samples was calculated using the above formula. Also, results were normalized to respective control groups corresponding to formula $N=N_0 \; x \; E^{\Delta\Delta CP}$.

Table 8. Primer sequences and conditions used for RT-PCR

Primer	Sequences	Annealing temperature
TIMP1	5´-CCTCTGTGGATATGTCCACA-3´ 3´-GGCAGTGATGTGCAAATTTC-5´	60°C
MMP2	5´-TGACGATGAGCTGTGGACTC-3´ 3´-CTGCTGTATTCCCGACCATT-5´	58°C
eNOS	5´-TCTACCGGGACGAGGTACTG-3´ 3´-CTGTCCTCAGGAGGTCTTGC-5´	60°C
iNOS	5´-GGGAGCCAGAGCAGTACAAG-3´ 3´-CATGGTGAACACGTTCTTGG-5´	60°C
sGC α	5´-GTGAAGAGCACCAAGCCTTC-3´ 3´-GGTCCAGCATGAAGTGGAAT-5´	61°C
sGC β	5´-GTGGTTTGCCAGAACCTTGT-3´ 3´-TTGACCAGCAATTTCCATCA-5´	62°C
PKG1	5´-GATGGAAGCTTGCCTAGGTG-3´ 3´-GCAAACGCTTCTACCACACA-5´	61.5°C
PKG2	5´-CGCTTTTGCCATGAAGTGTA-3´ 3´-GGAGAACACAGCTCCTCCAG-5´	61.5°C
ERα	5´-GTTGAAGCACAAGCGTCAGA-3´ 3´-AAGGTTGGCAGCTCTCATGT-5´	62°C
ERβ	5´-AAAGTAGCCGGAAGCTGACA-3´ 3´-CTGCTGCTGGGAGGAGATAC-5´	62°C
β Actin	5´-AGCCATGTACGTAGCCATCC-3´ 3´-ACCCTCATAGATGGGCACAG-5´	60°C

2.5 Statistical analysis

All values are expressed as mean ± standard error of the mean (SEM). Statistical analyses were performed with SPSS 11.0 by using Kruskal-Wallis and subsequent Mann-Whitney-*U* testing. A p value <0.05 was considered significant.

3. RESULTS

3.1. Model description

3.1.1. Food and water intake

Food and water consumption were monitored during the entire experiment, since their changes could influence the amount of ingested drugs. At the beginning of the study, the food intake was 25 g/day in males and 20 g/day in females, whereas water consumption was equal, 50 ml/day, for both sexes. After subtotal nephrectomy, an increase in water intake was seen in all SNX groups independent of treatment, reaching values of 70 ml/day in males and 65 ml/day in females at the end of the study. No changes in food intake were observed (91).

3.1.2. Body weight

Nine-week-old male and female Wistar rats were included in the study. They presented from study beginning a sexual dimorphism in body weight, females having a lower body weight than males, and this difference physiologically increases with age. At the end of the experiment, a significant body weight loss was observed in untreated SNX females compared to sham group (91), whereas no differences were seen between male groups.

Table 9. Effects of sex, subtotal nephrectomy (SNX), BAY 41-8543 (SNX+BAY) and hydralazine (SNX+Hydr) treatment on initial and final body weight (* $p<0.05$ vs. Sham; §§ $p<0.01$ and §§§ $p<0.001$ vs. females)

Groups	Initial body weight (g)	Final body weight (g)
F-Sham	236±1	329±7
F-SNX	245±3	304±5*
F-SNX+BAY	243±3	316±8
F-SNX+Hydr	229±3	300±9
M-Sham	370±9	581±11§§
M-SNX	364±5	573±13§§§
M-SNX+BAY	366±5	591±16§§§
M-SNX+Hydr	361±3	561±10§§§

3.1.3. Systolic blood pressure

Systolic blood pressure was monitored at weeks 0, 4, 12 and 18 in conscious, trained animals using the plethysmographic method. This enabled a better analysis of systolic blood pressure evolution after renal mass ablation. The model of mild uremia is characterized by an early increase in systolic blood pressure in both male and female untreated rats (M-SNX 137±4 mmHg and F-SNX 141±4 mmHg, 4 weeks after disease induction) when compared to sham-operated controls (M-Sham 124±6 mmHg and F-Sham 122±6 mmHg). After this time point, systolic blood pressure values remained relatively constant in male animals, whereas a progressive reduction was observed in females (91).
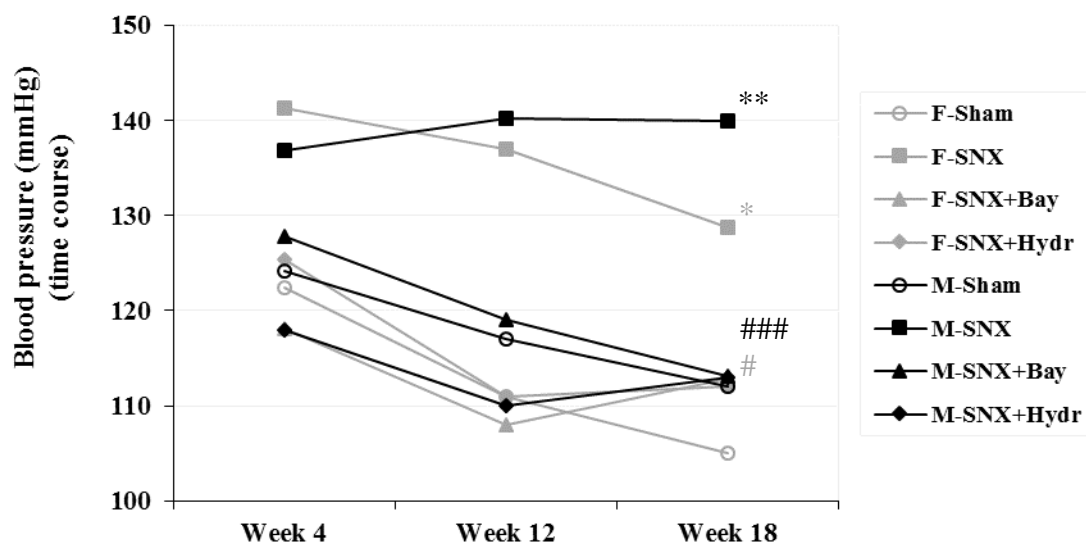

Figure 4. Effects of sex, subtotal nephrectomy (SNX), BAY 41-8543 (SNX+BAY) and hydralazine treatment (SNX+Hydr) on the time course of systolic blood pressure. Treatments were started 1 week after subtotal nephrectomy. Control animals underwent sham operation. Systolic blood pressure was measured in conscious animals using the plethysmographic method. (* $p < 0.05$ and ** $p < 0.01$ vs. Sham; # $p < 0.05$ and ### $p < 0.001$ vs. SNX).

Final systolic blood pressure was significantly higher in both untreated SNX groups (M-SNX 140±4 mmHg and F-SNX 129±4 mmHg) compared to control animals (M-Sham 112±5 mmHg and F-Sham 105±6 mmHg). BAY 41-8543 treatment induced a significant reduction of systolic blood pressure to 113±4 mmHg in males ($p < 0.001$) and 113±3 mmHg ($p < 0.05$) in females compared to untreated SNX groups. Hydralazine administration also lowered systolic blood pressure significantly to 113±3 mmHg ($p < 0.001$) in male and 112±1 mmHg ($p < 0.05$) in

female animals. Since there were no significant differences in the blood pressure lowering effect of BAY 41-8543 and hydralazine, the latter proved to be an appropriate control drug for the investigation of blood pressure-independent effects of BAY 41-8543. No significant sex-related differences in development of hypertension were observed, even if 18 weeks after disease induction female uremic rats exhibited slightly lower values of systolic blood pressure in comparison with corresponding male group.

3.1.4. Proteinuria

As illustrated in figure 5, after induction of mild renal insufficiency, a progressive increase in total urinary protein excretion was observed, indicating the degree of renal injury. At the end of the experiment, 18 weeks after renal ablation, SNX rats had a significantly higher proteinuria (M-SNX 191±35 mg/24h and F-SNX 472±63 mg/24h) in comparison with sham-operated groups (M-Sham 18±2 mg/24h and F-Sham 16±1 mg/24h). No effects on the degree of proteinuria could be observed in either BAY 41-8543-treated groups (199±47 mg/24h in males and 625±112 mg/24h in females) or in hydralazine-treated animals (males 148±20 mg/24h and females 497±104 mg/24h). All female SNX animals, independent of treatment, showed a significantly more accelerated progression of renal injury, as concluded from proteinuria, when compared to corresponding male groups (91).
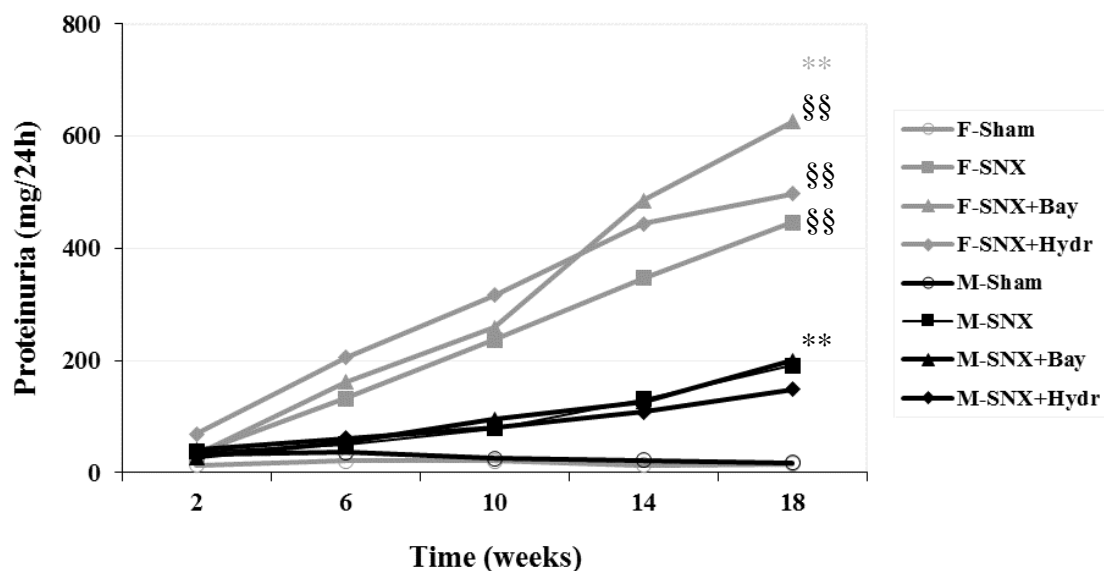

Figure 5. Impact of sex, subtotal nephrectomy (SNX), BAY 41-8543 (SNX+BAY) and hydralazine treatment (SNX+Hydr) on the time course of proteinuria. Treatments were started one week after SNX. Control animals underwent sham operation. Proteinuria was measured in 24 h-urine gained using metabolic cages. (** p<0.01 vs. Sham; §§ p<0.01 vs. males)

3.1.5. Histological markers of renal disease

3.1.5.1. Markers of glomerular injury

Compensatory glomerular hypertrophy, as reflected by glomerular tuft volume, was induced by SNX, independent of treatment, in both male (M-SNX +145 %, M-SNX+BAY +118 % and M-SNX+Hydr +134 %) and female (F-SNX +107 %, F-SNX+BAY +139 % and F-SNX+Hydr +124 %) animals in comparison with sham-operated groups (1368 ± 49 x10^3 µm³ in males and 1189 ± 53 x10^3 µm³ in females). The glomerular hypertrophic response was more pronounced in untreated SNX males than in females, a difference observed also in hydralazine-treated groups.
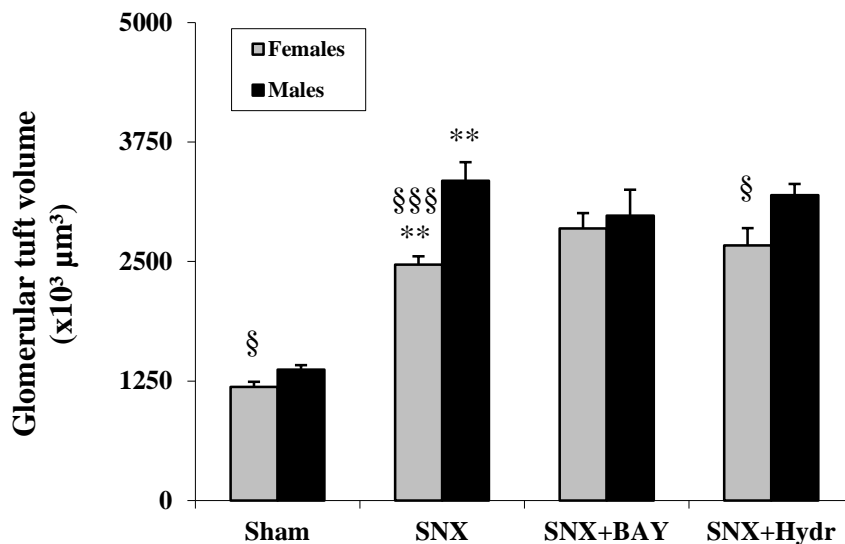

Figure 6. Effects of sex, subtotal nephrectomy (SNX), BAY 41-8543 (SNX+BAY) and hydralazine treatment (SNX+Hydr) on glomerular tuft volume 18 weeks after induction of mild renal insufficiency. Treatments were started one week after subtotal nephrectomy. Control animals underwent sham operation. (** $p<0.01$ vs. Sham; § $p<0.05$ and §§§ $p<0.001$ vs. males)

As shown in figure 7, mild uremia was characterized at glomerular level by mesangial and extracellular matrix expansion, which was quantified as glomerulosclerosis index (0.86 ± 0.14 vs. 0.09 ± 0.01 in males; 0.59 ± 0.08 vs.0.08 ± 0.02 in females). No beneficial effects of BAY 41-8543 (males 0.93 ± 0.19 and females 0.97 ± 0.16) or hydralazine treatment (males 0.76 ± 0.07 and females 0.79 ± 0.19) on the degree of glomerular injury were observed (91). Furthermore, no sex-related differences in glomerulosclerosis index were found.
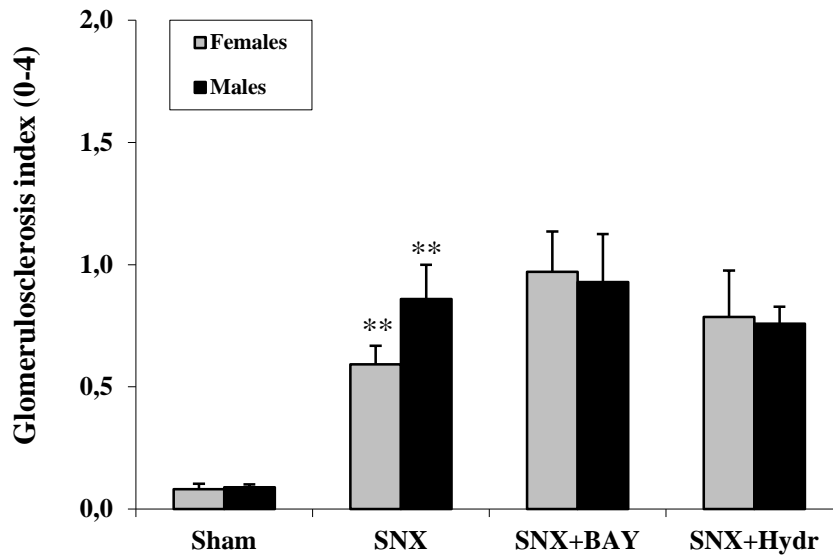
Figure 7. Influence of sex, subtotal nephrectomy (SNX), BAY 41-8543 (SNX+BAY) and hydralazine treatment (SNX+Hydr) on glomerulosclerosis index 18 weeks after induction of mild renal insufficiency. Treatments were started one week after subtotal nephrectomy. Control animals underwent sham operation. Glomerulosclerosis was scored on PAS-stained kidney sections. (** $p < 0.01$ vs. Sham)

3.1.5.2. Markers of tubulointerstitial damage

Tubulointerstitial injury (tubular dilatation and atrophy, inflammatory infiltration and interstitial fibrosis) accompanied the alterations seen in glomerular structure. As illustrated in figure 8, tubulointerstitial matrix score was significantly increased in all SNX male (M-SNX 39.2±8 %, M-SNX+BAY 40.7±9 % and M-SNX+Hydr 38.8±6 %) and female (F-SNX 38.8±4 %, F-SNX+BAY 38.7±8 % and F-SNX+Hydr 36.4±10 %) groups in comparison with sham-operated animals (M-Sham 0.7±0.3 % and F-Sham 0.5±0.2 %). No beneficial effects of BAY 41-8543, hydralazine treatment or protective effects of female sex on the development of tubulointerstitial damage were observed (91).

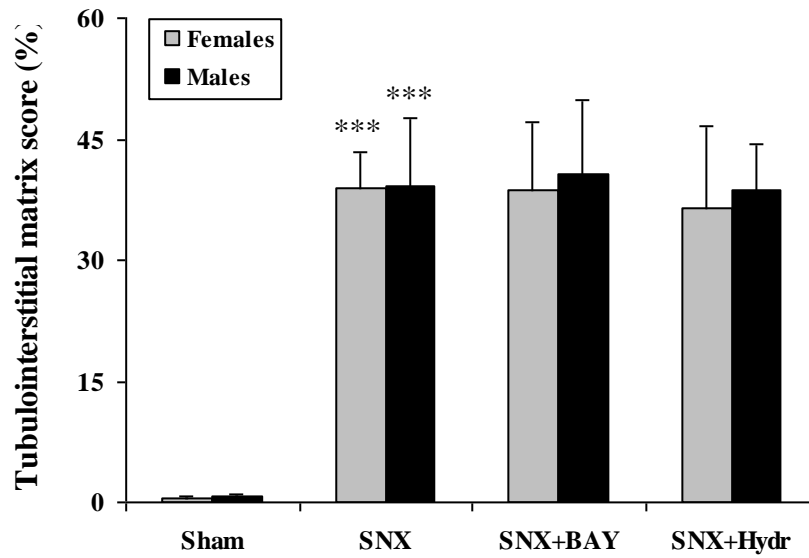Figure 8. Effects of sex, subtotal nephrectomy (SNX), BAY 41-8543 (SNX+BAY) and hydralazine treatment (SNX+Hydr) on tubulointerstitial matrix score 18 weeks after induction of mild renal insufficiency. Treatments were started one week after subtotal nephrectomy. Control animals underwent sham operation. Tubulointerstitial matrix expansion was scored on PAS-stained kidney sections. (*** $p<0.001$ vs. Sham)
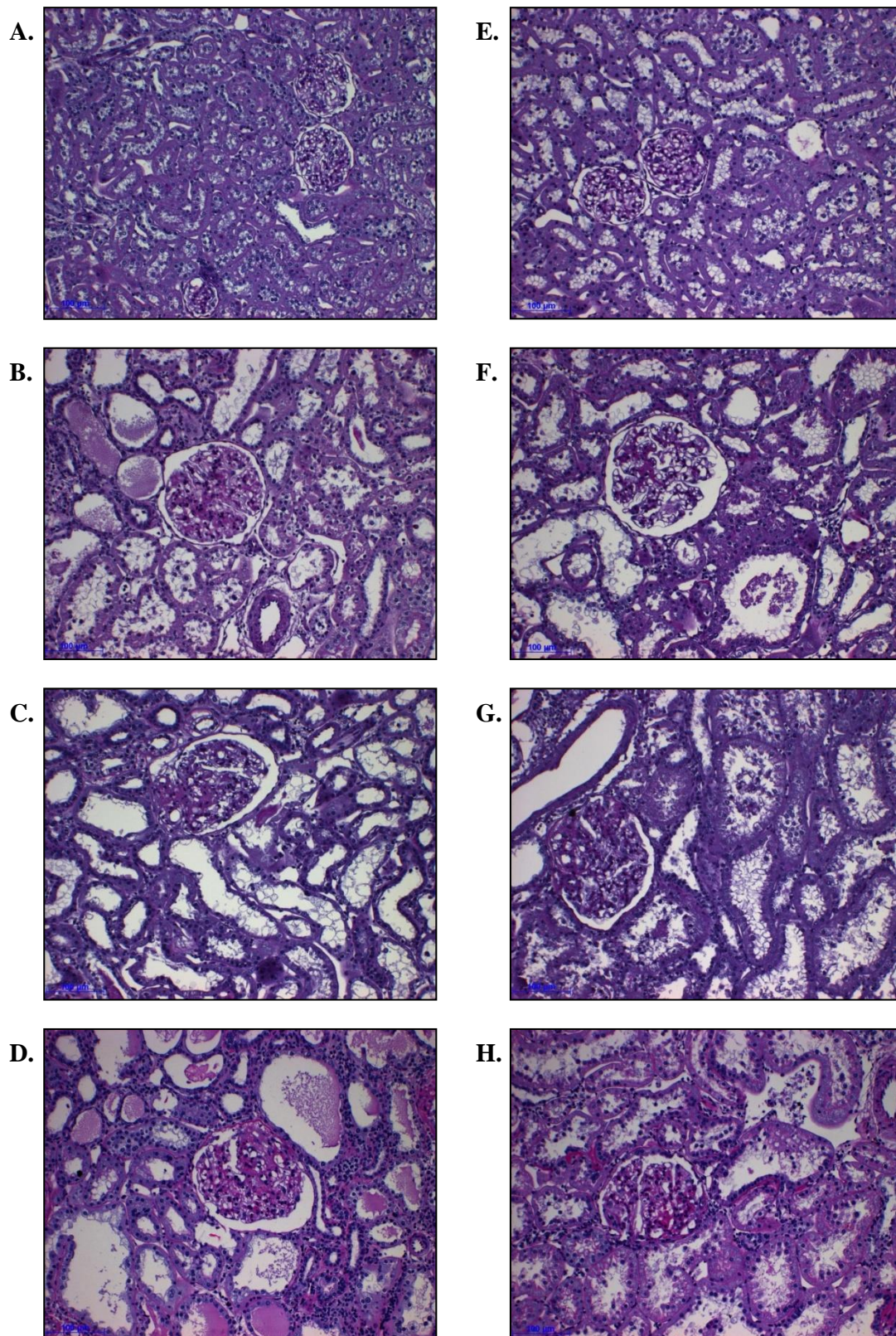
Figure 9. Representative histological images of PAS-stained kidney sections 18 weeks after induction of mild renal insufficiency in female and male sham-operated (A and E), SNX untreated (B and F), BAY 41-8543- (C and G) and hydralazine-treated (D and H). Treatments were started one week after subtotal nephrectomy. Magnification x200.

3.1.6. Parameters of renal function

Plasma creatinine levels, creatinine clearance and hematocrit were measured as indicators of renal excretory and endocrine function. As presented in table 11, SNX induced a significant increase of plasmatic creatinine and urea concentrations, whereas creatinine clearance, normalized to body weight, and hematocrit levels were significantly decreased (91). In concordance with the effects on proteinuria and histological markers of renal damage, treatment with BAY 41-8543 did not manage to improve renal function. Unexpectedly, a slight amelioration of some measured parameters was seen in hydralazine-treated animals. There were no sex-related differences observed for creatinine clearance, whereas the hematocrit reduction was more pronounced in male subtotally nephrectomised rats (M-SNX -17 % vs. F-SNX –3 %).

Table 10. Effects of sex, subtotal nephrectomy (SNX), BAY 41-8543 (SNX+BAY) and hydralazine treatment (SNX+Hydr) on renal excretory and endocrine function 18 weeks after induction of mild renal insufficiency. Treatments were started one week after subtotal nephrectomy. Control animals underwent sham operation. (** $p < 0.01$ vs. Sham; # $p < 0.05$ vs. SNX; § $p < 0.05$ and §§ $p < 0.01$ vs. males)

Group	Plasma creatinine (mg/dl)	Creatinine clearance (ml/min/100g BW)	Hematocrit (%)
F-Sham	0.34±0.02	0.65±0.03	49.4±1.3[§§]
F-SNX	0.78±0.04[**§]	0.30±0.02[**]	47.9±1.2
F-SNX+BAY	0.97±0.14	0.28±0.03	47.2±0.6
F-SNX+Hydr	0.60±0.06[#§]	0.44±0.05[#]	42.5±1.5[#§]
M-Sham	0.33±0.01	0.71±0.01	58.5±1.6
M-SNX	0.60±0.04[**]	0.38±0.04[**]	49.2±1.4[**]
M-SNX+BAY	0.83±0.14	0.31±0.04	49.5±1.5
M-SNX+Hydr	0.49±0.02[#]	0.46±0.02	48.4±1.9

3.2. Aortic remodelling

3.2.1. Aortic histomorphometric parameters

3.2.1.1. Lumen diameter

There were no significant changes of the lumen diameter of aorta thoracalis in untreated SNX groups compared to controls (1.86 ± 0.02 vs. 1.95 ± 0.03 mm in males and 1.60 ± 0.02 vs. 1.59 ± 0.02 mm in females). BAY 41-8543 and hydralazine treatment had also no effect on this parameter (M-SNX+BAY 2.00 ± 0.05 mm and M-SNX+Hydr 1.86 ± 0.04 mm; F-SNX+BAY 1.67 ± 0.03 mm and F-SNX+Hydr 1.68 ± 0.04 mm). The lumen diameter of aorta was significantly lower in females compared with males, independent of the study group, the difference being explained by the discrepancy in body size (91).

Figure 10. Influence of sex, subtotal nephrectomy (SNX), BAY 41-8543 (SNX+BAY) and hydralazine treatment (SNX+Hydr) on the lumen diameter of aorta thoracalis 18 weeks after induction of mild renal insufficiency. Treatments were started one week after subtotal nephrectomy. Control animals underwent sham operation. Aortic lumen diameter was measured on HE-stained slides. (§ $p < 0.05$, §§ $p < 0.01$ and §§§ $p < 0.001$ vs. males)

3.2.1.2. Media-to-lumen ratio

Media-to-lumen ratio was determined as a marker of vascular wall hypertrophy. Therefore, aortic cross-sectional lumen and media areas were measured on HE-stained sections. Since media cross-sectional area is dependent on the aortic dimensions, the augmentation of this parameter can be sometimes attributed to an increase in aortic diameter. Therefore, media-to-lumen ratio was used to detect hypertrophic modifications of the aortic medial layer, independent of aortic dimensions. Results are expressed as absolute and relative (% of control) values, the latter to allow comparison of aortic changes between sexes.

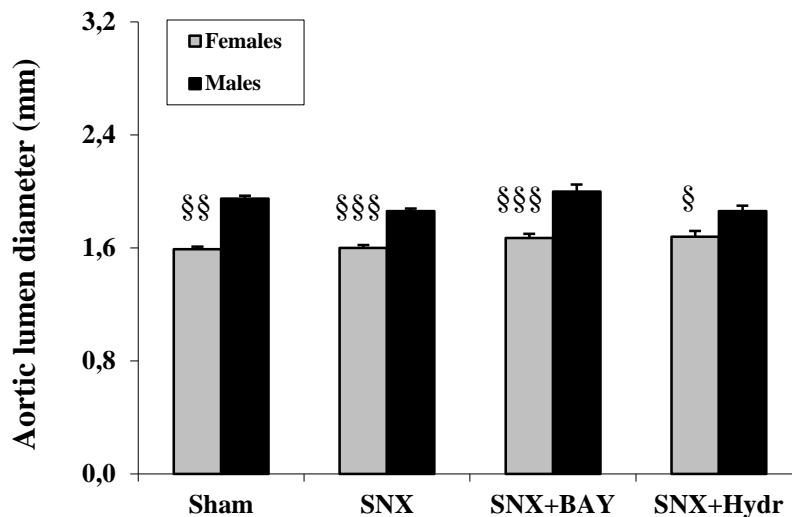Table 11. Effects of sex, subtotal nephrectomy (SNX), BAY 41-8543 (SNX+BAY) and hydralazine treatment (SNX+Hydr) on the aortic lumen and media cross-sectional area, and media-to-lumen ratio 18 weeks after induction of mild renal insufficiency. Lumen and media area of aorta thoracalis were measured on HE-stained slides at 25x magnification. (* $p<0.05$, ** $p<0.01$ and *** $p<0.001$ vs. Sham; # $p<0.05$ and ### $p<0.001$ vs. SNX; § $p<0.05$, §§ $p<0.01$ and §§§ $p<0.001$ vs. males)

Groups	Lumen Area (mm^2)	Media Area (mm^2)	Media-to-Lumen Ratio
F-Sham	$1.98\pm0.05^{\S\S}$	$0.60\pm0.03^{\S}$	$0.30\pm0.01^{\S\S}$
F-SNX	$2.02\pm0.06^{\S\S\S}$	$0.64\pm0.02^{\S\S\S}$	0.32 ± 0.01
F-SNX+BAY	$2.20\pm0.08^{\S\S\S}$	$0.64\pm0.02^{\S\S\S}$	$0.29\pm0.01^{\S}$
F-SNX+Hydr	$2.21\pm0.12^{\S}$	$0.71\pm0.05^{\S\S}$	$0.32\pm0.01^{\S}$
M-Sham	2.98 ± 0.08	0.73 ± 0.03	0.24 ± 0.01
M-SNX	$2.71\pm0.07^{*}$	$0.89\pm0.03**$	$0.33\pm0.01^{**}$
M-SNX+BAY	$3.16\pm0.17^{\#}$	0.83 ± 0.03	$0.27\pm0.01^{\#\#\#}$
M-SNX+Hydr	2.74 ± 0.12	1.01 ± 0.07	0.37 ± 0.01

As shown in table 13, mild renal insufficiency leads to a significant increase in aortic media cross-sectional area and media-to-lumen ratio only in male rats when compared to control groups. BAY 41-8543 treatment significantly lowered media-to-lumen ratio, while treatment with hydralazine failed to show any effect on this hypertrophic parameter. Thus, this study demonstrated for the first time that sGC-stimulator BAY 41-8543 exerts protective effects against uremic aortic remodelling. In female animals, neither mild renal insufficiency nor treatments with BAY 41-8543 or hydralazine influenced the aortic media-to-lumen ratio. Significant sex-related differences were observed between untreated SNX groups (figure 11), indicating pronounced hypertrophic remodelling of the aortic wall in male animals (91). These differences are blood pressure-independent since they are present among hydralazine-treated groups, too.
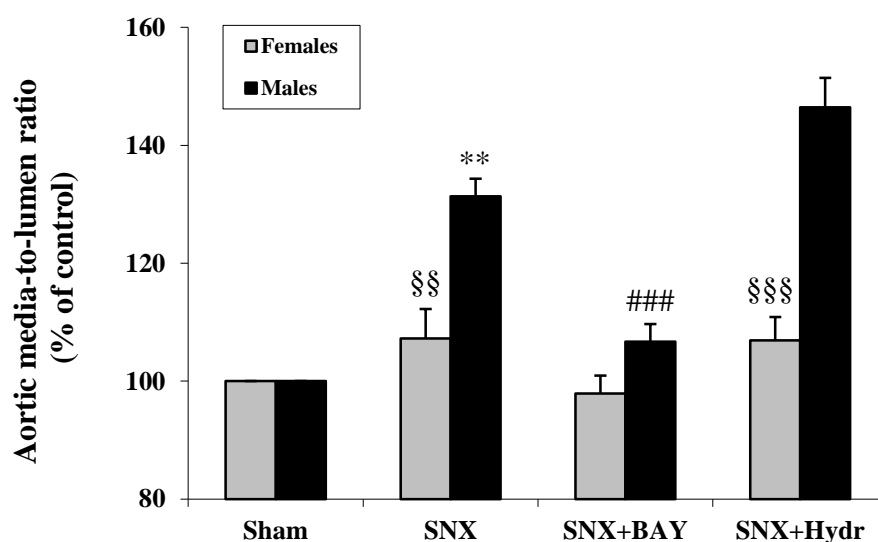

Figure 11. Impact of sex, subtotal nephrectomy (SNX), BAY 41-8543 (SNX+BAY) and hydralazine treatment (SNX+Hydr) on the media-to-lumen ratio of aorta thoracalis 18 weeks after induction of mild renal insufficiency. Treatments were started one week after subtotal nephrectomy. Sham-operated animals were used as controls. Aortic lumen and media cross-sectional areas were measured on HE-stained slides at x25 magnification. (** $p<0.01$ vs. Sham; ### $p<0.001$ vs. SNX; §§ $p<0.01$ and §§§ $p<0.001$ vs. males)

3.2.1.3. Media thickness and intima-media ratio

18 weeks after induction of mild renal insufficiency, a significant increase in media thickness of aorta was observed in male untreated SNX animals when compared to sham-

operated ones (131±3 vs. 103±1 µm, p<0.001). Female SNX rats showed only a slight and not significant thickening of aortic media (115±2 vs. 106±7 µm). Treatment with BAY 41-8543 significantly reduced aortic media thickness in both male (114±3 µm, p<0.1) and female groups (107±2 µm). Despite the lower blood pressure values, hydralazine-treated animals showed no decrease in aortic media thickness (130±2 µm in males and 121±2 µm in females). As presented in figure 12, significant sex differences in media thickening were observed in all SNX groups: untreated (127±3 % of control in males vs. 108±2 % of control in females, p<0.001), treated with BAY 41-8543 (males 111±3 vs. females 101±2 % of control, p<0.05) or with hydralazine (126±2 % of control in males vs. 114±2 % of control in females, p<0.01). Male animals developed more severe aortic hypertrophic remodelling.
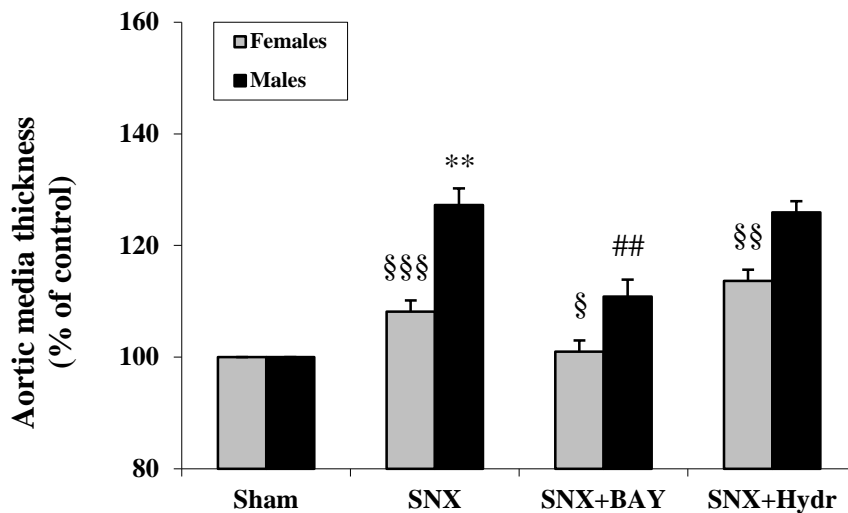
Figure 12. Effects of sex, subtotal nephrectomy (SNX), BAY 41-8543 (SNX+BAY) and hydralazine treatment (SNX+Hydr) on the media thickness of aorta thoracalis 18 weeks after induction of mild renal insufficiency. Treatments were started one week after subtotal nephrectomy. Sham-operated animals served as controls. Media thickness of aorta was measured on HE-stained slides at 400x magnification. (** p<0.01 vs. Sham; ## p<0.01 vs. SNX; § p<0.05, §§ p<0.01 and §§§ p<0.001 vs. males)

Figure 13. Representative histological pictures of aorta thoracalis wall 18 weeks after induction of mild renal insufficiency in female and male sham-operated (A and E), SNX untreated (B and F), BAY 41-8543 (C and G) and hydralazine-treated (D and H) animals. Treatments were started one week after subtotal nephrectomy. Aortic paraffin-embedded sections were HE-stained and analysed at 400x magnification.
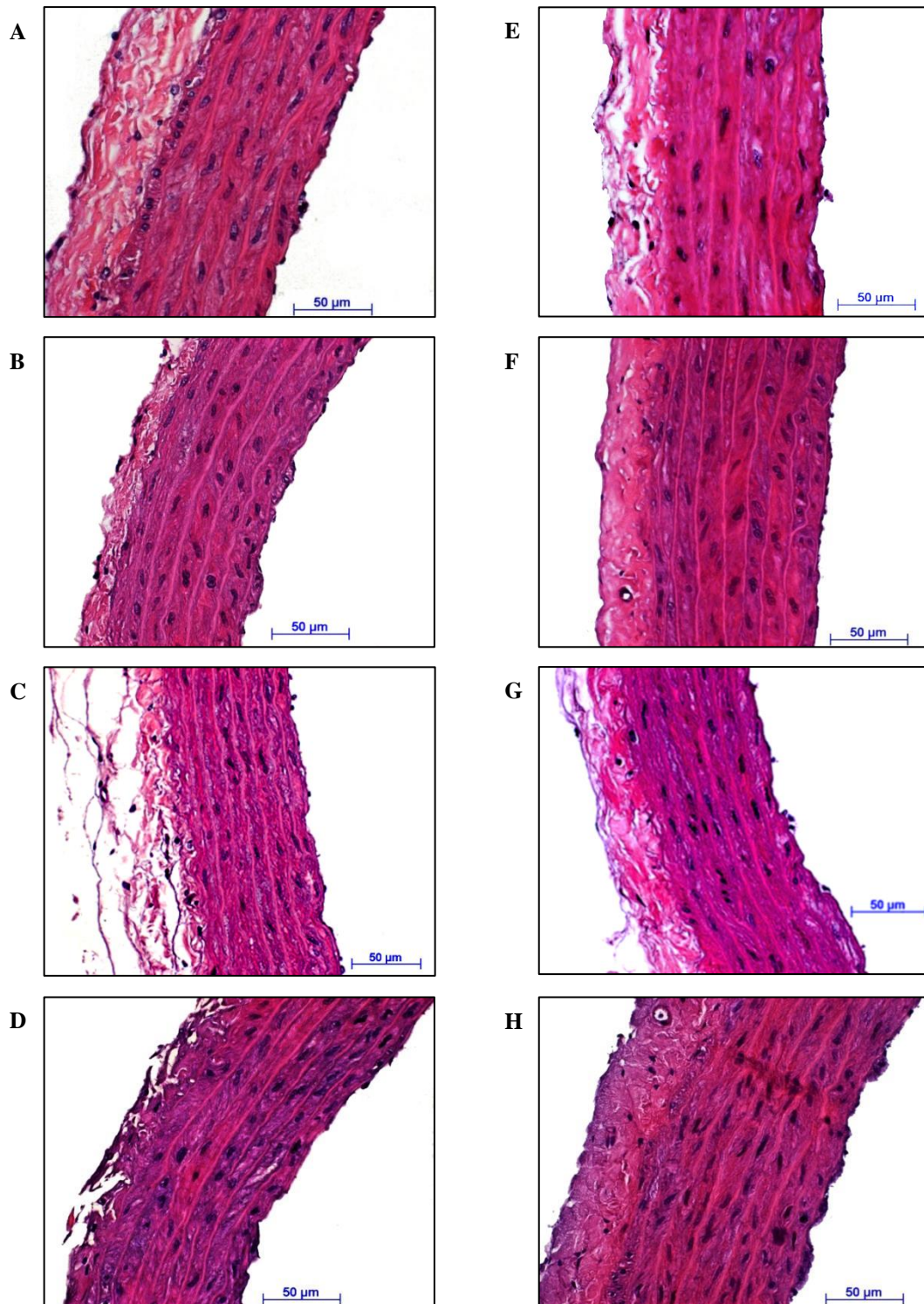
There was no intima proliferation observed 18 weeks after renal ablation (91). The intima-media ratio was found to be significantly reduced in male and female untreated SNX rats compared to corresponding sham groups (0.017 ± 0.0006 vs. 0.026 ± 0.0002 in males and 0.018 ± 0.0006 vs. 0.023 ± 0.0006 in females, $p<0.01$). This ratio was significantly ameliorated by BAY 41-8543 treatment (0.022 ± 0.0008 in males and 0.021 ± 0.0005 in females), but not by administration of hydralazine (0.018 ± 0.0004 in males and 0.018 ± 0.0007 in females, $p<0.001$ and $p<0.01$, respectively). Untreated SNX males showed a significantly more pronounced reduction of intima-media ratio than the corresponding female group (66.4 ± 2 vs. 79.6 ± 3 % of control, $p<0.01$), this sex-related difference being preserved also between hydralazine treated groups (68.2 ± 2 vs. 78.9 ± 3 % of control, $p<0.05$) (figure 14).
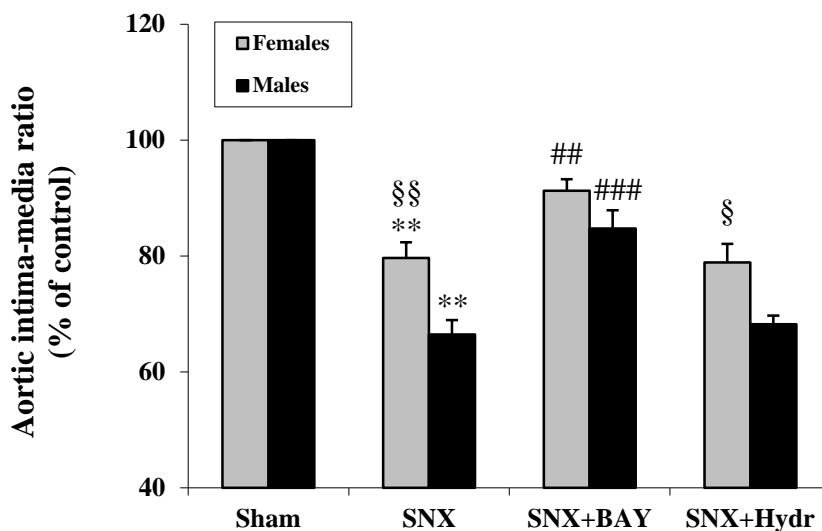
Figure 14. Impact of sex, subtotal nephrectomy (SNX), BAY 41-8543 (SNX+BAY) and hydralazine treatment (SNX+Hydr) on intima-media ratio of aorta thoracalis 18 weeks after induction of mild renal insufficiency. Treatments were started one week after subtotal nephrectomy. Sham-operated animals served as controls. Intima and media thickness of aorta were measured on HE-stained slides at 400x magnification. (*** $p<0.01$ vs. Sham; ## $p<0.01$ and ### $p<0.001$ vs. SNX; § $p<0.05$ and §§ $p<0.01$ vs. males)

3.2.2. Aortic VSMC proliferation

In order to investigate whether proliferation of vascular smooth muscle cells is involved in the observed aortic remodelling in our experimental model of mild renal insufficiency, we analysed the PCNA expression in aortic media using immunohistochemical staining. As shown in figure 15, untreated SNX males presented more PCNA-positive cells per aortic media cross-section than sham-operated ones (M-SNX +383 %; $p=0.05$). Compared to untreated SNX group, treatment with BAY 41-8543 significantly reduced the number of PCNA-positive cells (-79%, $p<0.05$), whereas hydralazine treatment showed only a minor effect (-27 %). In females, no significant differences were observed between study groups (F-SNX +83 %; F-SNX+BAY –26 % and F-SNX+Hydr –16 %). No sex-related differences were seen in either of the diseased groups (91).
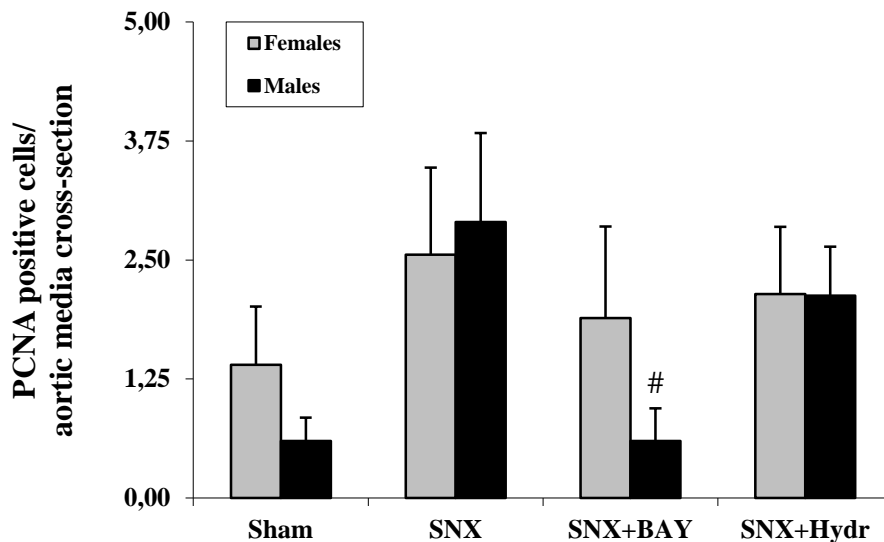
Figure 15. Effects of sex, subtotal nephrectomy (SNX), BAY 41-8543 (SNX+BAY) and hydralazine treatment (SNX+Hydr) on PCNA expression in the media layer of aorta thoracalis 18 weeks after induction of mild renal insufficiency. Treatments were started one week after subtotal nephrectomy. Sham-operated animals served as controls. Data are expressed as number of PCNA-positive cells per aortic media cross-section observed at 200x magnification. (# $p<0.05$ vs. SNX)

3.2.3. Aortic inflammatory infiltration

Immunohistological ED-1 staining of macrophages was performed in order to evaluate the chronic inflammatory infiltration of the aortic wall. Untreated SNX was associated with macrophage infiltration of the aortic wall, significant only in males (M-SNX +900 % and F-SNX +845 %) compared to corresponding sham groups (91). No significant effects of BAY 41-8543 treatment were observed (-23 % in males and –18 % in females), whereas hydralazine treatment reduced chronic inflammatory infiltration only in males (-75 % in males and +51 % in females) when compared to untreated SNX groups. There were no sex differences observed.

Figure 16. Influence of sex, subtotal nephrectomy (SNX), BAY 41-8543 (SNX+BAY) and hydralazine treatment (SNX+Hydr) on ED-1 positive cells infiltration of aorta thoracalis 18 weeks after induction of mild renal insufficiency. Treatments were started one week after subtotal nephrectomy. Sham-operated animals served as controls. Data are expressed as number of ED-1-positive cells per aortic cross-section observed at 200x magnification. (** $p < 0.01$ vs. Sham; # $p < 0.05$ vs. SNX)

3.2.4. Aortic extracellular matrix components

3.2.4.1. Collagen I

As shown in figure 17, mild renal insufficiency induced a significant increase in collagen I deposition in the media layer of aorta in both male (+112 %) and female (+110 %) untreated groups compared to sham-operated animals (7.6±0.7 % in males and 6.9±0.4 % in females). BAY 41-8543 treatment significantly inhibited the accumulation of collagen I in aortic media (-40 % in males and –35 % in females) in comparison with untreated SNX animals. Despite reducing blood pressure, treatment with hydralazine showed no beneficial influences (males –6 %, females +10%), thus proving that the anti-fibrotic effect of BAY 41-8543 is blood pressure-independent (91). Collagen I staining was found to be similar in both sexes, regardless of disease and treatments.
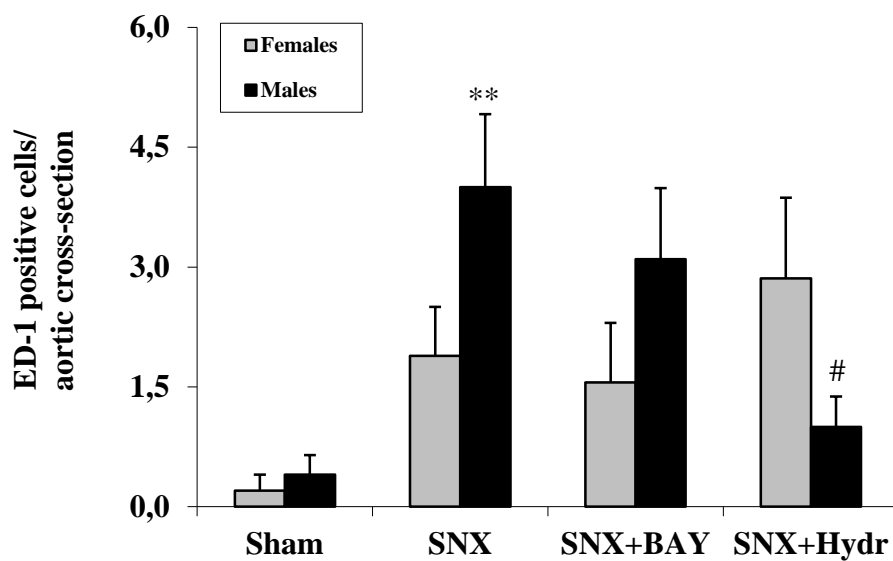

Figure 17. Effects of sex, subtotal nephrectomy (SNX), BAY 41-8543 (SNX+BAY) and hydralazine treatment (SNX+Hydr) on collagen I deposition in the media layer of aorta thoracalis 18 weeks after induction of mild renal insufficiency. Treatments were started one week after subtotal nephrectomy. Sham-operated animals served as controls. Data are expressed as % of positive area per aortic media cross-section measured at 200x magnification. (** $p<0.01$ vs. Sham; ## $p<0.01$ and ### $p<0.001$ vs. SNX)
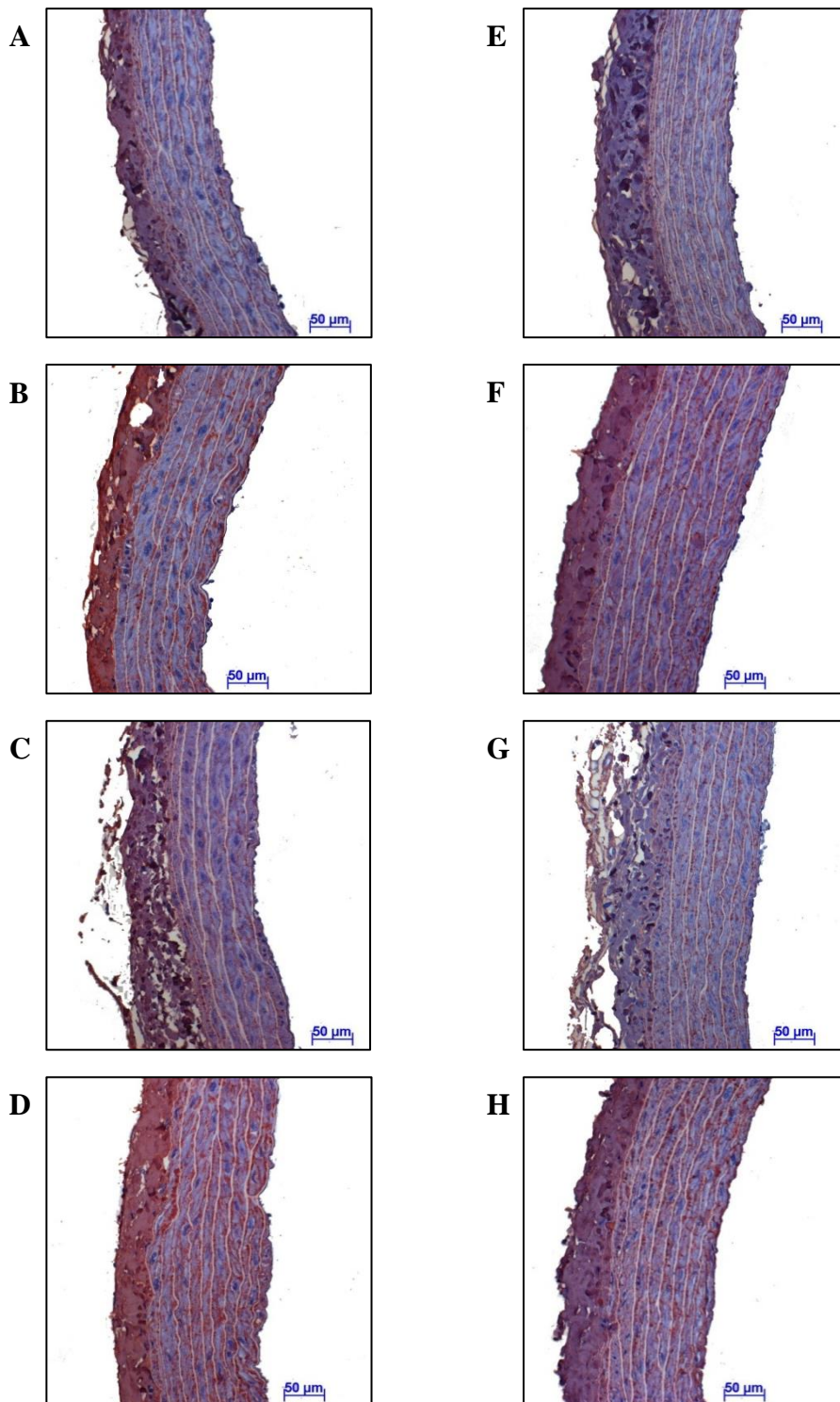
Figure 18. Representative histological pictures of collagen I staining of aortic wall 18 weeks after induction of mild renal insufficiency in female and male sham-operated (A and E), SNX untreated (B and F), BAY 41-8543 (C and G) and hydralazine-treated (D and H) animals. Treatments were started 1 week after subtotal nephrectomy. Magnification x200.

3.2.4.2. Elastin and elastin-to-collagen ratio

Aortic elastin protein expression was significantly down-regulated in untreated SNX groups (M-SNX –34 % and F-SNX –26%) in comparison with control animals (M-Sham 37.3±1.2 % and F-Sham 37.4±0.7 %). BAY 41-8543 treatment successfully prevented elastic fibre degradation (+34 % in males and +21 % in females), whereas no beneficial effects of hydralazine treatment were observed (+7 % in males and +6 % in females) when compared to untreated SNX animals. The elastin content of aortic media was slightly lower in male than in female untreated (p>0.05) and hydralazine-treated (p<0.05) groups.

Elastin-to-collagen ratio was calculated as an indirect marker of aortic wall stiffness. Mild renal insufficiency induced a marked reduction of this ratio (M-SNX -69 % and F-SNX –64 %) compared to control animals (M-Sham 5.1±0.6 and F-Sham 5.5±0.3). According to the beneficial effects on collagen I- and elastin-protein expression, treatment with BAY 41-8543 significantly increased the elastin-to-collagen ratio (+119 % in males and +80 % in females) in comparison with untreated SNX groups. No positive influence of hydralazine treatment was found (+13 % in males and –5 % in females) (91).
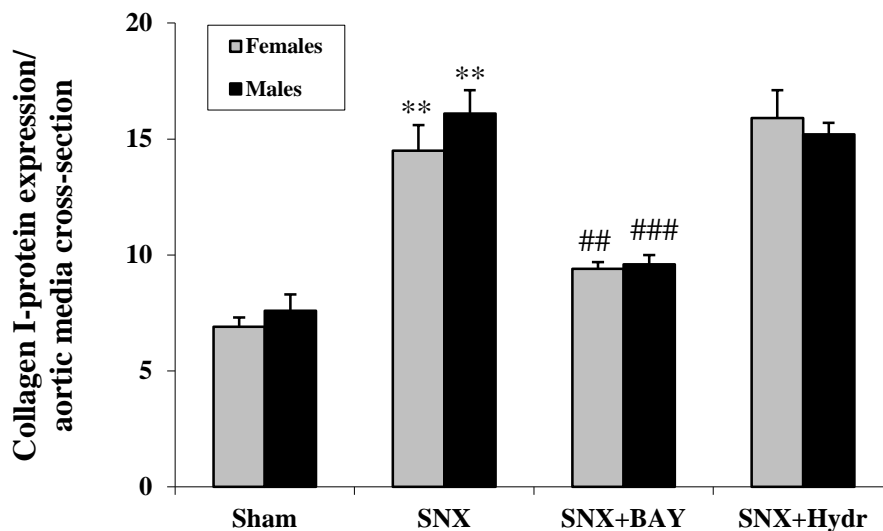
Figure 19. Effects of sex, subtotal nephrectomy (SNX), BAY 41-8543 (SNX+BAY) and hydralazine treatment (SNX+Hydr) on elastin deposition and elastin-to-collagen ratio in the media layer of aorta thoracalis 18 weeks after induction of mild renal insufficiency. Treatments were started one week after subtotal nephrectomy. Sham-operated animals served as controls. Elastin-protein levels are expressed as % of positive area per aortic media cross-section measured at 200x magnification. (** $p < 0.01$ vs. Sham; ## $p < 0.01$ and ### $p < 0.001$ vs. SNX; § $p < 0.05$ vs. males)

Figure 20. Representative histological images of elastin staining of aortic wall 18 weeks after induction of mild renal insufficiency in female and male sham-operated (A and E), SNX untreated (B and F), BAY 41-8543 (C and G) and hydralazine-treated (D and H) animals. Treatments were started one week after subtotal nephrectomy. Resorcin-fuchsin-stained aortic paraffin-embedded sections were analyzed at x200 magnification.

3.2.4.3. TIMP-1 mRNA relative expression

Aortic TIMP-1 mRNA expression was relativized to β-actin-mRNA levels (vs. β-actin) and normalized to control groups (vs. control). As illustrated in figure 21, aortic TIMP-1-mRNA relative expression was significantly up-regulated in SNX untreated animals, especially in males (M-SNX +304 % and F-SNX +160 %), compared to corresponding control groups. BAY 41-8543 limited TIMP-1 overexpression significantly in males (-58 %, p<0.01) but not in females (-24 %, p=NS), while no relevant beneficial effects were seen in hydralazine-treated groups (-34 % in males and –40% in females) when compared to untreated SNX rats. In sham-operated animals, TIMP-1 mRNA expression vs. β-actin was found to be higher in females (M-Sham 1.3±0.2 x10^{-6} vs. F-Sham 4.3±0.8 x10^{-6}; vs. β-actin). The changes in TIMP-1 mRNA expression in response to mild renal insufficiency were more pronounced in males (M-SNX 4.23±0.8 vs. F-SNX 2.69±0.6; vs. control), independent of blood pressure (M-SNX+Hydr 2.79±0.3 vs. F-SNX+Hydr 1.61±0.3; vs. control) (91).
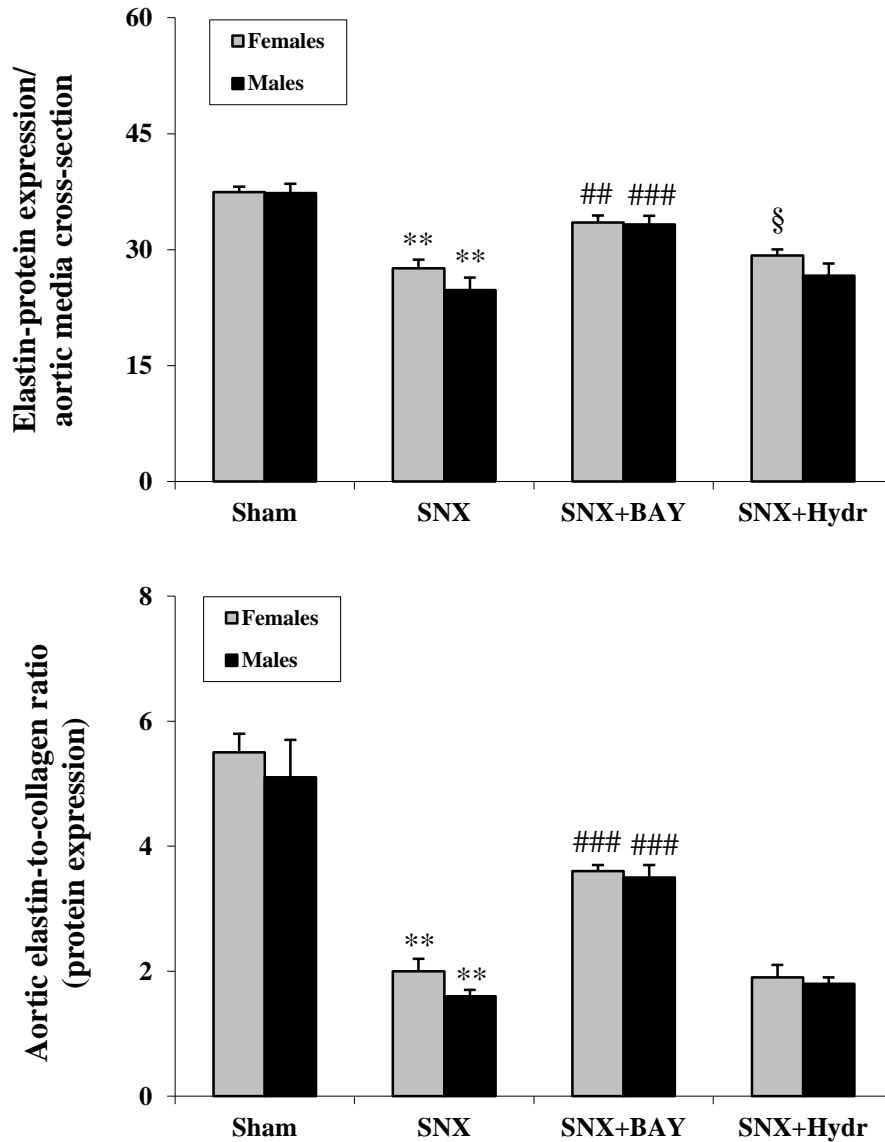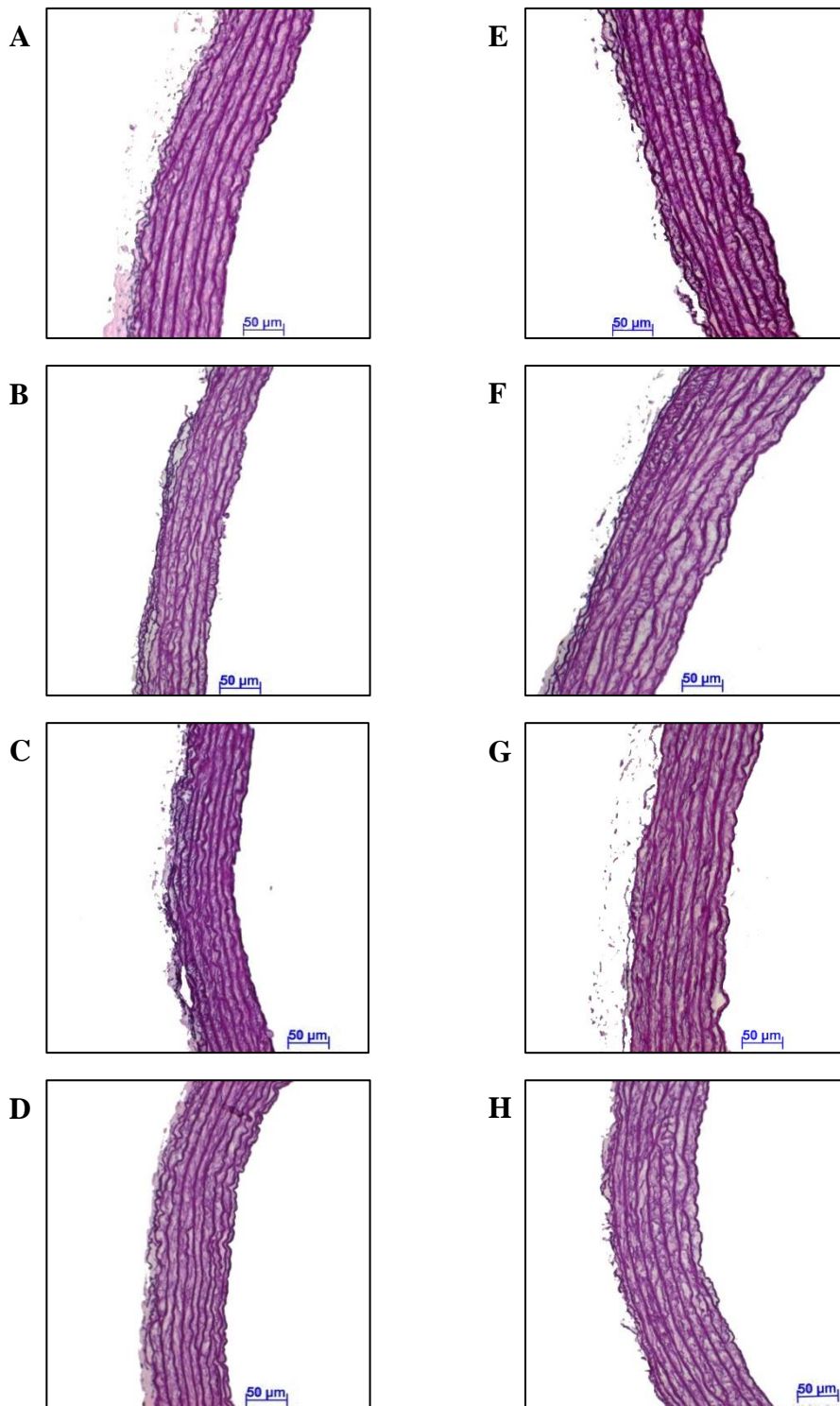

Figure 21. Impact of sex, subtotal nephrectomy (SNX), BAY 41-8543 (SNX+BAY) and hydralazine treatment (SNX+Hydr) on relative aortic TIMP-1 mRNA expression 18 weeks after induction of mild renal insufficiency. Treatments were started one week after subtotal nephrectomy. Sham-operated animals served as controls. TIMP-1-mRNA expression was relativized to β-actin and normalized to the respective control group. (* p<0.05 and ** p<0.01 vs. Sham; ## p<0.01 vs. SNX; § p<0.05 vs. males)

3.2.4.4. MMP-2 mRNA relative expression

Subtotal nephrectomy led to a significant up-regulation of relative aortic MMP-2 mRNA expression only in male rats (M-SNX +74 %) when compared to sham-operated ones (91). This change in aortic MMP-2 mRNA level was significantly ameliorated in the BAY 41-8543-treated group (-22 %), but not in hydralazine-treated animals (-11 %). In females, the relative aortic MMP-2-mRNA expression was not modified by SNX or therapeutic interventions. Significant sex-differences in relative aortic MMP-2 mRNA expression were observed within both untreated (M-SNX 1.78±0.14 vs. F-SNX 1.17±0.09; vs. control) and hydralazine-treated (males 1.58±0.09 vs. females 0.96±0.07; vs. control) SNX groups, while similar expression was seen in sham animals (M-Sham 0.025±0.003 vs. F-Sham 0.029±0.003; vs. β-actin).

Figure 22. Influence of sex, subtotal nephrectomy (SNX), BAY 41-8543 (SNX+BAY) and hydralazine treatment (SNX+Hydr) on aortic MMP-2 mRNA relative expression 18 weeks after induction of mild renal insufficiency. Treatments were started one week after subtotal nephrectomy. Sham-operated animals served as controls. MMP-2-mRNA expression was relativized to β-actin and normalized to the respective control group. (** $p < 0.01$ vs. Sham; # $p < 0.05$ vs. SNX; §§ $p < 0.01$ and §§§ $p < 0.001$ vs. males)

3.2.5.   *Aortic NO/cGMP signalling pathway*

At aortic level, relative eNOS mRNA expression was found to be significantly decreased in untreated SNX males (-41%) but not in females (+5 %) in comparison with control groups. BAY 41-8543 treatment restored relative aortic eNOS mRNA expression compared to untreated SNX groups, significantly in male animals (M-SNX+BAY +90 % and F-SNX+BAY +41 %), whereas no changes were seen in hydralazine-treated groups (M-SNX+Hydr +12 % and F-SNX+Hydr -29 %). eNOS mRNA expression was similar in male and female sham-operated animals (M-Sham 0.0019 ± 0.0004 and F-Sham 0.0014 ± 0.0003; vs. β-actin), but significant sex differences were observed after disease induction in untreated groups (males 0.63 ± 0.1 vs. females 1.14 ± 0.2; vs. control) (91).

Relative aortic iNOS mRNA expression was up-regulated in uremic animals (M-SNX +80 % and F-SNX +61 %) compared to controls, however, it did not reach statistical significance. Treatment with BAY 41-8543 normalized aortic iNOS mRNA levels in females (-46%) but not in the male group (-13 %), while hydralazine treatment showed no significant effects (M-SNX+Hydr -3 % and F-SNX+Hydr -25 %) when compared to untreated SNX animals. There were no sex-related differences observed in iNOS mRNA expression in either sham animals (M-Sham 0.017 ± 0.003 $x10^{-3}$ vs. F-Sham 0.019 ± 0.003 $x10^{-3}$; vs. β-actin) or in response to SNX (M-SNX 1.86 ± 0.2 vs. F-SNX 1.70 ± 0.3; vs. control).
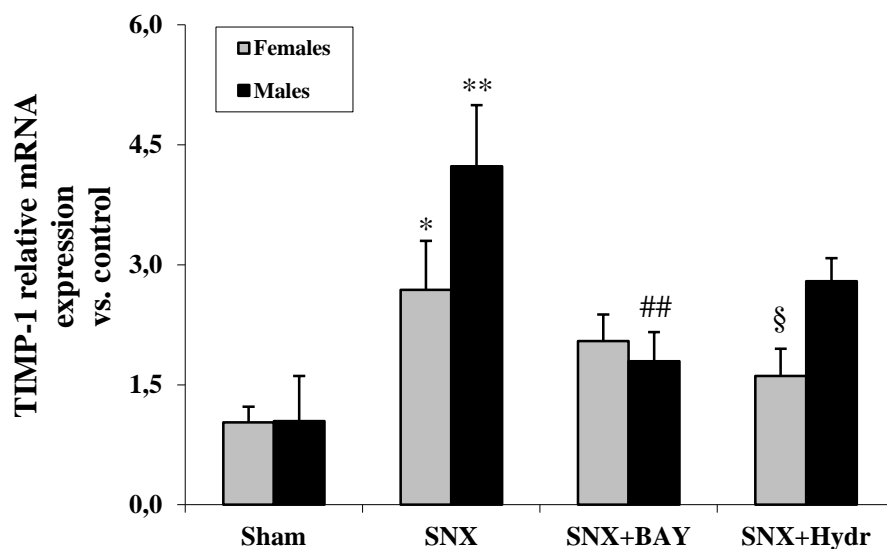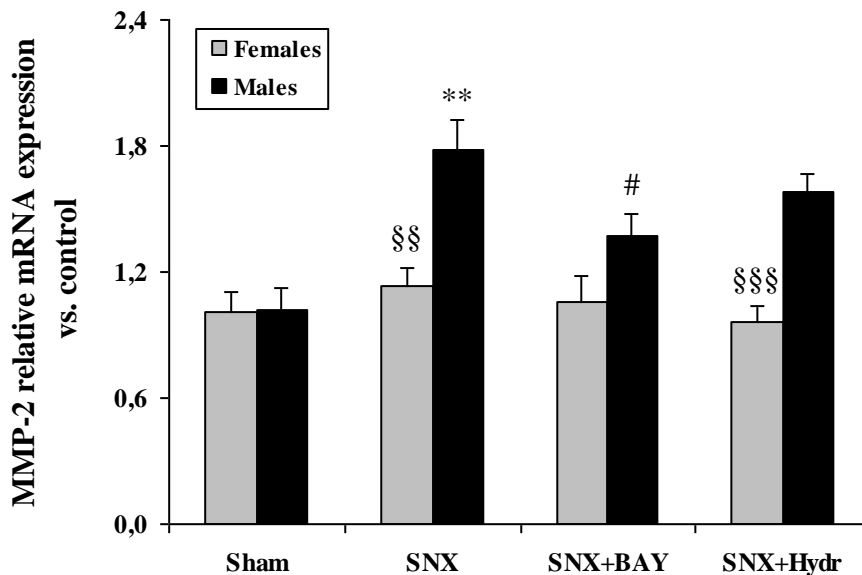
Figure 23. Effect of sex, subtotal nephrectomy (SNX), BAY 41-8543 (SNX+BAY) and hydralazine treatment (SNX+Hydr) on relative aortic eNOS and iNOS mRNA expression 18 weeks after induction of mild renal insufficiency. Treatments were started one week after subtotal nephrectomy. Sham-operated animals served as controls. eNOS- and iNOS -mRNA expression was relativized to β-actin and normalized to the respective control group. (* $p<0.05$ vs. Sham; # $p<0.05$ vs. SNX; § $p<0.05$ vs. females)

Figure 24. Impact of sex, subtotal nephrectomy (SNX), BAY 41-8543 (SNX+BAY) and hydralazine treatment (SNX+Hydr) on aortic relative mRNA expression of $\alpha 1$- and $\beta 1$-subunit of sGC 18 weeks after induction of mild renal insufficiency. Treatments were started one week after subtotal nephrectomy. Sham-operated animals served as controls. $\alpha 1$- and $\beta 1$-sGC-mRNA expression was relativized β-actin and normalized to the respective control group. (* $p < 0.05$ vs. Sham; § $p < 0.05$ vs. males)

As shown in figure 24, the relative mRNA expression of α1-subunit of sGC was similar in all male groups, independent of SNX or therapeutic intervention (M-SNX 1.20±0.18; M-SNX+BAY 1.38±0.19; M-SNX+Hydr 0.99±0.13; vs. control). In females, SNX led to a slight but significant decrease (-27 %), which was corrected by BAY 41-8543 (+46 %) but not by hydralazine (+21%) administration. Aortic β1-sGC mRNA expression was not modified by either SNX or by applied treatments. Same aortic mRNA expressions of α1-sGC (M-Sham 0.0022±0.0002 vs. F-Sham 0.0026±0.0003; vs. β-actin) and β1-sGC (M-Sham 0.0009±0.0001 vs. F-Sham 0.0011±0.0001; vs. β-actin) were found in male and female sham groups. Sex-related differences were observed only in relative α1-sGC mRNA expression in response to mild renal insufficiency (M-SNX 1.20±0.18 vs. F-SNX 0.75±0.07; vs. control).

Relative aortic PKG-1 mRNA expression followed the changes seen in mRNA levels of α1- and β1-subunit of sGC, as shown in figure 25. In males, PKG-1 mRNA expression remained unchanged when compared to the control group (M-SNX 1.16±0.10; M-SNX+BAY 1.01±0.06; M-SNX+Hydr 1.05±0.10; vs. control), while a slight down-regulation was observed in the untreated female SNX group (-27 %). BAY 41-8543 treatment brought PKG-1 mRNA expression back to normal levels (+46 %) in females, whereas no significant increase was seen in hydralazine-treated group (+17 %). Sex-related differences in PKG-1 mRNA expression were found only among untreated uremic animals (M-SNX 1.16±0.10 vs. F-SNX 0.77±0.07; vs. control).

Relative mRNA expression of PKG-2 at aortic level showed no significant variations in male (M-SNX 1.32±0.5; M-SNX+BAY 3.93±1.7; M-SNX+Hydr 2.39±0.6; vs. control) or female (M-SNX 1.96±0.4; M-SNX+BAY 1.05±0.2; M-SNX+Hydr 1.19±0.5; vs. control) animals compared to the corresponding sham group. Moreover, no significant effects of sex on aortic PKG-2 mRNA expression were observed.
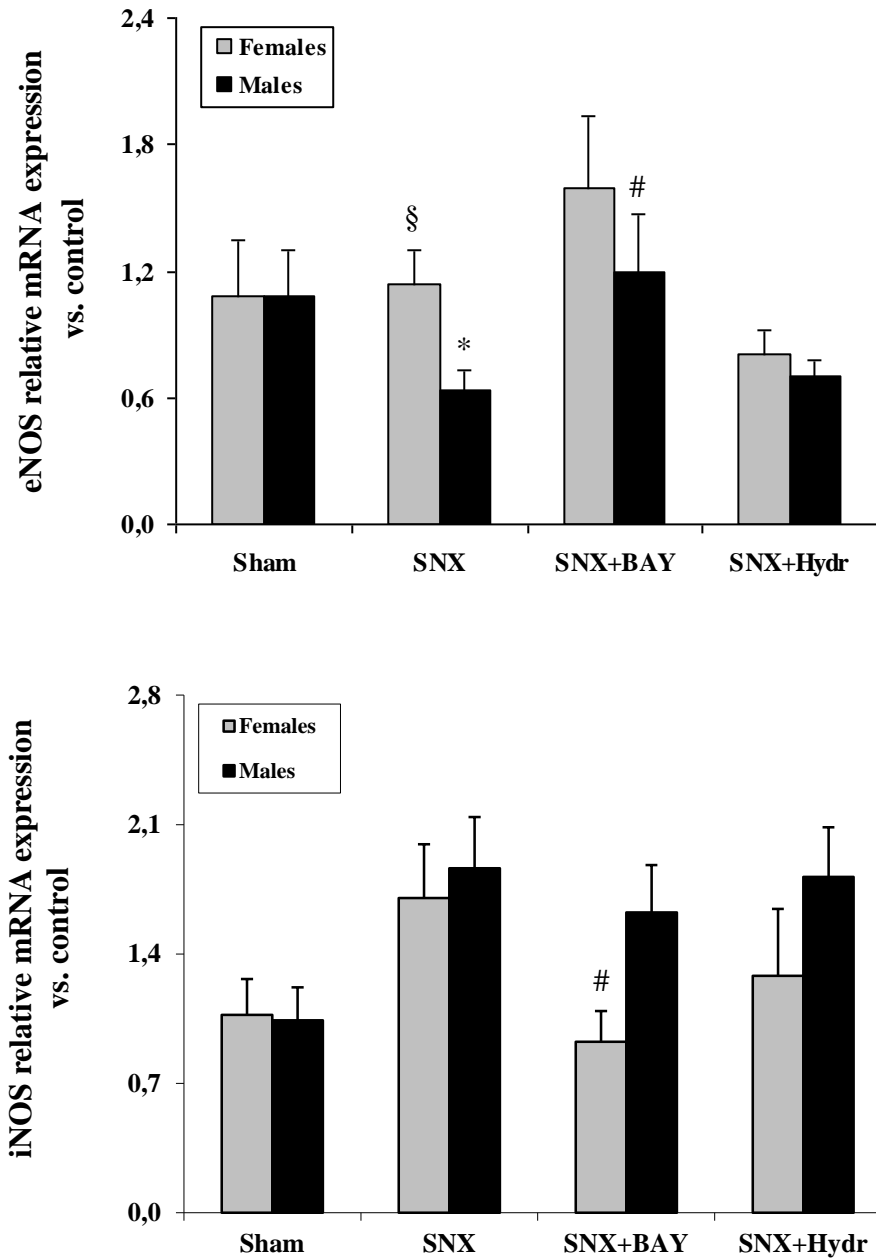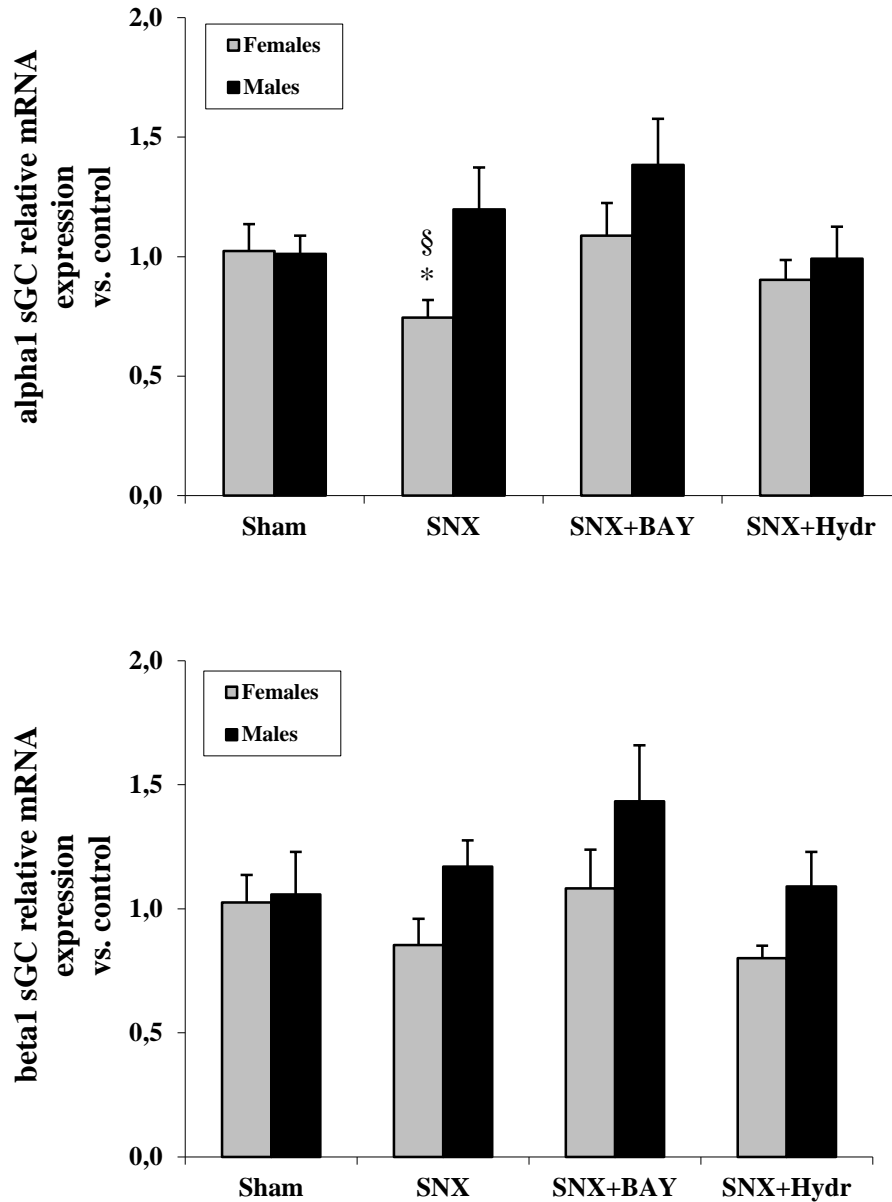
Figure 25. Effect of sex, subtotal nephrectomy (SNX), BAY 41-8543 (SNX+BAY) and hydralazine treatment (SNX+Hydr) on relative aortic PKG-1 and PKG-2 mRNA expression 18 weeks after induction of mild renal insufficiency. Treatments were started one week after subtotal nephrectomy. Sham-operated animals served as controls. PKG-1- and PKG-2-mRNA expression was relativized to β-actin and normalized to the respective control group. (* $p < 0.05$ vs. Sham; ## $p < 0.01$ vs. SNX; §§ $p < 0.01$ vs. males)

Plasma cGMP concentrations were measured as an indicator of systemic NO/cGMP signalling pathway activity. In untreated SNX animals, plasma cGMP levels were elevated in comparison with sham-operated groups (346±49 vs. 191±13 pmol/ml in males, $p < 0.01$; 487±103 vs. 257±29 pmol/ml in females, $p > 0.05$). Compared to untreated uremic groups, BAY 41-8543

treatment led to a significant increase of cGMP production in male animals (785 ± 147 pmol/ml) but not in females (429 ± 40 pmol/ml). The same effects were observed also in hydralazine-treated groups (663 ± 114 pmol/ml in males; 605 ± 66 pmol/ml in females). There were no sex differences seen in plasma cGMP levels among any of the experimental groups (91).
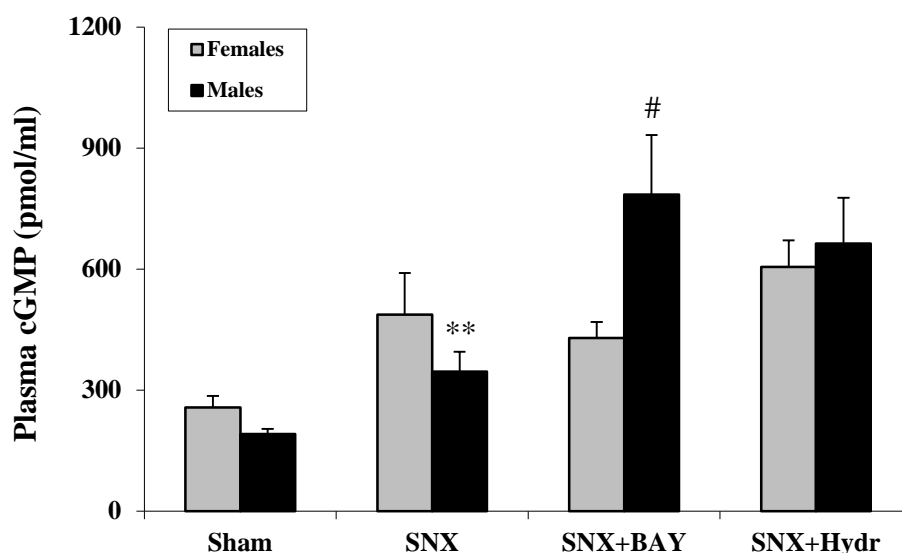
Figure 26. Effects of sex, subtotal nephrectomy (SNX), BAY 41-8543 (SNX+BAY) and hydralazine treatment (SNX+Hydr) on plasma cGMP concentration 18 weeks after induction of mild renal insufficiency. Treatments were started one week after subtotal nephrectomy. Sham-operated animals served as controls. CGMP levels were measured by ELISA in plasma samples pre-treated with IBMX, a phosphodiesterase inhibitor. (** $p<0.05$ vs. Sham; # $p<0.05$ vs. SNX)

3.2.6.   *Aortic ERα and ERβ mRNA expression*

As illustrated in figure 27, aortic mRNA expression of ERα and ERβ was not influenced by subtotal nephrectomy (M-SNX 1.07 ± 0.1 and 0.82 ± 0.2; F-SNX 1.25 ± 0.1 and 2.39 ± 0.5; vs. control), treatments with BAY 41-8543 (M-SNX+BAY 1.45 ± 0.2 and 0.71 ± 0.2; F-SNX+BAY 1.06 ± 0.2 and 1.46 ± 0.4; vs. control) or hydralazine (M-SNX+Hydr 0.88 ± 0.1 and 0.71 ± 0.2; F-SNX+Hydr 0.87 ± 0.1 and 1.13 ± 0.4; vs. control). There were also no significant sex differences in aortic ERα and ERβ mRNA expression, except untreated SNX groups, where the ERβ-mRNA level was found to be higher in females (91).
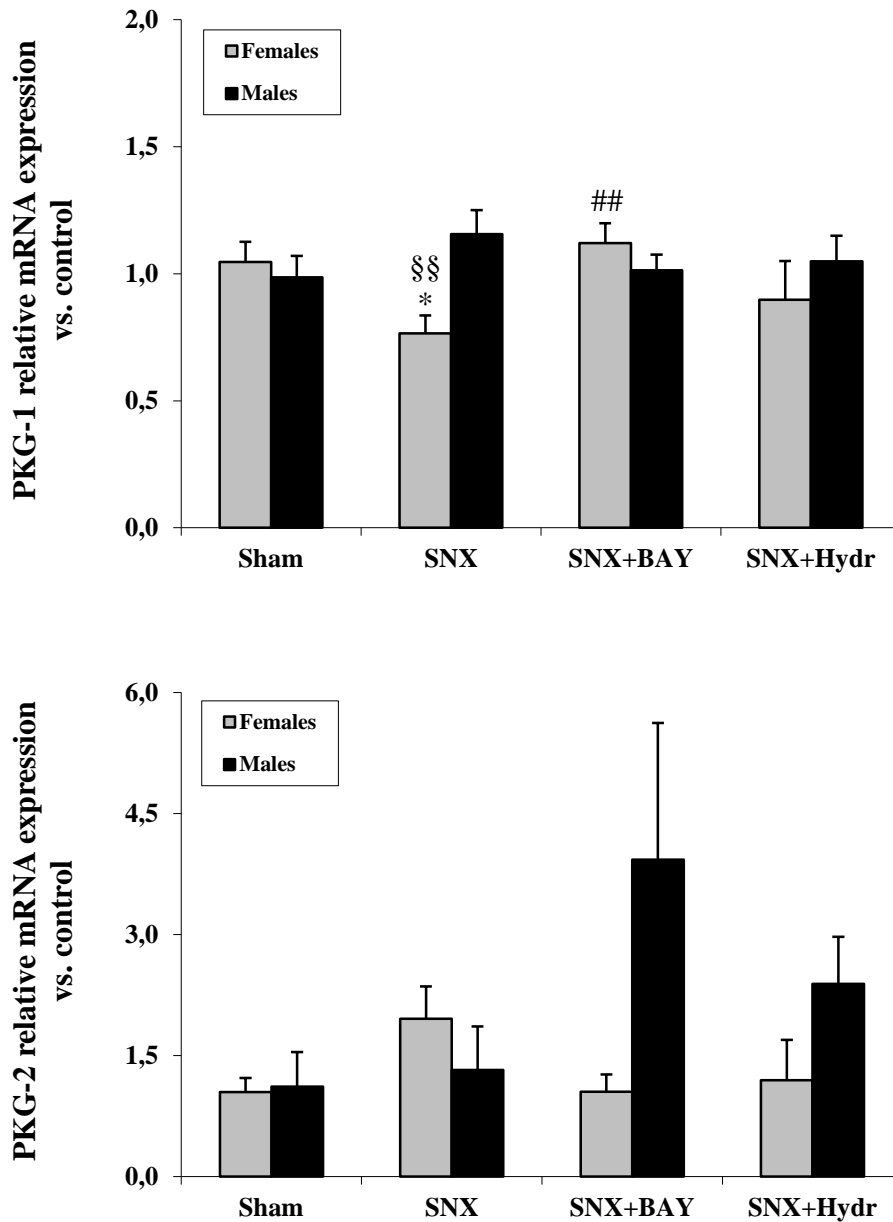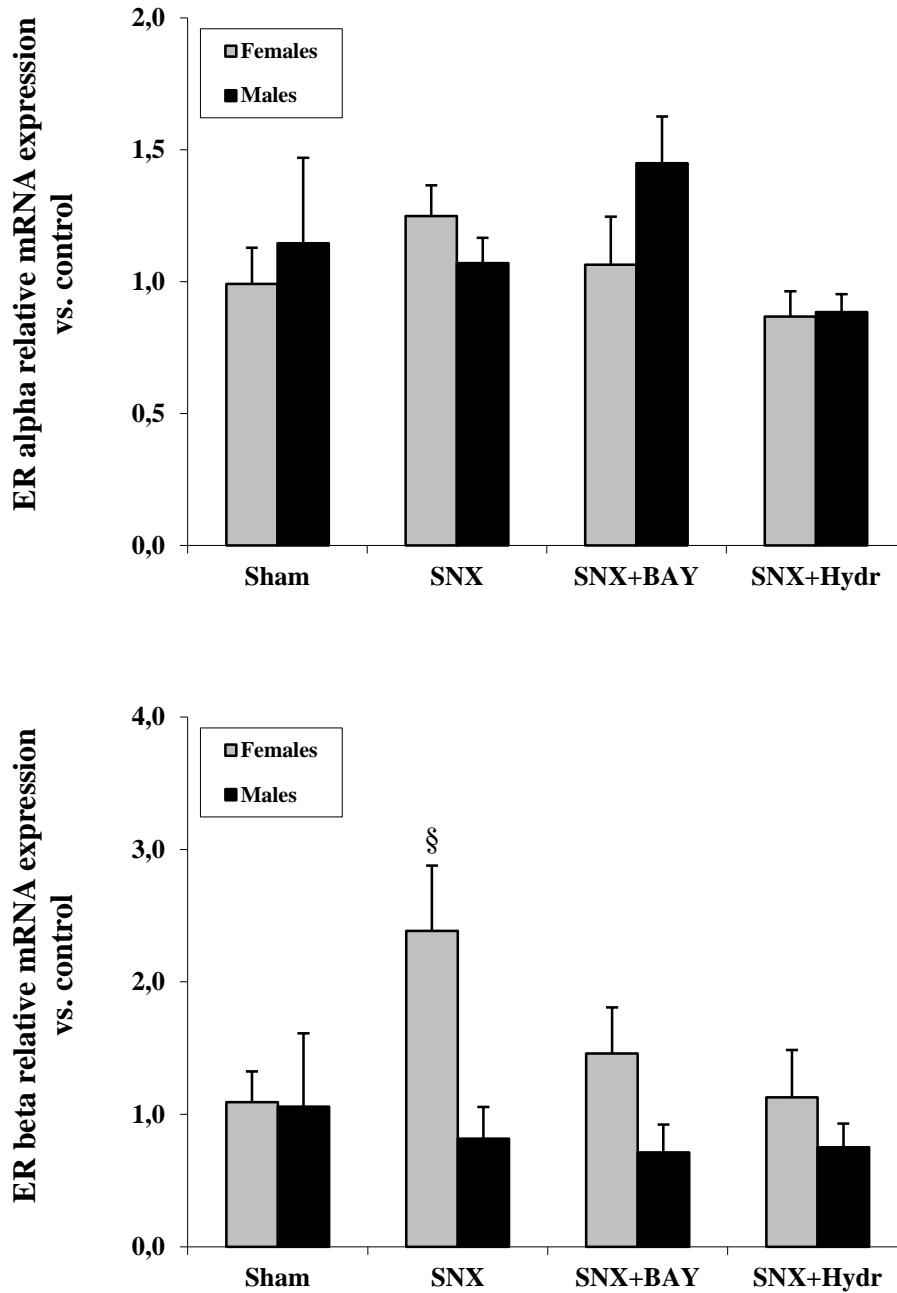
<u>Figure 27.</u> Influence of sex, subtotal nephrectomy (SNX), BAY 41-8543 (SNX+BAY) and hydralazine treatment (SNX+Hydr) on relative aortic ERα and ERβ mRNA expression 18 weeks after induction of mild renal insufficiency. Treatments were started one week after subtotal nephrectomy. Sham-operated animals served as controls. ERα- and ERβ-mRNA expression was relativized to β-actin and normalized to the respective control group. (§ $p<0.05$ vs. males)

4. DISCUSSION

The present study aimed to further characterize the uremic aortic remodelling process and the impact of biological sex and enhanced NO/cGMP signalling by BAY 41-8543 on uremia-induced alterations of the aorta in a rat model of subtotal nephrectomy. In the model employed, a relatively mild degree of impaired renal function led to marked hypertrophic remodelling and stiffening of the aortic wall over 18 weeks. With regard to the impact of gender, male animals presented more severe alterations as illustrated by increased media thickness, media-to-lumen ratio, VSMC proliferation, aortic macrophage infiltration and ECM turnover. Male rats showed decreased elastin-to-collagen ratios – a key morphological indicator of aortic wall stiffening – as a result of elevated collagen I and reduced elastin protein expression in the aortic wall. Furthermore, aortic remodelling in male uremic rats went along with reduced aortic eNOS expression, suggesting that impaired NO-cGMP signalling is an important pathomechanism. In turn, the less severe aortic pathology in female animals was linked to protective effects in the degree of aortic media thickness and media-to-lumen ratio, aortic VSMC proliferation, macrophage infiltration, MMP-2 and eNOS mRNA expression being not significantly altered in the presence of long-term mild uremia. With regard to stimulation of the eNOS/cGMP signalling pathway, the administration of BAY 41-8543 significantly ameliorated aortic remodelling and stiffening by inhibiting VSMC proliferation and normalizing expression of different ECM components and eNOS. In animals treated with the vasodilator hydralazine, no beneficial actions on aortic remodelling were found despite a similar reduction in systemic blood pressure (91). In the following, we will discuss the findings of this study in context with those of the published literature.

4.1. Critical evaluation of the methodology used

4.1.1. Experimental mild renal insufficiency

In this study, mild renal insufficiency was induced in male and female Wistar rats by subtotal (5/6) nephrectomy, a standard non-inflammatory model of progressive renal disease, using the ablation method introduced by Amann et al. (92). In the first step of the surgical procedure, the right kidney was removed, followed after two weeks by the second step consisting in ablation of 2/3 of the left kidney cortex. In comparison with other methods of renal mass reduction (infarction of renal artery branches or electrocoagulation of renal cortex), the ablation method used had the advantage that the amount of renal tissue removed was carefully controlled

and similar in all rats, thus allowing standardization of the induced renal damage. The model of SNX used induced a mild degree of renal dysfunction, presumably excluding the involvement of other factors, like severe anemia, dyselectrolytemia, and metabolic acidosis, characteristic of advanced renal failure (91). This does not represent a limitation, since there is strong evidence that even minor renal dysfunction (i.e. microalbuminuria or slightly reduced GFR) represents an independent cardiovascular risk factor, both vascular and cardiac alterations being identified already in early stages of CKD (1; 95; 96). Clinical and experimental studies showed that chronic renal failure is a state of impaired NO production and bioavailability. This represents an important pathogenic factor in the development of subsequent cardiovascular complications, including arterial remodelling (50). Therefore, the model of subtotal nephrectomy is suitable for investigating the role played by NO/cGMP pathway in uremic aortic remodelling and the effects of enhancing this pathway by the sGC stimulator, BAY 41-8543.

Given the differences in blood pressure between male and female SNX rats and the hypotensor effect of BAY 41-8543, hydralazine-treated animals were included in the study in order to asses blood pressure-independent effects of both biological sex and BAY 41-8543 treatment. Moreover, hydralazine treatment allowed identification of blood pressure-independent mechanisms involved in uremic aortic remodelling.

4.1.2. Enhancing NO/cGMP signalling with BAY 41-8543

Endothelial dysfunction due to impaired NO/cGMP signalling was identified as a major factor contributing to the pathophysiology of arterial remodelling in patients with CKD and hypertension, modulation of this pathway becoming an attractive therapeutic target. Studies investigating the effects of L-arginine supplementation on the course of renal disease described both beneficial and negative effects, the latter due to activation of iNOS, resulting in high cytotoxic concentrations of NO (97). Pharmacological NO donors, widely used in the treatment of ischemic coronary heart disease, induce systemic vasorelaxation, which is more pronounced in large veins than in resistance arteries, but their therapeutic potential is limited by development of tachyphylaxis after prolonged administration. In VSMCs of spontaneously hypertensive rats, reduced sGC expression with low cGMP level was observed despite enhanced eNOS-dependent NO production (98). Therefore, sGC stimulators, like BAY 41-8543, represent promising therapeutic tools that act selectively on sGC, thus increasing cGMP production and promoting the beneficial effects of NO as signal molecule, without having the side effects of L-arginine or NO donors. In addition, compared with other compounds of the same drug class (e.g. YC-1),

BAY 41-8543 shows no PDE inhibitory effects and has a higher potency after oral administration. This makes BAY 41-8543 a valuable tool for investigating the role of NO/cGMP signalling in the development of aortic remodelling.

4.2. Sex-related aspects and enhanced NO/cGMP signalling in mild renal insufficiency

Several sex- and treatment-related aspects in the progression to mild renal insufficiency must be discussed, even if these are not the main point in our study.

4.2.1. The rat model of mild renal insufficiency

Progression of renal disease following SNX can be divided into three phases. Phase 1 (first 2-4 weeks) is characterized by compensatory hypertrophy of remaining glomeruli. In phase 2 (up to 10 weeks), only minimal renal histological changes can be observed, followed by phase 3 (after 10 weeks), when glomerulosclerosis and tubulointerstitial fibrosis occur. This parallels the clinical progression of CKD that, independent of the underlying etiology, is characterized by persistent loss of functional nephrons leading finally to chronic renal failure. Glomerular hypertension plays the central role in the pathogenesis of renal disease in the model of subtotal nephrectomy. In response to significant inborn or acquired nephron number reduction, remaining glomeruli undergo compensatory structural (i.e. hypertrophy) and functional (i.e. hyperfiltration) adaptations leading to increased single nephron-glomerular filtration rate to maintain renal excretory function. This proved to be a "maladaptive" response, since alterations in glomerular hemodynamic with glomerular capillary hypertension promote and perpetuate glomerular injury in experimental models of reduced renal mass (99). Moreover, these nephrons lose their autoregulatory mechanisms, thus becoming more vulnerable to systemic hypertension (100). Hemodynamic changes at glomerular level are correlated with activation of RAAS. Beside its well-known vasoconstrictor effect, angiotensin II is also responsible for increased reactive oxygen species and decreased NO production, up-regulation of proinflammatory cytokines, profibrotic growth factors (with TGFβ as major player) and cell adhesion molecules, leading to mesangial cell proliferation, ECM expansion and macrophage infiltration and activation (101; 102; 103). Glomerular lesions are associated with tubulointerstitial inflammation, apoptosis of tubular cells with tubular atrophy, epithelial-mesenchymal transition and interstitial fibrosis.

In this model of subtotal nephrectomy, renal mass reduction was associated with early increase of systolic blood pressure, further contributing to progression of renal disease. This is consistent with findings of epidemiological studies showing that congenital deficit in nephron

number is correlated with development of hypertension and progressive renal disease in later life (104). Furthermore, a decrease in nephron number was observed in patients with essential hypertension (105).

4.2.2. Impact of sex on renal disease progression

Biological sex had a manifold impact on the degree of renal disease following subtotal nephrectomy was multifold. The degree of morphological kidney damage (glomerular and tubulointerstitial matrix expansion) and renal function impairment was found to be similar in male and female animals, despite a more pronounced glomerular hypertrophic response in the male SNX group. With regard to blood pressure, female rats showed a non-significant trend to less elevation, a finding that had been reported previously. However, the same sex differences in aortic remodelling were observed after lowering systolic blood pressure at similar levels in both sexes for hydralazine-treated animals. These results suggested that protective effects of female sex on uremic aortic remodelling were mediated, at least partially, by blood pressure-independent mechanisms. A significant difference was seen in the proteinuria levels, this was found to be more pronounced in female than in male uremic animals (91). Studies investigating the effects of gender and sex hormones on the progression of renal disease have shown important variations depending on the analysed species, animal strain and experimental model. The results of our study are comparable with the findings of Fleck et al. (106), who described a more severe degree of renal injury – as emerged from proteinuria and renal morphological changes - despite lower levels of systolic blood pressure in female than in male SNX Wistar rats. Several publications have nicely summarized or investigated the effects of biological sex on the progression of renal disease, showing different patterns depending on investigated animal model and underlying renal disease: from beneficial effects to none or even negative influence of female sex or estrogen replacement therapy (107; 108; 109; 110; 111). In animal models of remnant kidney, NOS inhibition-induced hypertension or ageing showed that the progression rate of renal disease is faster in males, with OVX accelerating and orchiectomy or estrogen replacement therapy attenuating disease progression (110; 112; 113; 114; 115). Clinical studies describe a slower progression of non-diabetic renal disease in women, but controversial data were provided for diabetic nephropathy. On the other hand, in a rodent model of diabetic nephropathy and in hyperlipidemic animals, female sex was found to exacerbate the progression of renal disease (116; 117; 118). Ovariectomy was demonstrated to attenuate renal injury induced by L-NAME and Ang II co-administration, whereas estradiol replacement therapy had

an aggravating effect (111). Other studies failed to show significant effects of estrogens on renal injury (107; 119). The mechanisms underlying sexual dimorphism in progression of renal disease are not completely understood. Besides sex-related differences in nephron numbers, and systemic and glomerular hemodynamics, other possible explanations include direct effects of sex hormones on different pathophysiological processes involved in renal disease progression. Estrogens were demonstrated to modulate RAAS, stimulate NO production, and interfere with renal fibrogenic process by influencing expression of ECM proteins, like collagen I and IV, and MMPs (107; 109; 120; 121; 122). For this study, it is important that the degree of impaired renal function was comparable between male and female animals; thus, the uremic stimulus for the aortic alterations over 18 weeks should not be accountable for sex differences.

4.2.3. Enhancing NO/cGMP signalling in mild renal insufficiency

sGC was demonstrated to be expressed at renal level in mesangial cells, podocytes, renal interstitial fibroblasts and VSMC, where it mediates antiproliferative and antifibrotic actions. Since CKD is associated with impaired NO production and/or signalling, pharmacological stimulation of sGC represents an attractive therapeutic tool.

As previously mentioned, BAY 41-8543 normalized blood pressure and thus interfered with the mechanical forces acting on the arterial wall and promoting structural and functional changes. In the present study, despite the significant reduction of systolic blood pressure, treatment with BAY 41-8543 showed no beneficial effects on parameters of renal disease (proteinuria, glomerular and tubulointerstitial matrix expansion, creatinine clearance) compared with untreated uremic animals (91). These results disagree with findings in experimental anti-Thy1 acute and chronic glomerulonephritis, where BAY 41-2272 treatment had antiproliferative and antiinflammatory effects and ameliorated markers of fibrosis (70; 71). However, neutral effects of sGC stimulation on proteinuria levels have been reported in other experimental studies as well (71; 123). This phenomenon was explained by the later start of the treatment, one week after disease induction, when glomerular changes were already present. Beneficial effects on renal structural alterations, albuminuria but not on plasma creatinine and urea levels were described in the renal mass ablation model after treatment with sGC activator HMR1766, in a dose that did not influence blood pressure (124). One could speculate that in conditions of increased oxidative stress, like in SNX, sGC activators could have a higher potency, since they act also on the oxidized form of the enzyme, whereas the action of sGC stimulators is limited to the reduced enzyme form.

4.3. Aortic remodelling in mild renal insufficiency

4.3.1. Aortic remodelling and stiffening in mild renal insufficiency

The present study demonstrated that in a model of mild renal insufficiency, thoracic aorta undergoes a remodelling process characterized by aortic wall hypertrophy and stiffening. A significant increase in media thickness and media cross-sectional area of thoracic aorta was observed in male untreated SNX rats compared to the sham-operated control group. This was accompanied by a low intima-media ratio and a significantly higher media-to-lumen ratio, the latter indicating hypertrophic remodelling of the aortic wall (91). These results are in agreement with data provided by investigations of Amann et al., who describe aortic media thickening with enlargement or preservation of lumen diameter in normotensive and hypertensive SNX rats (17; 19; 125).

Different cellular and molecular mechanisms can contribute to the development of aortic wall remodelling. In the present study, media thickening of aorta in untreated SNX males was associated with proliferation of VSMC and increased collagen I deposition in aortic media. In contrast, elastin content of the aortic wall was found to be significantly reduced in untreated SNX rats, with aortic elastic laminae being thinner and disrupted when compared with controls. The discrepancy between high collagen production, on one hand, and decreased synthesis or increased degradation of elastic fibres, on other hand, translates into reduced elastin-to-collagen ratio (91). It has already been described in the literature that viscoelastic properties of arterial wall, and consequently normal arterial functions, are strongly dependent of a balance between collagen and elastic fibres content. Stiffness, which best describes the viscoelastic properties of the aortic wall, expresses the relationship between pressure response and change in volume. At a low distending pressure, tension is produced in elastic fibres, while less extensible collagen fibres are responsible for tension generation at high distending pressure and the arterial wall becomes stiffer (7). Therefore, reduced elastin-to-collagen ratio is a reliable indirect indicator of aortic wall stiffening and impaired compliance.

A similar pattern of aortic remodelling was described by Amann et al. in normotensive SNX rats using the disector method. They found aortic wall thickening to be associated with pronounced hyperplasia and only moderate hypertrophy of VSMC, and expansion of extracellular matrix with decrease in relative elastic fibre content. The observed higher mean cell and nuclear volume of VSMC, together with expansion of the Golgi apparatus, suggest VSMC activation and phenotype alteration from contractile to a more secretory one. This results in

increased collagen content and further contributes to thickening of the aortic wall (17). Valuable data regarding cellular mechanisms involved in the process of aortic remodelling were provided by early studies in different animal models of hypertension. Using direct determination of cell numbers and DNA measurements, Owens and Schwartz found VSMC hypertrophy with hyperploidy of nuclei in aorta of SHR rats and rats with renovascular hypertension (15; 16). Olivetti et al. described hypertrophy and, to a lesser extent, hyperplasia of VSMC in the aorta of postnatal SHR rats (14).

The mitogenic response of VSMC to the uremic conditions, which was also described in the present study, could involve sympathetic over-activity (126) as well as growth-promoting effects of Ang II via stimulation of growing hormones like TGF-β and PDGF-AA (127).

Endothelial cells are also important players in the development of physiological and pathological vascular remodelling, an intact endothelium having been demonstrated to be a pre-requisite for normal vascular adaptation (5). This process involves detection and transduction of hemodynamic and/or humoral stimuli into biochemical signals that will further induce structural and functional alterations of the arterial wall. Endothelial cells, due to their strategic location at the blood-vessel wall interface, are the major candidates for this role. In response to different stimuli, endothelial cells react by generating vasoactive substances (nitric oxide, prostaglandins, endothelins etc), modulating the expression of adhesion molecules and ECM components (collagens, elastin, metalloproteinases, matrix-protease inhibitors). Following this idea, Amann et al. observed in experimental uremia the presence of enlarged endothelial cells with signs of cell activation (high number of intracellular vesicles and actin filaments, expansion of the Golgi apparatus) (125).

Male untreated SNX rats showed increased ECM turnover, with up-regulation of aortic TIMP-1 and MMP-2 relative mRNA-expression. This was associated with increased macrophage infiltration of the aortic wall (91). Vascular remodelling is a dynamic process that assumes both increased synthesis and accelerated degradation of different extracellular matrix components, allowing rearrangements of VSMC and fibre networks. Arterial resident cells, like endothelial cells and VSMC, as well as infiltrating inflammatory cells (macrophages) are known to produce MMPs and their inhibitors TIMPs. In normal human and animal arteries, local vascular cells constitutively express MMP-2 and the inhibitor TIMP-1, but no enzymatic activity was detected, suggesting a strict control of enzymes actions under normal conditions. In contrast, in different models of vascular disease, MMPs expression and activity were significantly up-regulated and associated with arterial structural changes, pointing towards MMPs as important players in arterial remodelling in both physiological and pathological conditions. Infiltrating inflammatory

cells like macrophages further contribute to MMP-2 and TIMP-1 overexpression either by direct enzyme release or by stimulating their synthesis and activation in neighbouring vascular cells (20; 21).

Increased tensile (pressure overload) and shear stress (volume overload) represent the major hemodynamic forces that act on the aortic wall and trigger compensatory structural alterations. Hypertension, a frequent finding in uremic humans and animal models, is an important contributing but not a necessary factor involved in pathogenesis of aortic remodelling. Based on the only moderate systolic blood pressure elevation following SNX, the present study suggests that increased blood pressure may represent a rather minor pathomechanism of uremia-induced aortic wall remodelling. Lowering systolic blood pressure with vasodilator hydralazine failed to prevent the aortic wall alterations, thus further supporting our theory and indicating that aortic remodelling can develop as an effect of uremia per se, at least partially independent of blood pressure levels. A major mechanism involved in the development of hypertension and progression of renal disease in humans and rodents with CKD is represented by activation of RAAS. However, the ablation method of SNX leads to considerably less activation of RAAS and lower values of blood pressure than those described in renal vascular ligation model. Besides being the most potent vasoconstrictor, Ang II acts on the adrenal glands, stimulating the aldosterone secretion and thus increasing the renal tubular sodium reabsorption and potassium excretion. Increased water retention is due to its passive reabsorption together with sodium and to the stimulation of vasopressin release from the posterior pituitary gland. Ang II also increases production of vasoactive substances, such as endothelin-1, platelet-derived growth factor (PDGF), basic fibroblast growth factor (bFGF) and TGF-β, which further contribute to the elevation of blood pressure, vascular cell proliferation, extracellular matrix protein synthesis and fibrosis. Moreover, sympathetic over-activity with high concentrations of plasma catecholamines was also demonstrated in renal failure and is partially an effect of Ang II. Low renalase levels, an oxidase produced by the kidney which catalyses catecholamine degradation, could also be involved (3; 127). The involvement of RAAS in structural alteration of the aortic wall is confirmed by the higher efficacy of ACE-inhibitors compared to other antihypertensive agents in prevention /reversal of aortic remodelling.

In this model of mild renal insufficiency, morphological and molecular alterations (reduced elastin-to-collagen ratio, increased ECM turnover) of the aortic wall were seen also in hydralazine-treated animals, in which systolic blood pressure was lowered to values compared to control groups. These results indicate that aortic remodelling can develop as an effect of uremia per se, at least partially independent of blood pressure levels (91).

Male uremic animals, independent of treatment, showed a lower hematocrit level. Volume overload and chronic increase in blood flow are factors that are more specific for CKD patients. These factors were shown to be important determinants of aortic remodelling by inducing vessel enlargement and wall hypertrophy. In patients with chronic renal failure, water and sodium retention, anemia and arteriovenous shunts promote volume/flow overload associated with increased regional and systemic blood flow and flow velocity. In conditions of severe anemia, the organism responds, trying to maintain an adequate oxygen delivery. Non-hemodynamic adaptive mechanisms are first activated: lower affinity of haemoglobin for oxygen, increased oxygen extraction and arteriovenous difference. If not sufficient, compensatory hemodynamic changes are induced: tachycardia and high stroke volume translated into increased cardiac output. Arteriovenous shunts, by lowering peripheral vascular resistance, lead to the same hemodynamic changes in both animal models and humans (128).

In addition to its pressor effect, endothelin-1 exerts important profibrotic actions, which seem to contribute to uremic vascular remodelling (9). Nevertheless, endothelin receptor blockade failed to attenuate aortic changes in experimental uremia, despite the prevention of small intramyocardial arteries remodelling (129).

Another factor that may be implicated in pathogenesis of aortic remodelling is represented by advanced glycation end-products (AGE), which form irreversible cross-links between collagen molecules. The resulted AGE-linked collagen is stiffer and resistant to hydrolytic degradation, leading to accumulation of structurally inadequate collagen with thickening and stiffening of the arterial wall. Moreover, AGE can also interact with elastin, reducing elastic matrix of arterial wall, and influence endothelial cells with inhibition of NO and increase of ROS production. In uremic patients, expression of AGE receptor was found to be up-regulated in endothelial cells (130).

Previous studies found that some of the vascular and cardiac effects of chronic renal insufficiency involve the permissive effect of parathormone (18). Experimental and clinical studies demonstrated in chronic renal disease an unbalance between calcification promoters (hyperphosphatemia, elevated CaxP product, secondary hyperparathyroidism, chronic inflammation) and inhibitors (low fetuin-A, BMP-7 serum concentrations, decreased local levels of matrix Gla protein), thus inducing VSMC phenotype alteration towards osteoblasts (131). These alterations are associated in CKD patients with media thickening and calcification, and increased stiffness of large conduit arteries.

In CKD patients, a complex association of proinflammatory status, increased oxidative stress and dyslipidemia further contributes to induction and progression of uremic vasculopathy.

Renal disease is accompanied by decreased apolipoprotein A-I and HDL levels, an important antioxidant with vasoprotective activity, and elevated triglycerides and LDL plasmatic concentrations. These changes were found to be associated with high PWV and increased intima-media thickness (7). Progressive deterioration of renal function in CKD leads to dyslipidemia and accumulation of uremic toxins, thus aggravating the oxidative stress and the inflammatory status. By acting through Ang II type 1 receptor (AT-1), Ang II stimulates generation of ROS by NADPH oxidase, myeloperoxidase (MPO) and other enzymes contributing to up-regulation of inflammatory markers (C reactive protein, fibrinogen, IL-6, TNF-α, adhesion molecules like E-selectin, ICAM-1, VCAM-1, and PAI-1) and spoliation of NO (12; 55; 127). In conditions of low tetrahydrobiopterin availability, eNOS itself, by uncoupling, is able to generate high amounts of superoxide. Thus, a vicious circle is closed, worsening endothelial dysfunction and arterial disease progression with hypertrophy and fibrosis of the aortic wall.

In patients with chronic renal failure, in comparison with age-, sex- and blood pressure-matched control subjects, large conduit arteries undergo structural remodelling characterized by dilatation and wall hypertrophy associated with increased arterial stiffness, alterations similar to those induced by ageing (7). Enlargement of aortic lumen was observed already at the onset of dialysis, indicating that the process of aortic remodelling starts early in the course of renal failure. This was confirmed by clinical trials that found aortic stiffening, reflected by increased PWV, to be significantly and independently correlated with renal function in subjects with mild to moderate renal dysfunction and normal or high blood pressure. In patients treated for hypertension, PWV increases more rapidly with age in those with higher baseline plasma creatinine levels, independent of mean blood pressure (1). Aortic stiffness was identified as an independent risk factor for cardiovascular mortality in both hypertensive and ESRD patients. In the latter, blood pressure reduction was associated with lower cardiovascular mortality only in those patients where PWV was also ameliorated (32). These studies also provided clinical evidences of beneficial effects of ACE inhibitors on aortic stiffness and cardiovascular mortality. Clinical trials confirmed, therefore, the hypothesis that, apart from hypertension, there are other factors more specific to uremia, which contribute to large artery remodelling in patients with chronic renal disease. Several important differences observed among patients with hypertensive and uremic aortic remodelling have to be mentioned in this context. In non-uremic hypertensive patients, large arteries respond to high blood pressure by wall hypertrophy with increased media-to-lumen ratio, and distensibility of aorta is similar to that observed in normotensive control subjects, when adjusted for differences in blood pressure (6; 18). Observations in ESRD patients showed proportional alterations of the aortic wall thickness and lumen diameter so that media-to-

lumen ratio was not significantly altered. This suggests an inadequate hypertrophic response of large arteries to combined flow and pressure overload. Konings et al. (13) proposes as a possible explanation the qualitative changes of the arterial wall components, which result in decreased aortic distensibility with high values of PWV that further amplify pressure load. Increased aortic stiffness in patients with chronic renal failure correlates with structural alterations, also described in experimental uremia: fibroelastic intima/media thickening, extracellular matrix expansion and, in particular models, high calcium content with media calcifications (17; 18; 125).

4.3.2. Aortic NO/cGMP signal transduction in mild renal insufficiency

Endothelial dysfunction represents a crucial factor in both physiological and pathological arterial remodelling. The results of the HOORN study indicate that endothelial dysfunction contributes to cardiovascular mortality even in patients with only mild renal insufficiency (2). Microalbuminuria, a marker of glomerular hyperfiltration and one of the early markers of renal disease, was shown to be correlated with impaired endothelial function. Nitric oxide deficiency and/or impaired signalling were demonstrated to be critically involved in the pathogenesis of CKD-associated endothelial dysfunction.

The present study analysed the expression of NO/cGMP signalling pathway components at aortic level and plasma cGMP concentration, as an indicator of systemic activity of this pathway, in hypertensive SNX rats. In male untreated SNX animals, renal mass ablation resulted at aortic level in decreased eNOS relative mRNA expression (91), this correlating with other published data. In the ablation model of SNX, Vaziri et al. showed significant reduction of aortic eNOS and iNOS protein levels which were associated with down-regulation of all NOS forms in the kidney (52; 54). By contrast, iNOS mRNA relative expression was found to be slightly but not significantly increased in our study, this being accompanied by increased macrophage infiltration of the aortic wall in male SNX group. Besides the expression of iNOS in macrophages, these inflammatory cells are able to induce iNOS expression in adjacent cells (VSMC, endothelial cells, fibroblasts), process mediated by production of proinflammatory cytokines, like TNF-α, IL-1. Contradictory data were presented by Aiello et al. in the infarction model of SNX. They demonstrated a progressive decline in renal iNOS but not eNOS protein expression, accompanied by increased aortic NOSs expression and activity (51). Different aortic NOSs expression in the ablation and infarction model of SNX is also reflected in NO synthesis. Therefore, plasma nitrite/nitrate levels are slightly reduced after renal mass ablation, whereas a significant increase of the same parameter is observed in the renal infarction model. Urinary

nitrite/nitrate levels are significantly reduced in both animal models of uremia, this alteration being also seen in CKD patients. The discrepant results concerning aortic NOSs expression and systemic NO synthesis observed in the two models of renal mass reduction could be explained by differences in blood pressure. In the infarction model characterized by development of severe hypertension, increased pressure and shear stress exert stimulatory effects on aortic eNOS expression, which overcome the inhibitory influence of CKD. Renal mass ablation leads to an only mild-moderate increase in vascular tonus, which is insufficient to induce up-regulation of aortic eNOS expression. This hypothesis was confirmed by the group of Vaziri in a model of renal mass reduction induced by electrocauterization of the renal cortex. This animal model was characterized by severe hypertension and associated with compensatory aortic eNOS up-regulation.

Further investigations in our study revealed no significant differences in relative mRNA expression of α- and β-subunit of sGC, PKG-1 and PKG-2, whereas plasma cGMP levels were significantly increased after renal mass ablation in untreated male rats (91). These results are consistent with those published by Sindhu et al. in a similar model of renal disease (132). In hypertension and aging, aortic sGC expression appears to be down-regulated (133).

We have to mention, as a limitation of our study, the fact that we could not provide data regarding aortic activity of the NO/cGMP signalling pathway (e.g. phosphorylated eNOS, endothelial function, aortic cGMP concentration). This was mainly due to the very limited aortic material we could harvest per animal and group, the already large set of aortic markers we analysed and the frame of animal number we were allowed to include in the experiments. Plasma cGMP level expresses the systemic activity of NO/cGMP signalling pathway and may not reflect the local activity of this pathway at aortic level. However, an increased cGMP concentration was previously described in patients with chronic kidney disease and – at renal level - in animal models of chronic glomerulosclerosis despite the NO deficiency (71; 134). This could involve higher natriuretic peptide level, reduced renal cGMP excretion as well as different regulation of NOSs- and sGC expressions depending on the investigated organ/cell type.

In the present study, alterations in expression of different NO/cGMP signal transduction components were not influenced by reduction of blood pressure with hydralazine. This suggests that the observed down-regulation of aortic eNOS expression involves blood pressure-independent effects of uremia per se.

4.4. Sex-specific aspects of uremic aortic remodelling

4.4.1. Sexual dimorphism in uremic aortic remodelling

The present study identified pronounced sexual dimorphism in the development of aortic remodelling in a rat model of mild renal insufficiency. Compared to male rats, aortic remodelling was less pronounced in female animals, a feature that may result from modulation of several underlying molecular mechanisms. Female sex exerted a protective effect against aortic hypertrophic remodelling, significant sex-related differences being observed for aortic media thickness and media-to-lumen ratio. In female animals, aortic VSMC proliferation, macrophage infiltration, MMP-2 and eNOS mRNA expression were not significantly altered after induction of mild uremia (91).

Since females reacted to SNX by a milder - although not statistically significant - increase in systolic blood pressure in comparison with male animals, it can be argued that the protective effects of female sex against uremic aortic remodelling were mediated by differences in blood pressure. Nonetheless, the same sex differences in aortic remodelling were observed after lowering systolic blood pressure at similar levels in both sexes in hydralazine-treated animals. These results suggested that beneficial effects of female sex on aortic remodelling in experimental mild renal insufficiency were mediated, at least partially, by blood pressure-independent mechanisms.

Previous experimental studies in different models of hypertension provided controversial data concerning the vascular effects of female sex hormones. Investigating the role of estrogens in pathogenesis of hypertension, several studies in SHR, Dahl salt-sensitive and deoxycorticosterone-salt hypertensive rats showed that blood pressure levels are higher in males than in females, OVX abolished this difference and estrogen treatment suppressed the development of hypertension in OVX females (72). Beneficial effects of estradiol treatment on aortic media thickening and lumen enlargement induced after OVX were described in normotensive Sprague Dawley rats (79). These observations confirm our findings of a blood pressure-independent mechanism being partially involved in mediating vasoprotective effects of female sex hormones. In uninephrectomized SHR stroke-prone rats, OVX induced aortic lumen dilatation and media thickening, alterations that could not be prevented by estradiol administration (77). Aortic wall hypertrophy was observed also in experimental renovascular hypertension, in this animal model OVX having no further influence on vascular remodelling. In

the same study, OVX alone did not induce media thickening of aorta, despite elevating blood pressure (78).

The decreased mitogenic response of VSMC in female uremic rats is consistent with previous findings of estrogens slowing proliferation rate of VSMC. This process can be mediated by direct effects of estrogens on VSMC, with suppression of growth factors (TGF-β, PDGF) production, but also by indirect effects on endothelial cells with enhancement of NO signalling (74). Kappert et al. described in VSMC isolated from rat aorta an inhibitory potential of estradiol on PDGF-induced proliferation, a process involving suppression of rac-1 (81).

Female sex hormones modulate expression of various adhesion molecules (i.e. E-selectin, VEGF) and proinflammatory cytokines (MCP-1), and inhibit production of ROS, thus interfering with the inflammatory response. These actions could explain the reduced macrophage infiltration of the aortic wall in female compared to male uremic animals in the present study (80).

In human aortic VSMC, both estradiol and testosterone treatments were shown to induce lower collagen I protein expression, but female sex hormone also increased elastin protein expression, while testosterone administration resulted in MMP-3 mRNA and protein up-regulation (135). Sex differences in MMP-2 expression in our study could be explained by differential regulation, since it is known that this gene is estrogen-regulated. Furthermore, the absence of MMP-2 up-regulation in uremic female animals is associated with reduced macrophage infiltration of the aortic wall. In the present study, no significant sex-related differences in collagen I, elastin or TIMP-1 expressions were found. Nevertheless, a slight trend could be observed for elastin and TIMP-1, female uremic animals showing less pronounced alterations of these parameters. This can be explained by the complex regulation (transcriptional, post-transcriptional, post-translational) and fragile but well controlled relation between synthesis and degradation of these ECM proteins. One can argue that in a complex pathological state like uremia, the vasoprotective effect of female sex hormones is the result of simultaneous discrete modulation of multiple molecular mechanisms involved in cell proliferation/differentiation, inflammation, ECM proteins synthesis/degradation. A significant higher number of animals would have been necessary to achieve significant sex-related differences.

Despite the beneficial effect of female sex in the development of uremic aortic hypertrophic remodelling, no significant sex-related differences in elastin-to-collagen ratio, as indirect marker of arterial stiffening, were observed in the present study. Previous clinical and experimental studies in different models of hypertension also provided controversial data concerning the vascular effects of ovariectomy and hormone replacement therapy. PWV, a marker of regional arterial stiffness, was found to be higher in men that in premenopausal

women, but carotid artery and global vascular stiffening were present more often in women (76; 136). The HOORN study showed in a general elderly population that even mild renal insufficiency is associated with development of LV hypertrophy only in male subjects, this being associated with an increased arterial stiffness (75). On the other hand, in subjects with type 2 diabetes, women have a greater incidence of aortic stiffening and left ventricular hypertrophy (73). In Sprague Dawley rats, OVX was demonstrated to significantly decrease aortic PWV without having any effect on media thickness or elastic modulus of thoracic aorta. Estradiol treatment in these rats normalized PWV and was associated with increased left ventricular mass. In the same study, different effects of estradiol replacement therapy on endothelial vasodilator function were described in the hindquarters and carotid arteries, suggesting once again a heterogeneous impact of estrogens on vascular function depending on the investigated vascular bed (79).

The present study showed that female uremic animals are protected against aortic remodelling independent of blood pressure values and despite a more rapid progression of renal disease. These results suggest that female sex hormones could differentially influence the pathogenesis of cardiovascular and renal disease, a hypothesis sustained by evidence of estrogens having divergent effects depending on strain, animal model and cell type.

4.4.2. Sex-related aspects in aortic NO/cGMP signal transduction

Preserved aortic mRNA expression of eNOS in uremic females but not in males, where it was down-regulated, suggests that conserved endothelial function is a mechanism involved in the protective effects of female sex on aortic remodelling. This is consistent with what is already known so far about female sex hormones and their interactions with NO/cGMP signal transduction.

A previous investigation showed that estrogens induce up-regulation of eNOS mRNA expression and this transcription activation is dependent on ERβ (85). In this model of mild uremia, aortic expression of ERβ was slightly up-regulated in SNX females, this is consistent with the increase of ERβ expression described in vascular diseases. *In vitro* studies demonstrated that NO production in human aortic endothelial cells was higher after 8h or more of estradiol treatment at concentrations of 10nM, with a parallel increase in eNOS protein expression (137). Furthermore, TNFα-induced eNOS down-regulation was prevented by estrogen in cultured endothelial cells (138). eNOS is situated to endothelial cell caveolae, special domains of cell membrane, where it colocalizes with estrogen receptors and other regulatory proteins like

caveolin-1, the latter binding to and inhibiting eNOS. Estradiol was able to remove the inhibitory effect of high caveolin-1 levels in cerebral arterioles of ovarectomized rats by reducing caveolin-1 concentration (139). However, in bovine aortic endothelial cells, estradiol stimulation increased after 48h the caveolin-1 expression, suggesting different actions depending on organism, tissue type and timing (140).

Modulation of NO/cGMP signalling pathway by female sex hormones implies also non-genomic activation of eNOS. This rapid effect is enabled by the colocalization of membrane-associated ER with eNOS and other regulatory proteins (calmodulin, caveolin-1) in caveolae. It was shown that, upon binding to ER in caveolae, estrogens can activate $G_{\alpha 1}$ protein and modulate the activity of MAPK and PI_3-kinase/Akt pathway and subsequently lead to eNOS phosphorylation on serine 1177, a critical residue for eNOS activation and modification of its calcium sensitivity. In addition, estrogens increase intracellular Ca^{2+} concentration by modulating the activity of ion channels and thus promote calmodulin binding to eNOS with dissociation of inactive eNOS-caveolin-1 complex, this leading to further stimulation of NO production. Besides stimulating NO production, female sex hormones further enhance NO/cGMP signalling due to their antioxidative effects that result in reduced NO scavenging by ROS (87; 88; 89).

No significant sex-related differences in plasmatic cGMP levels were seen in our study. Nevertheless, plasma cGMP concentrations reflect systemic activity of cGMP-producing enzymes and this parameter may not reflect local aortic activity of sGC.

However, investigation of molecular mechanisms linking female sex hormones with expression and activity of NO/cGMP signal transduction components was not the subject of this study, so that it cannot provide direct data about which of the known estrogens actions is involved in the protection of female SNX rats against uremic aortic remodelling. Further investigations in this direction, involving for example castration and hormone replacement therapy, could further elucidate the molecular mechanisms and signalling pathways involved in the protective effect of female sex hormones in the process of uremic aortic remodelling.

4.5. Effects of BAY 41-8543 on aortic remodelling in mild renal insufficiency

BAY 41-8543 treatment increased plasma cGMP concentrations in male uremic rats and successfully attenuated morphological remodelling of the aortic wall, normalizing aortic lumen diameter, media thickness and media-to-lumen ratio. The beneficial effects of BAY 41-8543 treatment were explained by inhibition of VSMC proliferation, significant decrease in collagen I

deposition and normalization of extracellular matrix turnover at the aortic level, as indicated by reduction of aortic TIMP-1 and MMP-2 expression. In addition, administration of BAY 41-8543 significantly inhibited degradation of elastic fibres, thus resulting in an increased elastin content of the aortic wall and a higher elastin-to-collagen ratio in comparison with untreated uremic animals. This points towards beneficial effects of BAY 41-8543 on the aortic function by reduction of the aortic wall stiffness. Furthermore, Bay 41-8543 treatment prevented the alterations of NO/cGMP signalling pathway components seen in untreated SNX animals (91).

Thus, this study demonstrates in a model of mild renal insufficiency the critical role played by NO/cGMP signal transduction in the pathogenesis of aortic remodelling and stiffening. This is the first evidence of beneficial effects of sGC stimulator BAY 41-8543 on aortic structural and functional alterations occurring in experimental mild uremia. These results suggest that BAY 41-8543 is a promising new pharmacological tool in the treatment of arterial remodelling.

In our renal ablation model, despite its hypotensor effect, hydralazine therapy did not manage to prevent/ameliorate aortic remodelling and stiffening. This indicates that the protective effects of BAY 41-8543 involve – at least in part – blood pressure-independent mechanisms.

4.5.1. Blood pressure reduction

In CKD patients and animal models of mild uremia, elevated blood pressure represents one of the important pathogenic factors involved in uremic aortic remodelling, even if there is evidence that this process can also develop in conditions of normotension. As previously mentioned, BAY 41-8543 normalized blood pressure. The mechanisms underlying the antihypertensive effects of BAY 41-8543 involve elevation of cGMP levels in VSMC with activation of PKG-1. This translates into reduction of intracellular Ca^{2+} concentration and induction of cell hyperpolarization, modifications that result in relaxation of VSMC with vasodilatation. Thus, by lowering blood pressure, BAY 41-8543 interferes with the mechanical forces acting on arterial wall and promoting structural and functional changes. Blood pressure-lowering effects of sGC stimulators, including BAY 41-8543, were previously demonstrated in high renin, low NO mice model of hypertension, rat model of L-NAME- and Ang II-induced hypertension and a canine model of tachypacing-induced heart failure (65; 66; 141; 142). Additionally, sGC stimulator riociguat (BAY 63-2521) was shown to reduce pressure in pulmonary circulation and thus ameliorate pulmonary vascular remodelling in patients with pulmonary arterial hypertension and chronic thromboembolic pulmonary hypertension (68; 69).

4.5.2. Antiproliferative effects of BAY 41-8543

Proliferation of VSMC was indicated as one of the major cellular mechanisms underlying aortic media thickening in experimental uremia. BAY 41-8543 treatment, by increasing cGMP levels, significantly reduced the mitogenic response of aortic VSMC in uremic male rats. This finding is in line with antiproliferative effects of sGC stimulator YC-1, the prototype of BAY 41-8543, on VSMC demonstrated *in vitro* in rat thoracic aorta VSMC and *in vivo* in balloon-injured rat carotid arteries. These effects of YC-1 on VSMC were mediated through elevation of sGC activity and cGMP concentration, inhibition of TGF-β1 secretion and down-regulation of focal adhesion kinase (FAK) protein expression. Both TGF-β1 and FAK are known to stimulate cell growth and proliferation and to modulate cell survival, thereby playing an active role in vascular disease induction and progression. Further inhibitory effects on VSMC proliferation were seen after administration of sGC stimulator BAY 41-2272 in a rat model of chronic pulmonary hypertension, this translating into reduced muscularization of pulmonary arteries (67).

4.5.3. Antiinflammatory effects of BAY 41-8543

Chronic renal insufficiency is a state of increased inflammatory status and oxidative stress, alterations that are observed also at the aortic wall level. Consequently, the expression of various adhesion molecules and chemoattractant proteins in endothelial cells is markedly up-regulated, leading to increased leukocyte adhesion and inflammatory infiltration of the aortic wall. Infiltrating macrophages further aggravate vascular disease by production of proinflammatory and profibrotic cytokines and proteins involved in extracellular matrix homeostasis (MMPs, TIMPs). It has been shown that sGC stimulators can inhibit P-selectin expression in endothelial cells and platelets in vitro and reduce leukocyte rolling and adhesion in vivo, pointing towards modulator effects of sGC and cGMP on the vascular inflammatory response (143). In the present study, increased aortic macrophage infiltration in uremic rats, as documented by ED-1 staining, was slightly but not significantly reduced in BAY 41-8543-treated animals. Because of the very small cross-section area of aorta and low number of macrophages/aortic cross-section, it is difficult to obtain statistically significant differences between study groups, this representing a methodological limitation in the evaluation of aortic inflammatory infiltration.

4.5.4. Impact of BAY 41-8543 on extracellular matrix components

Signalling through NO/cGMP pathway modulates not only proliferation, but also the phenotype of VSMC. Under certain conditions (inflammation, increased oxidative stress), VSMC can alter their phenotype from a contractile/differentiated one to a more secretory/de-differentiated one. This process involves loss of contractile proteins, low expression of signalling proteins (membrane receptors, ion channels), high levels of extracellular matrix proteins (e.g. collagen, fibronectin, thrombospondin), growth factors (e.g. PDGF) and growth factor receptors. The involvement of NO/cGMP signal transduction in this process is suggested by *in vitro* and *in vivo* evidence for a pro-differentiation role of NO donors, cGMP analogues, PKG-transfection and PDE inhibitors. Moreover, expression of sGC and PKG was down-regulated in VSMC with synthetic phenotype. PKG transfection was shown to decrease collagen I production and MMP-2 expression in cultured VSMC (47). Thus, by stimulating cGMP production, BAY 41-8543 can inhibit fibroproliferative transformation of VSMC and so reduce accumulation of extracellular matrix proteins, whereby both mechanisms are involved in structural remodelling and stiffening of arterial wall in this study. Administration of BAY 41-8543 significantly reduced collagen I protein deposition and TIMP-1 and MMP-2 relative mRNA expression in the aortic wall of uremic rats (91). Similar effects on MMP-2 expression were described after YC-1 treatment in the balloon-injured rat carotid artery model; this is associated with inhibition of MMP-2 enzymatic activity (57). Even if there are a few investigations suggesting opposite effects of cGMP-activated PKG (proproliferative effects, increased expression of adhesion molecules), the majority of studies shows inhibitory effects of cGMP on VSMC proliferation and de-differentiation.

4.5.5. Effects of BAY 41-8543 on NO/cGMP signaling pathway

In the present study treatment with BAY 41-8543 prevented the decrease in aortic eNOS mRNA expression, suggesting that the beneficial effects of BAY 41-8543 on aortic uremic remodelling could also be partially explained by normalization of aortic NO/cGMP signalling.

In our renal ablation model, despite its hypotensor effect, hydralazine therapy failed to prevent/ameliorate aortic remodelling and stiffening. This indicates that the protective effects of BAY 41-8543 involve – at least in part – blood pressure-independent mechanisms.

In conclusion, this study shows that experimental mild renal insufficiency leads to pronounced aortic hypertrophic remodelling and stiffening in Wistar rats. The results of this study suggest that aortic wall alterations can develop as an effect of uremia per se, at least partially independent of blood pressure levels. Aortic morphological, cellular and molecular alterations undergo a sex-dependent regulatory process. Vascular disease was more severe in male animals and was mediated by proliferation of aortic VSMC, macrophage infiltration of the aortic wall, enhanced extracellular matrix turnover with elevated collagen I deposition, decreased elastin content and up-regulated TIMP-1 and MMP-2 aortic mRNA expression, and was related to decreased aortic eNOS expression. In turn, specific sGC/cGMP stimulation by BAY 41-8543 significantly ameliorates the aortic wall remodelling and stiffening, an effect that occurred in a blood pressure-independent manner. BAY 41-8543 reduced the mitogenic response of aortic VSMC, the aortic collagen I deposition and extracellular matrix turnover, and normalised aortic eNOS expression. The findings in this experimental model of mild, long-term uremia suggest that pharmacological stimulation of the sGC enzyme may be a novel therapy concept for pathological arterial wall remodelling seen in patients with impaired renal function.

REFERENCE LIST

1. Briet M, Boutouyrie P, Laurent S and London GM. Arterial stiffness and pulse pressure in CKD and ESRD. Kidney Int. 2011, Bd. 82, S. 388-400.

2. Stam F, van Guldener C, Becker A, Dekker JM, Heine RJ, Bouter LM, Stehouwer CDA. Endothelial dysfunction contributes to renal function-associated cardiovascular mortality in a population with mild renal insufficiency: the Hoorn study. J.Am.Soc.Nephrol. 2006, 17, S. 537-545.

3. Schiffrin EL, Lipman ML, Mann JF. Chronic kidney disease: effects on the cardiovascular system. Circulation . 2007, Bd. 116, S. 85-97.

4. dos Santos RL, da Silva FB, Ribeiro RF Jr, Stefanon I. Sex hormones in the cardiovascular system. Horm Mol Biol Clin Investig. 2014, Bd. 18(2), S. 89-103.

5. Tronc F, Wassef M, Esposito B, Henrion D, Glagov S, Tedgui A. Role of NO in flow-induced remodeling of the rabbit common carotid artery. Arterioscler.Thromb.Vasc.Biol. 1996, Bd. 16, S. 1256-1262.

6. Nichols WW, O'Rourke MF, McDonald DA. McDonald's blood flow in arteries: theoretical, experimental and clinical principles. Hodder Arnold. 6th ed. London, 2011.

7. London GM, Marchais SJ, Guerin AP, Metivier F, Adda H. Arterial structure and function in end-stage renal disease. Nephrol.Dial.Transplant. . 2002, Bd. 17, S. 1713-1724.

8. Meeus F, Kourilsky O, Guerin AP, Gaudry C, Marchais SJ, London GM. Pathophysiology of cardiovascular disease in hemodialysis patients. Kidney Int.Suppl. 2000, 76, S. S140-S147.

9. Demuth K, Blacher J, Guerin AP, Benoit MO, Moatti N, Safar ME, London GM. Endothelin and cardiovascular remodelling in end-stage renal disease. Nephrol.Dial.Transplant. 1998, Bd. 13, S. 375-383.

10. Passauer J, Pistrosch F, Bussemaker E, Lassig G, Herbrig K, Gross P. Reduced agonist-induced endothelium-dependent vasodilation in uremia is attributable to an impairment of vascular nitric oxide. J.Am.Soc.Nephrol. 2005, Bd. 16, S. 959-965.

11. Wever R, Boer P, Hijmering M, Stroes E, Verhaar M, Kastelein J, Versluis K, Lagerwerf F, van Rijn H, Koomans H, Rabelink T. Nitric oxide production is reduced in patients with chronic renal failure. Arterioscler.Thromb.Vasc.Biol. 1999, 19, S. 1168-1172.

12. Himmelfarb J, Stenvinkel P, Ikizler TA, Hakim RM. The elephant in uremia: oxidant stress as a unifying concept of cardiovascular disease in uremia. Kidney Int. 2002, 62, S. 1524-1538.

13. Konings CJ, Dammers R, Rensma PL, Kooman JP, Hoeks AP, Kornet L, Gladziwa U, van der Sande FM, Leunissen KM. Arterial wall properties in patients with renal failure. Am.J.Kidney Dis. 2002, Bd. 39, S. 1206-1212.

14. Olivetti G, Melissari M, Marchetti G, Anversa P. Quantitative structural changes of the rat thoracic aorta in early spontaneous hypertension. Tissue composition, and hypertrophy and hyperplasia of smooth muscle cells. Circ.Res. 1982, 51, S. 19-26.

15. Owens GK, Schwartz SM. Alterations in vascular smooth muscle mass in the spontaneously hypertensive rat. Role of cellular hypertrophy, hyperploidy, and hyperplasia. Circ.Res. 1982, 51, S. 280-289.

16. Owens GK, Schwartz SM. Vascular smooth muscle cell hypertrophy and hyperploidy in the Goldblatt hypertensive rat. Circ.Res. 1983, 53, S. 491-501.

17. Amann K, Wolf B, Nichols C, Törnig J, Schwarz U, Zeier M, Mall G, Ritz E. Aortic changes in experimental renal failure: hyperplasia or hypertrophy of smooth muscle cells? Hypertension. 1997, 29, S. 770-775.

18. Amann K, Tornig J, Flechtenmacher C, Nabokov A, Mall G, Ritz E. Blood-pressure-independent wall thickening of intramyocardial arterioles in experimental uraemia: evidence for a permissive action of PTH. Nephrol.Dial.Transplant. 1995, 10, S. 2043-2048.

19. Amann K, Munter K, Wessels S, Wagner J, Balajew V, Hergenröder S, Mall G, Ritz E. Endothelin A receptor blockade prevents capillary/myocyte mismatch in the heart of uremic animals. J.Am.Soc.Nephrol. 2000, 11, S. 1702-1711.

20. Galis ZS, Khatri JJ. Matrix metalloproteinases in vascular remodeling and atherogenesis: the good, the bad, and the ugly. Circ.Res. 2002, 90, S. 251-262.

21. Raffetto JD, Khalil RA. Matrix metalloproteinases and their inhibitors in vascular remodeling and vascular disease. Biochem.Pharmacol. 2008, 75, S. 346-359.

22. Briet M, Schiffrin EL. Treatment of arterial remodeling in essential hypertension. Curr Hypertens Rep. 2013, Bd. 15(1), S. 3-9.

23. Shahin Y, Khan JA, Chetter I. Angiotensin converting enzyme inhibitors effect on arterial stiffness and wave reflections: a meta-analysis and meta-regression of randomised controlled trials. Atherosclerosis. 2012, Bd. 221(1), S. 18-33.

24. Virdis A, Ghiadoni L, Qasem AA, Lorenzini G, Duranti E, Cartoni G, Bruno RM, Bernini G, Taddei S. Effect of aliskiren treatment on endothelium-dependent vasodilation and aortic stiffness in essential hypertensive patients. Eur Heart J. 2012, Bd. 33(12), S. 1530-1538.

25. de Souza F, Muxfeldt E, Fiszman R, Salles G. Efficacy of spironolactone therapy in patients with true resistant hypertension. Hypertension . 2010, Bd. 55(1), S. 147-152.

26. Kostis JB, Packer M, Black HR, Schmieder R, Henry D, Levy E. Omapatrilat and enalapril in patients with hypertension: the Omapatrilat Cardiovascular Treatment vs. Enalapril (OCTAVE) trial. Am.J.Hypertens. 2004, Bd. 17, S. 103-111.

27. Mitchell GF, Izzo JL, Jr., Lacourciere Y, Ouellet JP, Neutel J, Qian C, Kerwin LJ, Block AJ, Pfeffer MA. Omapatrilat reduces pulse pressure and proximal aortic stiffness in patients with systolic hypertension: results of the conduit hemodynamics of omapatrilat international research study. Circulation. 2002, Bd. 105, S. 2955-2961.

28. Schmitt M, Qasem A, McEniery C, Wilkinson IB, Tatarinoff V, Noble K, Klemes J, Payne N, Frenneaux MP, Cockcroft J, Avolio A. Role of natriuretic peptides in regulation of conduit artery distensibility. Am.J.Physiol Heart Circ.Physiol. 2004, Bd. 287, S. H1167-H1171.

29. Vlachopoulos C, Hirata K, O'Rourke MF. Effect of sildenafil on arterial stiffness and wave reflection. Vasc.Med. 2003, Bd. 8, S. 243-248.

30. London GM, Pannier B, Guerin AP, Marchais SJ, Safar ME, Cuche JL. Cardiac hypertrophy, aortic compliance, peripheral resistance, and wave reflection in end-stage renal disease. Comparative effects of ACE inhibition and calcium channel blockade. Circulation. 1994, Bd. 90, S. 2786-2796.

31. London GM, Pannier B, Vicaut E, Guerin AP, Marchais SJ, Safar ME, Cuche JL. Antihypertensive effects and arterial haemodynamic alterations during angiotensin converting enzyme inhibition. J.Hypertens. 1996, Bd. 14, S. 1139-1146, .

32. Guerin AP, Blacher J, Pannier B, Marchais SJ, Safar ME, London GM. Impact of aortic stiffness attenuation on survival of patients in end-stage renal failure. Circulation. 2001, 103, S. 987-992.

33. Furchgott RF, Zawadzki JV. The obligatory role of endothelial cells in the relaxation of arterial smooth muscle by acetylcholine. Nature. 1980, Bd. 288, S. 373-376.

34. Ignarro LJ, Buga GM, Wood KS, Byrns RE, Chaudhuri G. Endothelium-derived relaxing factor produced and released from artery and vein is nitric oxide. Proc.Natl.Acad.Sci.U.S.A . 1987, Bd. 84, S. 9265-9269.

35. Palmer RM, Ferrige AG, Moncada S. Nitric oxide release accounts for the biological activity of endothelium-derived relaxing factor. Nature. 1987, Bd. 327, S. 524-526.

36. Beckman JS, Koppenol WH. Nitric oxide, superoxide, and peroxynitrite: the good, the bad, and ugly. Am.J.Physiol . 1996, Bd. 271, S. C1424-C1437.

37. Palmer RM, Ashton DS, Moncada S. Vascular endothelial cells synthesize nitric oxide from L-arginine. Nature. 1988, Bd. 333, S. 664-666.

38. Reyes AA, Karl IE, Klahr S. Role of arginine in health and in renal disease. Am.J.Physiol. 1994, Bd. 267, S. F331-F346.

39. Förstermann U, Sessa WC. Nitric oxide synthases: regulation and function. Eur Heart J. 2012, Bd. 33(7), S. 829-837,837a-837d.

40. Bachmann S, Mundel P. Nitric oxide in the kidney: synthesis, localization, and function. Am.J.Kidney Dis. 1994, Bd. 24, S. 112-129.

41. Nathan CF, Hibbs JB, Jr. Role of nitric oxide synthesis in macrophage antimicrobial activity. . Curr.Opin.Immunol. . 1991, Bd. 3, S. 65-70.

42. Stamler JS, Singel DJ, Loscalzo J. Biochemistry of nitric oxide and its redox-activated forms. Science. 1992, Bd. 258, S. 1898-1902.

43. Derbyshire ER, Marletta MA. Structure and regulation of soluble guanylate cyclase. Annu Rev Biochem. 2012, Bd. 81, S. 533-559.

44. Dudzinski DM, Igarashi J, Greif D, Michel T. The regulation and pharmacology of endothelial nitric oxide synthase. . Annu.Rev.Pharmacol.Toxicol. 2006, Bd. 46, S. 235-276.

45. Filippov G, Bloch DB, Bloch KD. Nitric oxide decreases stability of mRNAs encoding soluble guanylate cyclase subunits in rat pulmonary artery smooth muscle cells. . J.Clin.Invest 100:942-948, 1997. 1997, Bd. 100, S. 942-948.

46. Gewaltig MT, Kojda G. Vasoprotection by nitric oxide: mechanisms and therapeutic potential. Cardiovasc.Res. 2002, 55, S. 250-260.

47. Lincoln TM, Wu X, Sellak H, Dey N, Choi C. Regulation of vascular smooth muscle cell phenotype by cyclic GMP and cyclic GMP-dependent protein kinase. Front Biosci. 2006, 11, S. 356-367.

48. Rybalkin SD, Yan C, Bornfeldt KE, Beavo JA. Cyclic GMP phosphodiesterases and regulation of smooth muscle function. . Circ.Res. 2003, Bd. 93, S. 280-291.

49. Maurice DH, Ke H, Ahmad F, Wang Y, Chung J, Manganiello VC. Advances in targeting cyclic nucleotide phosphodiesterases. Nat Rev Drug Discov. . 2014 , Bd. 13(4), S. 290-314.

50. Baylis C. Nitric oxide deficiency in chronic kidney disease. Am.J.Physiol Renal Physiol. 2008, Bd. 294, S. F1-F9.

51. Aiello S, Noris M, Todeschini M, Zappella S, Foglieni C, Benigni A, Corna D, Zoja C, Cavallotti D, Remuzzi G. Renal and systemic nitric oxide synthesis in rats with renal mass reduction. Kidney Int. 1997, 52, S. 171-181.

52. Kim SW, Lee J, Paek YW, Kang DG, Choi KC. Decreased nitric oxide synthesis in rats with chronic renal failure. J.Korean Med.Sci. 2000, 15, S. 425-430.

53. Roczniak A, Fryer JN, Levine DZ, Burns KD. Downregulation of neuronal nitric oxide synthase in the rat remnant kidney. J.Am.Soc.Nephrol. 1999, Bd. 10, S. 704-713.

54. Vaziri ND, Ni Z, Wang XQ, Oveisi F, Zhou XJ. Downregulation of nitric oxide synthase in chronic renal insufficiency: role of excess PTH. Am.J.Physiol. 1998, 274, S. F642-F649.

55. Vaziri ND, Oveisi F, Ding Y. Role of increased oxygen free radical activity in the pathogenesis of uremic hypertension. Kidney Int. 1998, Bd. 53, S. 1748-1754.

56. Huang PL, Huang Z, Mashimo H, Bloch KD, Moskowitz MA, Bevan JA, Fishman MC. Hypertension in mice lacking the gene for endothelial nitric oxide synthase. Nature. 1995, 377, S. 239-242.

57. Liu YN, Pan SL, Peng CY, Guh JH, Huang DM, Chang YL, Lin CH, Pai HC, Kuo SC, Lee FY, Teng CM. YC-1 [3-(5'-hydroxymethyl-2'-furyl)-1-benzyl indazole] inhibits neointima formation in balloon-injured rat carotid through suppression of expressions and activities of matrix metalloproteinases 2 and 9. J.Pharmacol.Exp.Ther. 2006, 316, S. 35-41.

58. Hassid A, Arabshahi H, Bourcier T, Dhaunsi GS, Matthews C. Nitric oxide selectively amplifies FGF-2-induced mitogenesis in primary rat aortic smooth muscle cells. Am.J.Physiol. 1994, 267, S. H1040-H1048.

59. Wolfsgruber W, Feil S, Brummer S, Kuppinger O, Hofmann F, Feil R. A proatherogenic role for cGMP-dependent protein kinase in vascular smooth muscle cells. Proc.Natl.Acad.Sci.U.S.A. 2003, 100, S. 13519-13524.

60. Radomski MW, Palmer RM, Moncada S. Endogenous nitric oxide inhibits human platelet adhesion to vascular endothelium. Lancet. 1987, 2, S. 1057-1058.

61. Wilkinson IB, Franklin SS, Cockcroft JR. Nitric oxide and the regulation of large artery stiffness: from physiology to pharmacology. Hypertension. 2004, 44, S. 112-116.

62. Friebe A, Koesling D. Mechanism of YC-1-induced activation of soluble guanylyl cyclase. . Mol.Pharmacol. . 1998, Bd. 53, S. 123-127.

63. Stasch JP, Becker EM, Alonso-Alija C, Apeler H, Dembowsky K, Feurer A, Gerzer R, Minuth T, Perzborn E, Pleiss U, Schröder H, Schroeder W, Stahl E, Steinke W, Straub A, Schramm M. NO-independent regulatory site on soluble guanylate cyclase. Nature. 2001, 410, S. 212-215.

64. Stasch JP, Alonso-Alija C, Apeler H, Dembowsky K, Feurer A, Minuth T, Perzborn E, Schramm M, Straub A. Pharmacological actions of a novel NO-independent guanylyl cyclase stimulator, BAY 41-8543: in vitro studies. Br.J.Pharmacol. 2002, 135, S. 333-343.

65. Stasch JP, Dembowsky K, Perzborn E, Stahl E, Schramm M. Cardiovascular actions of a novel NO-independent guanylyl cyclase stimulator, BAY 41-8543: in vivo studies. Br.J.Pharmacol. 2002, 135, S. 344-355.

66. Boerrigter G, Costello-Boerrigter LC, Cataliotti A, Tsuruda T, Harty GJ, Lapp H, Stasch JP, Burnett JC Jr. Cardiorenal and humoral properties of a novel direct soluble guanylate cyclase stimulator BAY 41-2272 in experimental congestive heart failure. Circulation. 2003, 107, S. 686-689.

67. Dumitrascu R, Weissmann N, Ghofrani HA, Dony E, Beuerlein K, Schmidt H, Stasch JP, Gnoth MJ, Seeger W, Grimminger F, Schermuly RT. Activation of soluble guanylate cyclase reverses experimental pulmonary hypertension and vascular remodeling. Circulation. 2006, 113, S. 286-295.

68. Ghofrani HA, Hoeper MM, Halank M, Meyer FJ, Staehler G, Behr J, Ewert R, Weimann G, Grimminger F. Riociguat for chronic thromboembolic pulmonary hypertension and pulmonary arterial hypertension: a phase II study. Eur Respir J. 2010, 36(4), S. 792-799.

69. Grimminger F, Weimann G, Frey R, Voswinckel R, Thamm M, Bölkow D, Weissmann N, Mück W, Unger S, Wensing G, Schermuly RT, Ghofrani HA. First acute haemodynamic study of soluble guanylate cyclase stimulator riociguat in pulmonary hypertension. The European Respiratory Journal. 2009, 4, S. 785–792.

70. Peters H, Wang Y, Loof T, Martini S, Kron S, Kramer S, Neumayer HH. Expression and activity of soluble guanylate cyclase in injury and repair of anti-thy1 glomerulonephritis. Kidney Int. 2004, 66, S. 2224-2236.

71. Wang Y, Kramer S, Loof T, Martini S, Kron S, Kawachi H, Shimizu F, Neumayer HH, Peters H. Stimulation of soluble guanylate cyclase slows progression in anti-thy1-induced chronic glomerulosclerosis. Kidney Int. 2005, 68, S. 47-61.

72. Orshal JM, Khalil RA. Gender, sex hormones, and vascular tone. Am.J.Physiol Regul.Integr.Comp Physiol. 2004, 286, S. R233-R249.

73. Reckelhoff JF. Sex steroids, cardiovascular disease, and hypertension: unanswered questions and some speculations. Hypertension. 2005, 45, S. 170-174.

74. Mendelsohn ME, Karas RH. The protective effects of estrogen on the cardiovascular system. N.Engl.J.Med. 1999, 340, S. 1801-1811.

75. Henry RM, Kamp O, Kostense PJ, Spijkerman AM, Dekker JM, Nijpels G, Heine RJ, Bouter LM, Stehouwer CD. Mild renal insufficiency is associated with increased left ventricular mass in men, but not in women: an arterial stiffness-related phenomenon--the Hoorn Study. Kidney Int. 2005, 68, S. 673-679.

76. London GM, Guerin AP, Pannier B, Marchais SJ, Stimpel M. Influence of sex on arterial hemodynamics and blood pressure. Role of body height. Hypertension. 1995, 26, S. 514-519.

77. Gross ML, Ritz E, Korsch M, Adamczak M, Weckbach M, Mall G, Berger I, Hansen A, Amann K. Effects of estrogens on cardiovascular structure in uninephrectomized SHRsp rats. Kidney Int. 2005, 67, S. 849-857.

78. Mendonca LS, Fernandes-Santos C, Mandarim-de-Lacerda CA. Cardiac and aortic structural alterations due to surgically-induced menopause associated with renovascular hypertension in rats. Int.J.Exp.Pathol. 2007, 88, S. 301-309.

79. Tatchum-Talom R, Martel C, Marette A. Influence of estrogen on aortic stiffness and endothelial function in female rats. Am.J.Physiol Heart Circ.Physiol. 2002, 282, S. H491-H498.

80. Tostes RC, Nigro D, Fortes ZB, Carvalho MH. Effects of estrogen on the vascular system. Braz.J.Med.Biol.Res. 2003, 36, S. 1143-1158.

81. Kappert K, Caglayan E, Huntgeburth M, Baumer AT, Sparwel J, Uebel M, Rosenkranz S. 17Beta-estradiol attenuates PDGF signaling in vascular smooth muscle cells at the postreceptor level. Am.J.Physiol Heart Circ.Physiol. 2006, 290, S. H538-H546.

82. Mendelsohn ME, Karas RH. Molecular and cellular basis of cardiovascular gender differences. Science. 2005, 308, S. 1583-1587.

83. Qiu H, Tian B, Resuello RG, Natividad FF, Peppas A, Shen YT, Vatner DE, Vatner SF, Depre C. Sex-specific regulation of gene expression in the aging monkey aorta. Physiol Genomics. 2007, Bd. 29, S. 169-180.

84. Forte P, Kneale BJ, Milne E, Chowienczyk PJ, Johnston A, Benjamin N, Ritter JM. Evidence for a difference in nitric oxide biosynthesis between healthy women and men. Hypertension. 1998, Bd. 32, S. 730-734.

85. Nuedling S, Karas RH, Mendelsohn ME, Katzenellenbogen JA, Katzenellenbogen BS, Meyer R, Vetter H, Grohe C. Activation of estrogen receptor beta is a prerequisite for estrogen-dependent upregulation of nitric oxide synthases in neonatal rat cardiac myocyte. FEBS Lett. 2001, Bd. 502, S. 103-108.

86. Wagner AH, Schroeter MR, Hecker M. 17beta-estradiol inhibition of NADPH oxidase expression in human endothelial cells. . FASEB J. 2001, Bd. 15, S. 2121-2130.

87. Chambliss KL, Shaul PW. Estrogen modulation of endothelial nitric oxide synthase. Endocr.Rev. 2002, 23, S. 665-686.

88. Edwards DP. Regulation of signal transduction pathways by estrogen and progesterone. Annu.Rev.Physiol. 2005, 67, S. 335-376.

89. Khalil RA. Sex hormones as potential modulators of vascular function in hypertension. Hypertension. 2005, 46, S. 249-254.

90. Gray GA, Sharif I, Webb DJ, Seckl JR. Oestrogen and the cardiovascular system: the good, the bad and the puzzling. Trends Pharmacol Sci. 2001, Bd. 22(3), S. 152-156.

91. Stancu B, Krämer S, Loof T, Mika A, Amann K, Neumayer HH, Peters H. Soluble guanylate cyclase stimulator BAY 41-8543 and female sex ameliorate uremic aortic remodeling in a rat model of mild uremia. J Hypertens. 2015, 33, S. 1907-1921 .

92. Amann K, Irzyniec T, Mall G, Ritz E. The effect of enalapril on glomerular growth and glomerular lesions after subtotal nephrectomy in the rat: a stereological analysis. J.Hypertens. 1993, 11, S. 969-975.

93. Evgenov OV, Pacher P, Schmidt PM, Hasko G, Schmidt HH, Stasch JP. NO-independent stimulators and activators of soluble guanylate cyclase: discovery and therapeutic potential. Nat.Rev.Drug Discov. 2006, 5, S. 755-768.

94. Gurney AM, Allam M. Inhibition of calcium release from the sarcoplasmic reticulum of rabbit aorta by hydralazine. Br.J.Pharmacol. . 1995, Bd. 114, S. 238-244.

95. Ritz E, McClellan WM. Overview: increased cardiovascular risk in patients with minor renal dysfunction: an emerging issue with far-reaching consequences. J.Am.Soc.Nephrol. 2004, 15, S. 513-516.

96. Sarnak MJ, Levey AS, Schoolwerth AC, Coresh J, Culleton B, Hamm LL, McCullough PA, Kasiske BL, Kelepouris E, Klag MJ, Parfrey P, Pfeffer M, Raij L, Spinosa DJ, Wilson PW, American Heart Association Councils on Kidney in Cardiovascular Disease, High Blood Pressure Research, Clinical Cardiology, and Epidemiology and Prevention. Kidney disease as a risk factor for development of cardiovascular disease: a statement from the American Heart Association Councils on Kidney in Cardiovascular Disease, High Blood Pressure Research, Clinical Cardiology, and Epidemiology and Prevention. Hypertension. 2003, 42, S. 1050-1065.

97. Peters H, Border WA, Noble NA. From rats to man: a perspective on dietary L-arginine supplementation in human renal disease. Nephrol Dial Transplant. . 1999, Bd. 14(7), S. 1640-1650.

98. Kagota S, Tamashiro A, Yamaguchi Y, Sugiura R, Kuno T, Nakamura K, Kunitomo M. Downregulation of vascular soluble guanylate cyclase induced by high salt intake in spontaneously hypertensive rats. Br.J.Pharmacol. 2001, 134, S. 737-744.

99. Brenner BM. Nephron adaptation to renal injury or ablation. Am.J.Physiol. 1985, Bd. 249, S. F324-F337.

100. Chen JK, Chen J, Neilson EG, Harris RC. Role of mammalian target of rapamycin signaling in compensatory renal hypertrophy. J.Am.Soc.Nephrol. 2005, Bd. 16, S. 1384-1391.

101. Noble NA, Border WA. Angiotensin II in renal fibrosis: should TGF-beta rather than blood pressure be the therapeutic target? Semin.Nephrol. 1997, Bd. 17, S. 455-466.

102. Peters H, Noble NA. Angiotensin II and L-arginine in tissue fibrosis: more than blood pressure. Kidney Int. 1997, Bd. 51, S. 1481-1486.

103. Ruiz-Ortega M, Lorenzo O, Suzuki Y, Ruperez M, Egido J. Proinflammatory actions of angiotensins. Curr.Opin.Nephrol.Hypertens. 2001, Bd. 10, S. 321-329.

104. Brenner BM, Chertow GM. Congenital oligonephropathy and the etiology of adult hypertension and progressive renal injury. Am.J.Kidney Dis. 1994, Bd. 23, S. 171-175.

105. Keller G, Zimmer G, Mall G, Ritz E, Amann K. Nephron number in patients with primary hypertension. N.Engl.J.Med. 2003, Bd. 348, S. 101-108.

106. Fleck C, Appenroth D, Jonas P, Koch M, Kundt G, Nizze H, Stein G. Suitability of 5/6 nephrectomy (5/6NX) for the induction of interstitial renal fibrosis in rats--influence of sex, strain, and surgical procedure. Exp.Toxicol.Pathol. 2006, 57, S. 195-205.

107. Silbiger S, Neugarten J. Gender and human chronic renal disease. Gender medicine. 5, Suppl A, 2008, S. 3-10.

108. Zimmermann MA, Sullivan JC. Hypertension: what´s sex got to do with it? Physiology. 28(4), 2013, S. 234-244.

109. Carrero, JJ. Gender differences in chronic kidney disease: underpinnings and therapeutic implications. Kidney Blood Press Res. 33, 2010, S. 383-392.

110. Lemos CC, Mandarim-de-Lacerda CA, Dorigo D, Coimbra TM, Bregman R. Chronic renal failure in male and female rats. J.Nephrol. 18, 2005, S. 368-373.

111. Oestreicher EM, Guo C, Seely EW, Kikuchi T, Martinez-Vasquez D, Jonasson L, Yao T, Burr D, Mayoral S, Roubsanthisuk W, Ricchiuti V, Adler GK. Estradiol increases proteinuria and angiotensin II type 1 receptor in kidneys of rats receiving L-NAME and angiotensin II. Kidney Int. 70, 2006, S. 1759-1768.

112. Antus B, Hamar P, Kokeny G, Szollosi Z, Mucsi I, Nemes Z, Rosivall L. Estradiol is nephroprotective in the rat remnant kidney. Nephrol.Dial.Transplant. 2003, Bd. 18, S. 54-61.

113. Sainz J, Osuna A, Wangensteen R, de Dios LJ, Rodriguez-Gomez I, Duarte J, Moreno JM, Vargas F. Role of sex, gonadectomy and sex hormones in the development of nitric oxide inhibition-induced hypertension. Exp.Physiol . 2004, Bd. 89, S. 155-162.

114. Verhagen AM, Attia DM, Koomans HA, Joles JA. Male gender increases sensitivity to proteinuria induced by mild NOS inhibition in rats: role of sex hormones. Am.J.Physiol Renal Physiol . 2000, Bd. 279, S. F664-F670.

115. Sandberg K. Mechanisms underlying sex differences in progressive renal disease. Gend.Med. 2008, Bd. 5, S. 10-23.

116. Rosenmann E, Yanko L, Cohen AM. Female sex hormone and nephropathy in Cohen diabetic rat (genetically selected sucrose-fed). Horm.Metab Res. 1984, Bd. 16, S. 11-16.

117. Gades MD, Stern JS, van Goor H, Nguyen D, Johnson PR, Kaysen GA. Estrogen accelerates the development of renal disease in female obese Zucker rats. Kidney Int. . 1998, Bd. 53, S. 130-135.

118. Joles JA, van Goor H, Koomans HA. Estrogen induces glomerulosclerosis in analbuminemic rats. Kidney Int. . 1998, Bd. 53, S. 862-868.

119. Baylis C. Age-dependent glomerular damage in the rat. Dissociation between glomerular injury and both glomerular hypertension and hypertrophy. Male gender as a primary risk factor. J.Clin.Invest. 1994, Bd. 94, S. 1823-1829.

120. Karl M, Berho M, Pignac-Kobinger J, Striker GE, Elliot SJ. Differential effects of continuous and intermittent 17beta-estradiol replacement and tamoxifen therapy on the prevention of glomerulosclerosis: modulation of the mesangial cell phenotype in vivo. Am.J.Pathol. 2006, Bd. 169, S. 351-361.

121. McGuire BB, Watson RW, Perez-Barriocanal F, Fitzpatrick JM, Docherty NG. Gender differences in the renin-angiotensin and nitric oxide systems: relevance in the normal and diseased kidney. Kidney Blood Press Res. . 2007, Bd. 30, S. 67-80.

122. Neugarten J, Acharya A, Lei J, Silbiger S. Selective estrogen receptor modulators suppress mesangial cell collagen synthesis. Am.J.Physiol Renal Physiol . 2000, Bd. 279, S. F309-F318.

123. Kalk P, Godes M, Relle K, Rothkegel C, Hucke A, Stasch JP, Hocher B. NO-independent activation of soluble guanylate cyclase prevents disease progression in rats with 5/6 nephrectomy. Br J Pharmacol. 2006, 148, S. 853–859.

124. Benz K, Orth SR, Simonaviciene A, Linz W, Schindler U, Rutten H, Amann K. Blood pressure-independent effect of long-term treatment with the soluble heme-independent guanylyl cyclase activator HMR1766 on progression in a model of noninflammatory chronic renal damage. Kidney Blood Press Res. 2007, 30, S. 224-233.

125. Amann K, Neususs R, Ritz E, Irzyniec T, Wiest G, Mall G. Changes of vascular architecture independent of blood pressure in experimental uremia. Am.J.Hypertens. 1995, 8, S. 409-417.

126. Campese VM. Is hypertension in chronic renal failure neurogenic in nature? Nephrol.Dial.Transplant. 1994, 9, S. 741-742.

127. Schiffrin EL, Touyz RM. From bedside to bench to bedside: role of renin-angiotensin-aldosterone system in remodeling of resistance arteries in hypertension. Am.J.Physiol Heart Circ.Physiol . 2004, Bd. 287, S. H435-H446.

128. London GM. Cardiovascular disease in chronic renal failure: pathophysiologic aspects. Semin.Dial. 2003, Bd. 16, S. 85-94.

129. Nabokov AV, Amann K, Wessels S, Munter K, Wagner J, Ritz E. Endothelin receptor antagonists influence cardiovascular morphology in uremic rats. Kidney Int. 1999, Bd. 55, S. 512-519.

130. Abel M, Ritthaler U, Zhang Y, Deng Y, Schmidt AM, Greten J, Sernau T, Wahl P, Andrassy K, Ritz E. Expression of receptors for advanced glycosylated end-products in renal disease. Nephrol.Dial.Transplant. 1995, Bd. 10, S. 1662-1667.

131. Ketteler M, Schlieper G, Floege J. Calcification and cardiovascular health: new insights into an old phenomenon. Hypertension. 2006, Bd. 47, S. 1027-1034.

132. Sindhu RK, Ehdaie A, Vaziri ND, Roberts CK. Effects of chronic renal failure on caveolin-1, guanylate cyclase and AKT protein expression. Biochim.Biophys.Acta. 2004, 1690, S. 231-237.

133. Kloss S, Bouloumie A, Mulsch A. Aging and chronic hypertension decrease expression of rat aortic soluble guanylyl cyclase. Hypertension. 2000, 35, S. 43-47.

134. Sitter T, Holzgartner V, Wolfram G, Toepfer M, Klare B, Gerzer R, Schiff H. Assessment of hypervolemia by cyclic 3′,5′-guanonsine monophosphate in pediatric patient on hemodialysis. Nephron. 83, 1999, S. 287–288.

135. Natoli AK, Medley TL, Ahimastos AA, Drew BG, Thearle DJ, Dilley RJ, Kingwell BA. Sex steroids modulate human aortic smooth muscle cell matrix protein deposition and matrix metalloproteinase expression. Hypertension. 2005, 46, S. 1129-1134.

136. Hayward CS, Kelly RP. Gender-related differences in the central arterial pressure waveform. J.Am.Coll.Cardiol. . 1997, 30, S. 1863-1871.

137. Hishikawa K, Nakaki T, Marumo T, Suzuki H, Kato R, Saruta T. Up-regulation of nitric oxide synthase by estradiol in human aortic endothelial cells. FEBS Lett. 1995, 360, S. 291-293.

138. Sumi D, Hayashi T, Jayachandran M, Iguchi A. Estrogen prevents destabilization of endothelial nitric oxide synthase mRNA induced by tumor necrosis factor alpha through estrogen receptor mediated system. Life Sci. 2001, 69, S. 1651-1660.

139. Xu HL, Galea E, Santizo RA, Baughman VL, Pelligrino DA. The key role of caveolin-1 in estrogen-mediated regulation of endothelial nitric oxide synthase function in cerebral arterioles in vivo. J.Cereb.Blood Flow Metab. 2001, 21, S. 907-913.

140. Jayachandran M, Hayashi T, Sumi D, Iguchi A, Miller VM. Temporal effects of 17beta-estradiol on caveolin-1 mRNA and protein in bovine aortic endothelial cells. Am.J.Physiol Heart Circ.Physiol. 2001, 281, S. H1327-H1333.

141. Masuyama H, Tsuruda T, Kato J, Imamura T, Asada Y, Stasch JP, Kitamura K, Eto T. Soluble guanylate cyclase stimulation on cardiovascular remodeling in angiotensin II-induced hypertensive rats. Hypertension. 2006, 48, S. 972-978.

142. Zanfolin M, Faro R, Araujo EG, Guaraldo AM, Antunes E, De Nucci G. Protective effects of BAY 41-2272 (sGC stimulator) on hypertension, heart, and cardiomyocyte hypertrophy induced by chronic L-NAME treatment in rats. J.Cardiovasc.Pharmacol. 2006, 47, S. 391-395.

143. Ahluwalia A, Foster P, Scotland RS, McLean PG, Mathur A, Perretti M, Moncada S, Hobbs AJ. Antiinflammatory activity of soluble guanylate cyclase: cGMP-dependent down-regulation of P-selectin expression and leukocyte recruitment. Proc Natl Acad Sci U S A. 2004, 101, S. 1386-1391.

ABBREVIATIONS

°C	Degrees Celsius
π	Pi mathematical constant (=3.14159…)
Akt	Proteinkinase B
APAAP	Alkaline phosphatase and anti-alkaline phosphatase
ATP	Adenosine triphosphate
Ca^{2+}	Calcium ion
CaM	Calmodulin
Cav1	Caveolin 1
cDNA	Complementary DNA
cGMP	Cyclic monophosphate
dATP	Deoxyadenosine 5´-triphosphate
dCTP	Deoxycytidine 5´-triphosphate
dGTP	Deoxyguanosine 5´-triphosphate
dTTP	Deoxytymidine 5´-triphosphate
DEPC	Diethyl pyrocarbonate
DNA	Deoxyribonucleic acid
dsDNA	Double-strain DNA
ECM	Extracellular matrix
EDTA	Ethylenediaminetetraacetic acid
ELISA	Enzyme-linked immunoabsorbent assay
eNOS	Endothelial nitric oxide synthetase
ER	Estrogen receptor
GAPDH	Glyceraldehyde-3-phosphate dehydrogenase
GTP	Guanosine 5´-triphosphate
HRP	Horseradish peroxidase

h	Hours
HE	Hematoxylin-eosin
H_2SO_4	Sulphuric acid
HCl	Hydrochloric acid
IBMX	3-Isobuthyl-1-methylxanthine
Ig	Immunoglobulin
iNOS	Inducible nitric oxide synthase
M	Molar concentration
min	Minutes
MAPK	Mitogen-activated protein kinase
$MgCl_2$	Magnesium chloride
mM	Millimolar concentration
mmHg	Millimeters mercury
MMP	Matrix metalloproteinase
MuLV	Murine leukemia virus
mRNA	Messenger ribonucleic acid
NaCl	Natrium chloride
NADPH	Nicotineamide adenine dinucleotide phosphatise reductase
nm	Nanometres
NO	Nitric oxide
NOS	Nitric oxide synthases
nNOS	Neuronal nitric oxide synthase
PAS	Periodic acid Schiff
PBS	Phosphate-buffered saline
PCNA	Proliferating cell nuclear antigen
PCR	Polymerase chain reaction

PDE	Phosphodiesterase
PKG	cGMP-dependent protein kinase
pmol	Picomol
p.o.	Per os
RNA	Ribonucleic acid
RNase	Ribonuclease
rpm	Revolutions per minute
RPMI	Roswell Park Memorial Institute medium
RT-PCR	Real-time polymerase chain reaction
sec	Seconds
sGC	Soluble guanylate cyclase
αSMA	Alpha Smooth muscle actin
SNX	Subtotal nephrectomy
TBS	Tris-buffered saline
TGFβ	Transforming growth factor beta
TIMP1	Tissue inhibitor of metalloproteinase 1
VSMC	Vascular smooth muscle cell

Eidesstattliche Versicherung

Ich, Bianca Stancu, versichere an Eides statt durch meine eigenhändige Unterschrift, dass ich die vorgelegte Dissertation mit dem Thema „Effects of sex and enhanced nitric oxide/cGMP signalling on aortic remodelling in experimental mild renal insufficiency" selbstständig und ohne nicht offengelegte Hilfe Dritter verfasst und keine anderen als die angegebenen Quellen und Hilfsmittel genutzt habe.

Alle Stellen, die wörtlich oder dem Sinne nach auf Publikationen oder Vorträgen anderer Autoren beruhen, sind als solche in korrekter Zitierung (siehe „Uniform Requirements for Manuscripts (URM)" des ICMJE -*www.**icmje**.org*) kenntlich gemacht. Die Abschnitte zu Methodik (insbesondere praktische Arbeiten, Laborbestimmungen, statistische Aufarbeitung) und Resultaten (insbesondere Abbildungen, Graphiken und Tabellen) entsprechen den URM (s.o) und werden von mir verantwortet.

Meine Anteile an etwaigen Publikationen zu dieser Dissertation entsprechen denen, die in der untenstehenden gemeinsamen Erklärung mit dem Betreuer angegeben sind. Sämtliche Publikationen, die aus dieser Dissertation hervorgegangen sind und bei denen ich Autorin bin, entsprechen den URM (s.o) und werden von mir verantwortet.

Die Bedeutung dieser eidesstattlichen Versicherung und die strafrechtlichen Folgen einer unwahren eidesstattlichen Versicherung (§156,161 des Strafgesetzbuches) sind mir bekannt und bewusst.

Datum   Unterschrift

Anteilserklärung an erfolgten Publikationen

Bianca Stancu hatte folgenden Anteil an den folgenden Publikationen:

<u>Publikation:</u>

Stancu B, Krämer S, Loof T, Mika A, Amann K, Neumayer HH, Peters H, Soluble guanylate cyclase stimulator BAY 41-8543 and female sex ameliorate uremic aortic remodeling in a rat model of mild uremia, Journal of Hypertension, 2015 Sep;33(9):1907-21. doi: 10.1097/HJH.0000000000000648.

<u>Beitrag im Einzelnen:</u>

Bianca Stancu hat gemeinsam mit dem Letzt- und Zweitautor die experimentelle Studie geplant, hat selbstständig den Tierversuch durchgeführt (Betreuung der Tieren, Randomisierung, Verabreichung der Medikamenten, in-vivo Messungen, Entnahme der Blutproben und Organe), war an den chirurgischen Eingriffen (die durch Fr. S. Krämer ausgeführt wurden) und an den Weiterverarbeitung der Proben für die histologischen und molekularbiologischen Analysen mitbeteiligt, hat selbstständig die histologischen Untersuchungen der Nierengewebe (Glomerulosclerosis Index) und Aorta thoracalis sowie die cGMP-Bestimmung mittels ELISA durchgeführt und war an der statistischen Auswertung mitbeteiligt. Bianca Stancu hat den Entwurf für das Manuskript und seine revidierte Version im Rahmen des Publikationsverfahrens erstellt. Nach Rückmeldung und Diskussion mit den Mitautoren hat sie die jeweils zur Publikation eingereichten Manuskriptversionen erstellt.

Unterschrift, Datum und Stempel des betreuenden Hochschullehrers

Unterschrift der Doktorandin

LEBENSLAUF

Mein Lebenslauf wird aus datenschutzrechtlichen Gründen in der elektronischen Version meiner Arbeit nicht veröffentlicht.

LEBENSLAUF

Mein Lebenslauf wird aus datenschutzrechtlichen Gründen in der elektronischen Version meiner Arbeit nicht veröffentlicht.

LEBENSLAUF

Mein Lebenslauf wird aus datenschutzrechtlichen Gründen in der elektronischen Version meiner Arbeit nicht veröffentlicht.

PUBLIKATIONSLISTE

B. Stancu, S. Krämer, T. Loof, A. Mika, K. Amann, H-H. Neumayer, H. Peters: Soluble guanylate cyclase stimulator BAY 41-8543 and female sex ameliorate uremic aortic remodeling in a rat model of mild uremia; Journal of Hypertension, 2015 Sep;33(9):1907-21. doi: 10.1097/HJH.0000000000000648

AKNOWLEDGEMENTS